Longtom-2 & ST1

VIC/P54

Well Completion Report

Interpretive Data

February 2006

CONTENTS

FIGURES **Page**

APPENDICES

ENCLOSURES

1. WELL SUMMARY

Longtom-2 is located approximately 31 kms from the nearest landfall in southeastern Victoria. It lies approximately 27.7 km west-southwest of the Snapper Field, 12.5 km southeast of the Tuna Field, 17 km southwest of the Marlin Field and 15.5 km northeast of the Patricia Baleen Field in the production permit Vic/P54 (Figure 1). The well was designed as an appraisal well to test the gas column encountered within the Admiral Formation 'A' Sandstone in the Longtom-1/ST1 well, and the deeper and undrilled sandstones of the same formation that were not explored by Longtom-1/ST1. The Longtom structure is mapped as a three-way dip closure buttress, formed by the juxtaposition of the Emperor Sub-group sandstones and shales on the southern downthrown side against the Strzelecki Group on the northern upthrown side along a major WNW-ESE trending fault (Figure 2).

Longtom-2 was spudded at 09:00 hrs on November 10, 2004 by the Ocean Patriot rig, in 56.8 m of water. The vertical well reached a total depth of -2385.1 mTVDAHD (2422.0 mMDRT) at 15:00hrs on November 19, 2004.

In addition to the acquisition of logging-while-drilling data (Sperry-Sun LWD), the following suite of wireline logs was run:

Run 1: RCI-GR
Run 2: RCI-GR
Run 3: RCI-GR
Run 4: RCI-GR
Run 5: VSP/Checkshot Survey
Run 6: CCL-GR
Run 7: CCL-GR

All RCI runs were unsuccessful as the tool hung up and was unable to pass 1919.0 mMDRT. A second CCL was required as the gamma tool on the first run stopped functioning.

The top of the primary objective Admiral Formation was intersected at -1992.3 mTVDAHD (2019.0 mMDRT), 27.7 m low to prognosis (Figure 3). The Upper unit was subsequently labelled the 'A' Sandstone. Deeper sandstone packages ('B to F' Sandstone) were also encountered within the Admiral Formation prior to intersecting the Longtom Volcanics Member in this well. Problems were encountered whilst drilling Longtom-2, with increasing gas readings unable to be verified as the chromatograph was not functional. Gas system readings were erratic and it was found to be a calibration error. Total average gas values prior to -2295.2 mTVDAHD (2330.0 mMDRT) are not reliable as a result. Below this level, following an "on the fly" recalibration, several significant gas peaks (up to 23.6%) were recorded over a background of 5.6% to 6.5%. No hydrocarbon shows were observed within the Longtom-2 well.

A sidetrack, Longtom-2 ST1, was drilled to cut core and perform drill stem testing. A total of 36.0 m of core was cut from within the Admiral Formation, with 98.9% recovery. No gas data is available for the sidetrack and no hydrocarbon shows were observed.

Drill stem testing was carried out at two levels within the Admiral Formation. DST #1, in the Lower Admiral Formation, resulted in a final gas flow rate of

VIC/P 54

LONGTOM-2 & ST1 LOCATION MAP

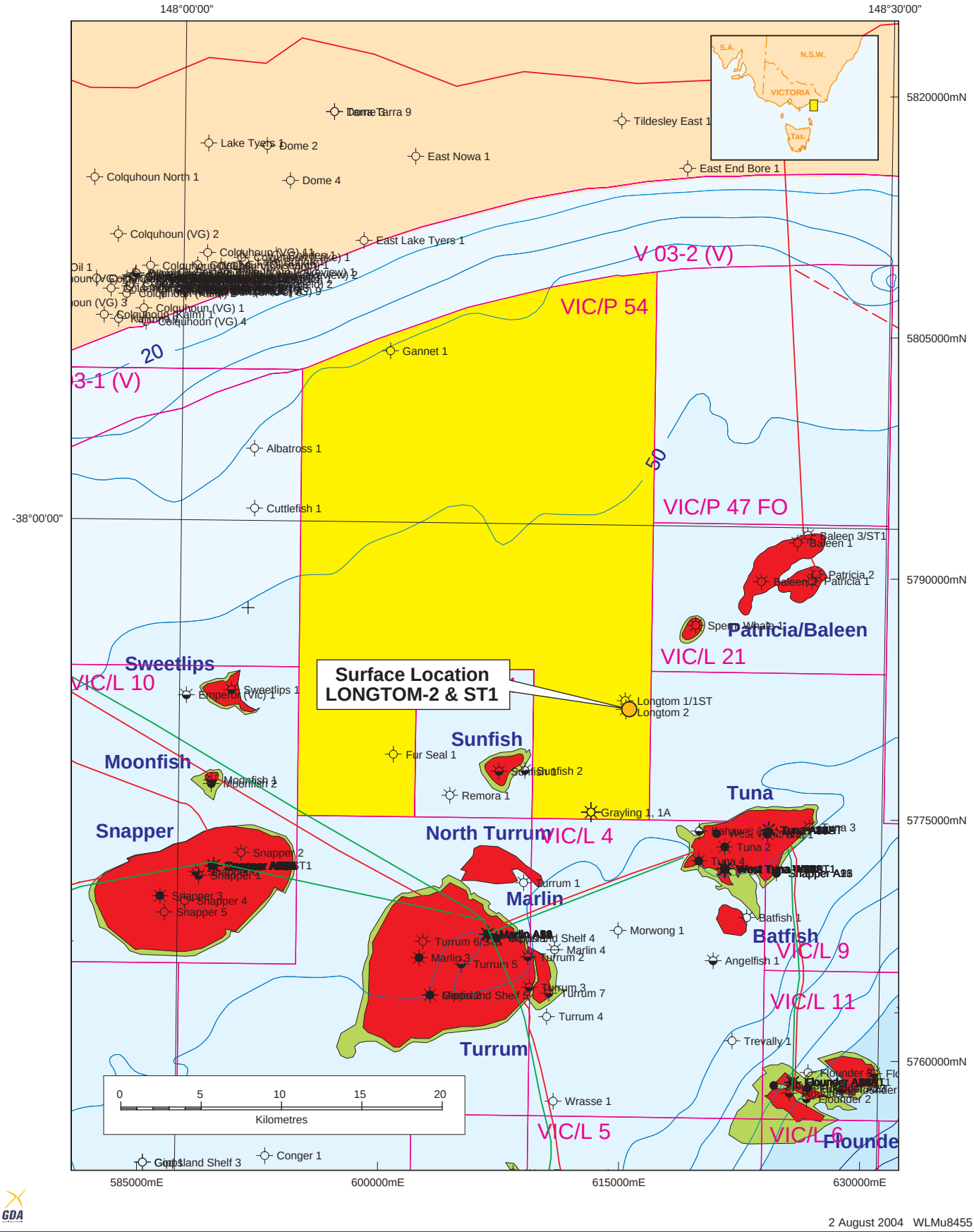

Figure 1

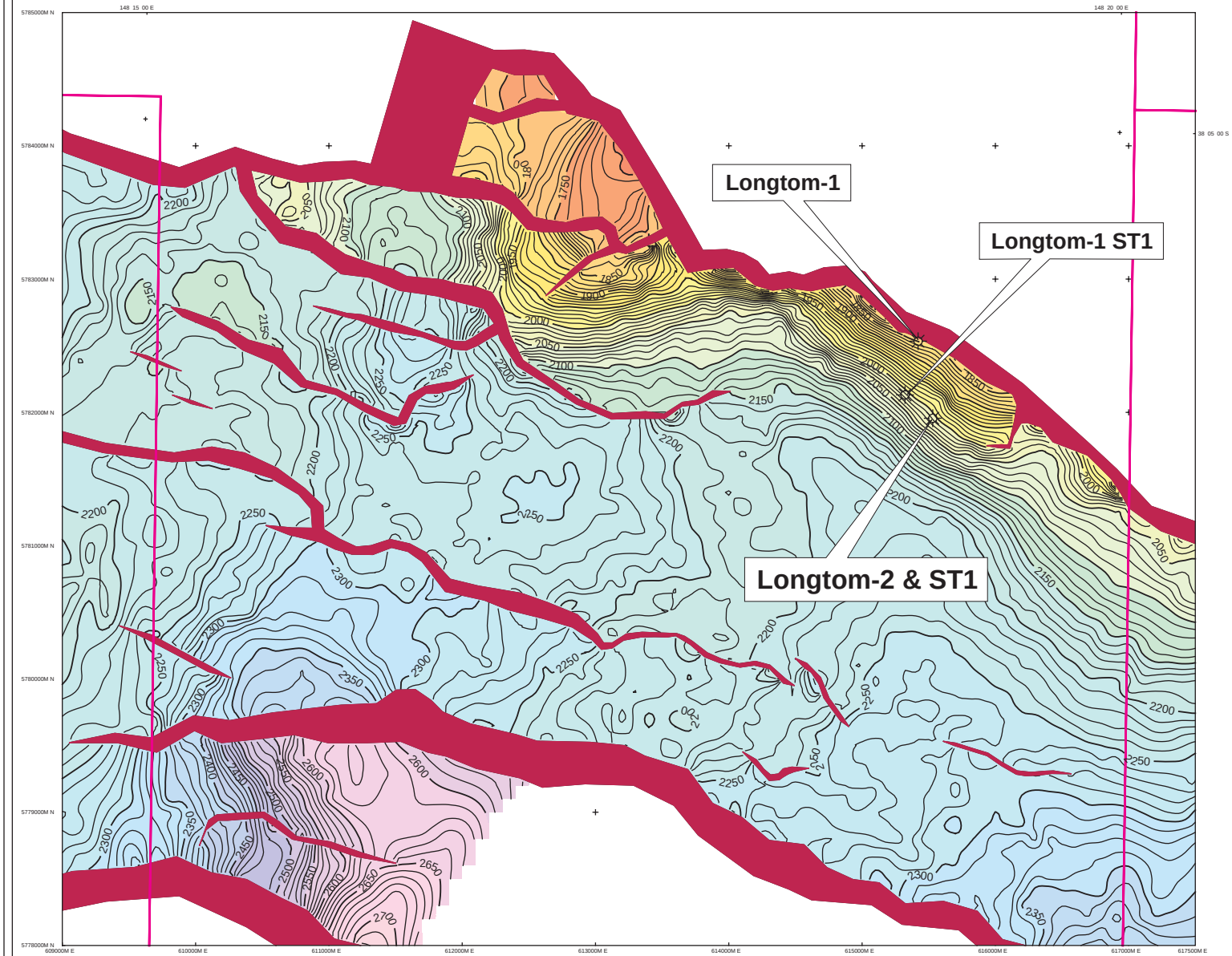
Longtom-1
Longtom-1 ST1
Longtom-2 & ST1
148 15 00 E
148 20 00 E
38 05 00 S
5785000M N
5784000M N
5783000M N
5782000M N
5781000M N
5780000M N
5779000M N
5778000M N
609000M E
610000M E
611000M E
612000M E
613000M E
614000M E
615000M E
616000M E
617000M E
617500M E
0
1
KILOMETRES
0
0.50
MILES
UNIVERSAL TRANSVERSE MERCATOR PROJECTION
G.R.S. 1980 SPHEROID
CENTRAL MERIDIAN 147 00 00 E
Mapsheet datum: "Unknown"
GDA
Apache ENERGY
VIC/P54
LONGTOM-2 & ST1
Top Admiral Fm.
Postdrill Depth Structure Map
C. I. = 10m
Author : RLK
Mapsheet : LONGTOM
Map File : /vicp54_longtom-2_091_ADML_D.map
Date : August 1, 2005
Scale :
Plan No. : RLKU9049

Figure 2

LONGTOM-2 & ST1

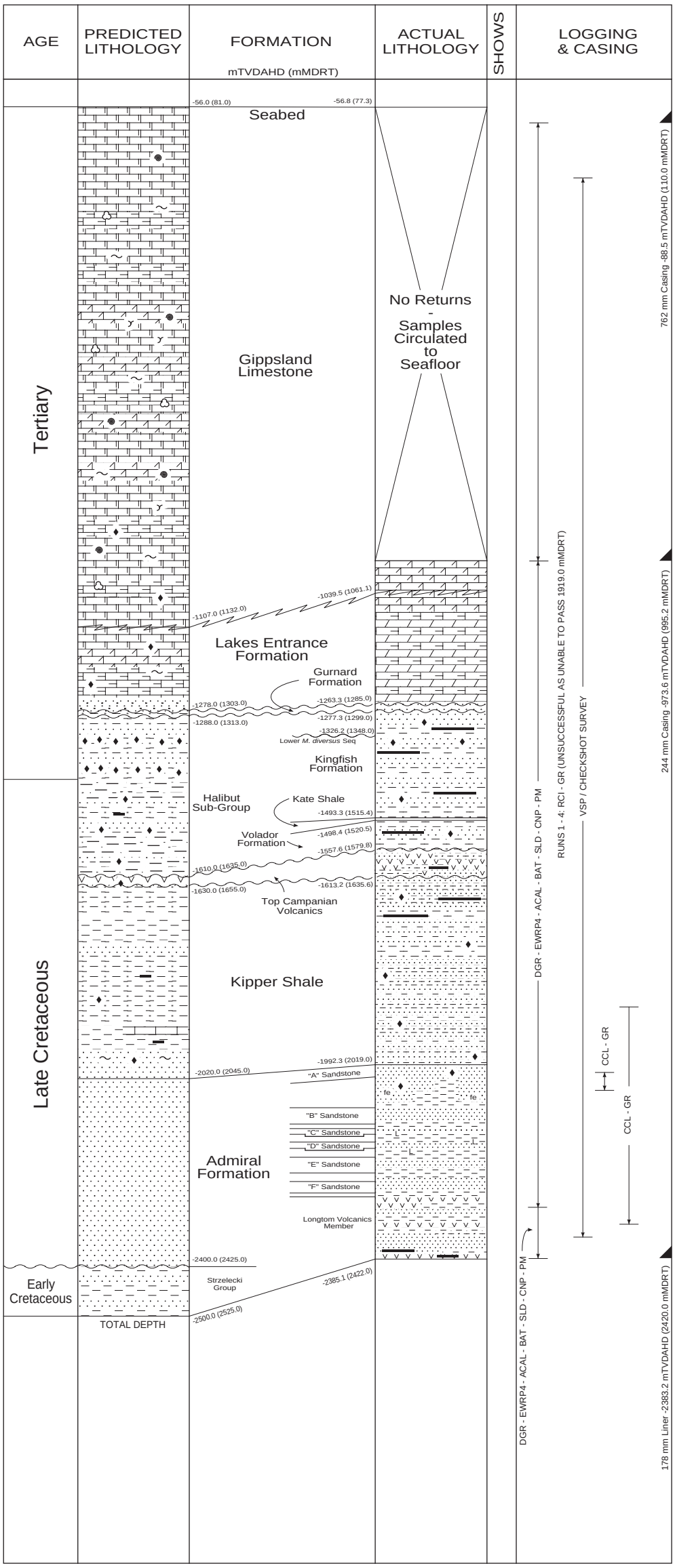

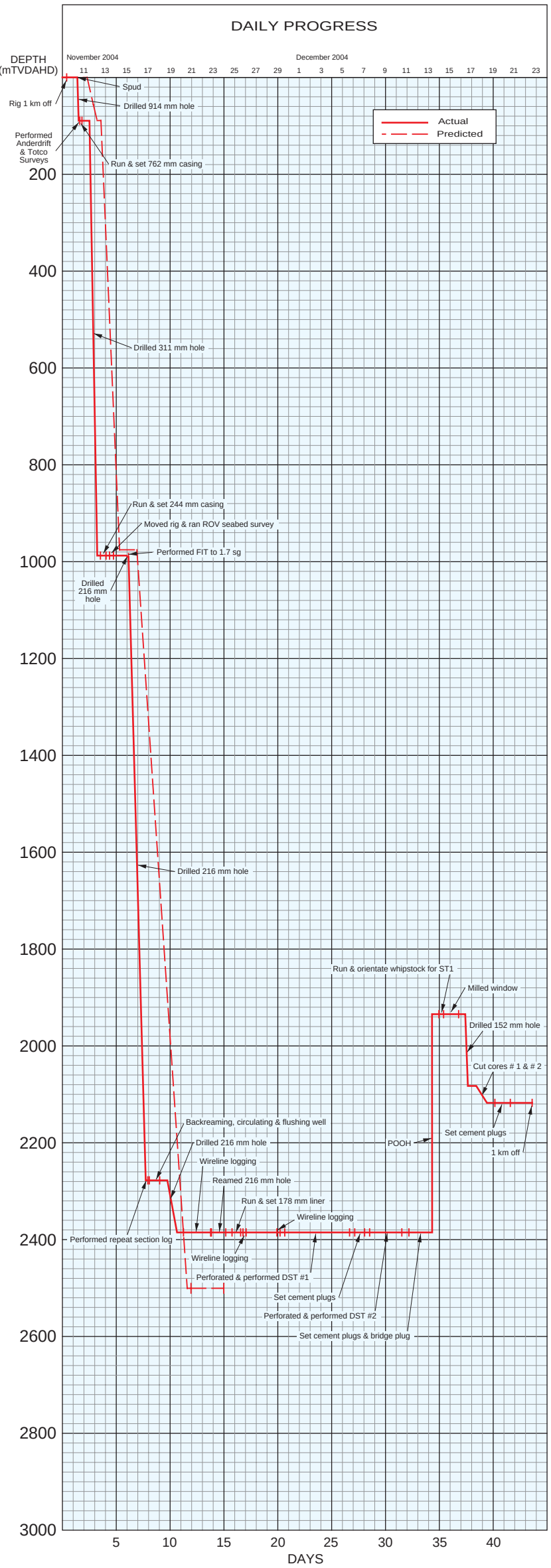

LATITUDE :	38° 06' 11.89" S	UTM:	5,781,904.33 mN
LONGITUDE :	148° 19' 00.92" E		615,462.43 mE
SEISMIC LINE :	IL 3711, XL 8925	LONGTOM-2	
ELEVATION R.T.:	21.5 m above AHD	SPUD DATE:	10 November 2004, 09:00 hrs
WATER DEPTH :	56.8 m below AHD	REACHED T.D.:	19 November 2004, 15:00 hrs
SEA BED :	78.3 m below R.T.		
STATUS :	P & A, Gas Discovery	LONGTOM-2 ST1	
RIG :	Ocean Patriot	KICKED OFF:	17 December 2004, 06:00 hrs
RIG RELEASED :	22 December 2004, 14:30 hrs	REACHED T.D.:	18 December 2004, 10:00 hrs

Apache ENERGY

VIC/P-54

GIPPSLAND BASIN

LONGTOM-2 & ST1

PREDICTED vs ACTUAL SECTION & WELL HISTORY

Author :	WCR	Date :	September 2005
Drawn :	Perth Exploration Dept.	Plan No.	ASu8944

Figure 3

19.1mmscf/d (unstabilised, at the end of the test). DST #2, in the Upper Admiral Formation, failed to flow to surface due to severe formation damage.

Petrophysical analysis has interpreted the Longtom-2 well intersected a 259.3 m gross gas column that contained 94.9 m net pay. Average porosity and calculated water saturations are 18.9% and 39.9%, respectively. No gas-water contact was evident on log analysis and the base of the sandstone unit represents a 'gas-down-to' level.

Longtom-2/ST1, a gas discovery, was plugged and abandoned and the rig was released at 14:30 hrs on December 22, 2004 when 1 km from location.

2. WELL INDEX SHEET

Well:	Longtom-2 & ST1	**Operator:**	Apache Energy Limited
Well Type:	Exploration	**Partners:**	Apache Northwest Pty Ltd
Basin:	Gippsland		Nexus Energy Vic P54 Pty Ltd
Tenement:	VIC/P-54		
Objective:	Admiral Formation sandstones		
Status:	P & A, Gas Discovery		
Spudded:	09:00 hrs 10 November, 2004	**Latitude:**	38° 06' 11.89" S
TD Reached:	15:00 hrs 19 November, 2004	**Longitude:**	148° 19' 00.92" E
Kicked Off Sidetrack:	06:00 hrs 17 December, 2004	**Northing:**	5,781,904.33 mN
TD Reached in Sidetrack	10:00 hrs 18 December, 2004	**Easting:**	615,462.43 mE
Rig Released:	14:30 hrs 22 December, 2004		
Total Depth:	mTVDAHD (mMDRT)		
Longtom-2	-2385.1 (2422.0)		
Longtom-2 ST1	-2118.1 (2148.0)		
RT Elevation:	21.5 m above AHD	**Datum:**	GDA94, Spheroid GRS80
Water Depth:	56.8 m below AHD	**Projection:**	MGA Zone 55, CM 147º E
Drill. Contr.:	Diamond Offshore	**Seis Loc:**	Northern Fields 3D
Rig (Type):	Ocean Patriot (Semi-Sub)		Inline 3711, Crossline 8925

Formations

Subgroup	**Formation/Marker**	**Tops**		
		mMDRT	**mTVDAHD**	**mTVT**
Seaspray	Gippsland Limestone (Seabed)	78.3	-56.8	982.7
	Lakes Entrance Formation	1061.1	-1039.5	223.8
Cobia	Gurnard Formation	1285.0	-1263.3	14.0
Halibut	Kingfish Formation	1299.0	-1277.3	216.0
	Lower *M. diversus* seq	1348.0	-1326.2	N/A
	Kate Shale	1515.4	-1493.3	5.1
	Volador Formation	1520.5	-1498.4	59.2
Golden Beach	Top Campanian Volcanics	1579.8	-1557.6	55.6
Emperor	Kipper Shale	1635.6	-1613.2	379.1
	Admiral A Sandstone	2019.0	-1992.3	26.6
	Base Admiral A Sandstone	2044.2	-2016.9	62.3
	Admiral B Sandstone	2108.0	-2079.2	33.0
	Base Admiral B Sandstone	2141.9	-2112.2	9.2
	Admiral C Sandstone	2151.4	-2121.4	11.5
	Base Admiral C Sandstone	2163.2	-2132.9	15.8
	Admiral D Sandstone	2179.4	-2148.7	12.7
	Base Admiral D Sandstone	2192.5	-2161.4	17.9
	Admiral E Sandstone	2210.9	-2179.3	31.7
	Base Admiral E Sandstone	2243.5	-2211.0	17.4
	Admiral F Sandstone	2261.4	-2228.4	23.2
	Base Admiral F Sandstone	2285.3	-2251.6	7.8
	Longtom Volcanics Member	2293.3	-2259.4	>125.7
	Total Depth	2422.0	-2385.1	

Well Index Sheet (cont.)

Hole and Casing Details

Hole Size (mm)	Interval (mMDRT)	Interval (mTVDAHD)	Casing Size (mm)	Depth (mMDRT)	Depth (mTVDAHD)
Longtom-2					
914	78.3 to 111.0	-56.8 to -89.5	762	110.0	-88.5
311	111.0 to 1009.0	-89.5 to -987.4	244	995.2	-973.6
216	1009.0 to 2422.0	-987.4 to -2385.1	178	2420.0	-2383.2
Longtom-2 ST1 kicked off at 1960.0 mMDRT.					
152	1960.0 to 2148.0	-1934.5 to -2118.1	No casing set in sidetrack.		

MWD/LWD Logs

Bit No.	Log Suite	Interval (mMDRT)	Max °C	Hole Size (mm)	Remarks
Longtom-2					
2	DGR-EWRP4-ACAL-BAT-PM	111.0 to 1009.0	26	311	All recorded data recovered at surface.
3	DGR-EWRP4-ACAL-BAT-SLD-CNP-PM	1009.0 to 2312.0	99	216	All recorded data recovered at surface.
4	DGR-EWRP4-ACAL-BAT-SLD-CNP-PM	2312.0 to 2422.0	90	216	POOH to run wireline logs. SDL tool failed prior to running in hole.

Wireline Logs

Suite	Run	Log Suite	Interval (mMDRT)	BHT (°C)	Remarks
Longtom-2					
1	1	RCI-GR	N/A	N/A	Hung up at 1854.0 mMDRT. POOH.
	2	RCI-GR	N/A	N/A	Unable to pass 1854.0 mMDRT. POOH.
	3	RCI-GR	N/A	N/A	Unable to pass 1815.0 mMDRT. POOH.
	4	RCI-GR	N/A	N/A	Unable to pass 1919.0 mMDRT. POOH.
	5	VSP/Checkshot Survey	2377.0 to 220.0	N/A	29 levels recorded.
	6	CCL-GR	2035.0 to 2072.0	N/A	GR stopped functioning. POOH.
	7	CCL-GR	2350.0 to 1900.0	N/A	

* Hours since circulation stopped.

Well Index Sheet (Cont.)

Cement Plugs

Plug No.	Interval (mMDRT)	Tagged
Longtom-2		
1JW	2274.0 to 2230.0	Y
1RS	2230.0 to 2172.0	Y
2a	2172.0 to 2062.0	N
2b	2062.0 to 1986.0	N
3	1980.0 to 1960.0	N
Longtom-2 ST1		
4a	2148.0 to 2078.0	Y
4b	2078.0 to 1976.0	N
4c	1976.0 to 1881.0	Y
5	907.0 to 802.0	Y
6	170.0 to 100.0	N

Testing: Drillstem testing was carried out over the following intervals:

DST #1: Lower Admiral Formation
Perforation Intervals: -2153.1 to -2161.4 mTVDAHD (2184.0 to 2192.5 mMDRT)
-2180.8 to -2211.0 mTVDAHD (2212.5 to 2243.5 mMDRT)

Results: Cumulative Gas Produced = 7.65 mmscf
Cumulative Condensate = 20.2 bbl
Avg Condensate/Gas Ratio = 2.6 bbl/mmscf
Cumulative Water Produced = 11.1 bbl
Average Water/Gas Ratio = 1.45 bbl/mmscf
Final Gas Flow Rate = 19.1 mmscf/d (unstabilised, at the end of the test)
Extrapolated Stabilised Flow = 13.6 mmscf/d at Psf=1472 psia
Wellhead AOF = 14.9 mmscf/d

DST #2: Upper Admiral Formation
Perforation Intervals: -1999.1 to -2018.2 mTVDAHD (2026.0 to 2045.5 mMDRT)
-2083.5 to -2091.8 mTVDAHD (2112.5 to 2121.0 mMDRT)
-2095.2 to -2112.7 mTVDAHD (2124.5 to 2142.5 mMDRT)

Results: No flow to surface.

Coring: Two conventional cores were cut in Longtom-2 ST1**.**

Core #1: -2082.5 to -2100.1 mTVDAHD (2112.0 to 2130.0 mMDRT)
18.0 m cut (97.8% recovery)

Core #2: -2100.1 to -2117.6 mTVDAHD (2130.0 to 2148.0 mMDRT)
18.0 m cut (100% recovery)

Comments: The surface position is 4.2 m on a bearing of 150.0º (T) from the intended Longtom-2 location.

No logs were run in Longtom-2 ST1. Depths (mTVDAHD) have been calculated based on correlation of core gamma (Longtom-2 ST1) with FEWD gamma (Longtom-2).

3. GEOLOGY

3.1 Summary of Regional Geology

The Longtom structure is located within the Rosedale Fault System on the southern edge of the Northern Terrace of the Gippsland Basin (Figure 1). The Gippsland Basin is located at the eastern end of the major Late Jurassic to Late Cretaceous rift system that formed the southern edge of the Australian continent. It developed as a series of asymmetrical grabens in response to the break-up of Australia and Antarctica during the Early Cretaceous, and separation of Australia from the Lord Howe Rise/Campbell Plateau during the Late Cretaceous.

Clastic deposition commenced during the Early Cretaceous and continued in the basin at least until the Miocene in onshore regions. The onshore western part of the basin is dominated by terrestrial pre-rift succession of the Early Cretaceous Strzelecki Group which is Albian and older in age. The eastern offshore part has a much more complete and complex sedimentary record and all of the economic hydrocarbon accumulations. The offshore portion of the basin also has a thick interval of carbonates, the Gippsland Limestone that was deposited during the Miocene.

The structural evolution of the Gippsland Basin involved extensional and compressional events. Two phases of superimposed extension associated with southeastern Australian rifting events affected the region. Extension resulted in a series of NW-SE to WNW-ESE orientated en-echelon basement-involved normal faults on both the northern and southern margins of the basin. The en-echelon, soft-linked dog-leg pattern of normal faults on both the southern and northern margins of the basin is a characteristic of basement involvement in faulting, suggesting pre-existing structural grain influencing the orientation of subsequent faults. Locally, on the basin margins, these faults accommodate large syn-depositional thickness variations.

During the Cenomanian and Turonian, sediments of the syn-rift phase were deposited in lacustrine and lake margin settings (Emperor Sub-Group). The separation of the Lord Howe Rise and the onset of the Tasman Sea opening to the east of the Gippsland Basin during the Santonian were responsible for generating a basin-wide unconformity surface referred to as the Longtom Unconformity. This unconformity separates the underlying lacustrine Emperor Sub-Group from the overlying braided fluvial, deltaic to paralic and shallow marine rocks of the Golden Beach Sub-Group. Shallow marine depositional environments within the Golden Beach Sub-Group are only recorded from the eastern part of the basin. As the Tasman Sea rifting progressed to seafloor spreading in the mid-Campanian (*T. lilliei* biozone), basaltic volcanism within the basin and on the basin flanks reached a peak, covering much of the Golden Beach coastal plain environment with basic extrusives. The unconformity at the top of the Golden Beach Sub-Group is known as the Seahorse Unconformity.

Following this volcanic episode the sediments of the Halibut Sub-Group were deposited during the late syn-rift to post-rift thermal subsidence phase of basin evolution. These were deposited in fluvial, alluvial, deltaic and paralic environments in a basin that opened out to the east onto a developing ocean. The majority of the Halibut Sub-Group was deposited in a non-marine coastal plain setting behind a generally NE-SW orientated beach-barrier complex. During the deposition of the Halibut Sub-Group syn-depositional growth was achieved via

extensional reactivation of pre-existing NW-SE to WNW-ESE faults. This faulting progressively ceased during the Paleocene to Eocene. Towards the end of the Lower Eocene the coastal plain was well established with fluvial systems feeding a strand line beach/barrier system.

Compressional tectonics began to affect the Gippsland Basin from the Early Eocene. Uplift and inversion of the central region and northern margins initiated at this stage caused erosion and generation of initially fluvially incised canyon systems. Within the eastern part of the basin several erosional monadnocks are formed within these canyon systems. In eastern parts of the basin significant amounts of erosion have resulted in a prominent unconformity surface which cuts down into the Halibut Sub-Group to the level of the Maastrichtian Volador Formation. The section underlying the Top Latrobe Unconformity in the western part of the basin is much younger than in eastern parts of the basin. Backstepping (or transgressing) of a series of barrier beach/strandline complexes from east to west occurred during the Eocene. Subsequent to this period of incision and downcutting several pulses of relative sea-level rise took place as subsidence and sedimentation rates slowed, allowing flooding/transgressive pulses to gradually push the shoreline system towards the NW. The depositional lows (eroded canyons) are flooded first preferentially as Eocene offshore marine facies, e.g. the Flounder Formation, are deposited. By the Middle Eocene the palaeo-shoreline had transgressed westwards. By the end of the Eocene the palaeo-shoreline is believed to have moved inland from Lakes Entrance. In most of the offshore areas deposition of condensed glauconitic siltstones and shales replaced deposition of coarse siliciclastics.

Northwest directed compression and transpression began in the Early Eocene and continued episodically with varying intensity through to the Pliocene. Major pulses of compression subsequent to the Early Eocene affected the basin during the Lower Oligocene, Middle Miocene and Pliocene. A series of NE to ENE trending anticlines are the result of this compression. Whilst many of the resultant compressional features are eroded and partially truncated, suggesting periods of sub-aerial exposure, several structures in the west of the basin are not eroded, suggesting they were not emergent sub-aerially.

The marine marls of the Lakes Entrance formation record the final marine transgression in the Early Oligocene. Locally, this succession onlaps onto the flanks of the earlier formed compressional features. From the Mid-Miocene onwards a thick limestone unit, the Gippsland Limestone, was deposited. Major incisions during the mid to Late Miocene are interpreted as offshore erosion/mass wasting events that may have been initiated during compressional reactivation. These incisions are infilled by prograding limestone depositional wedges, which are ultimately responsible for creating the present day shelf-slope break.

The presence of mature source rock intervals within the basin is evidenced by significant oil and gas reserves in the basin. Within the Central Deep portion of the basin coals, coaly or carbonaceous shales of the Strzelecki Group, Golden Beach and Halibut Sub-Groups have all contributed to the oil and gas pools reservoired in the basin. The most prolific source rock intervals however, are suggested to be within the lower coastal plain facies of the Golden Beach and Halibut Sub-Groups. Contributions from source rock intervals in more marine-influenced shales in the eastern parts of the basin have been noted. The regional top seal for the reservoirs in the Gippsland Basin is the Lakes Entrance Formation, however, the presence of volcanics, shales, coaly shales, coals and glauconitic shales related to marine flooding within the Golden Beach and Halibut Sub-Groups

have been proven at several intersections to provide valid top seals and cross-fault seals. Within the Latrobe Group there are several proven reservoir levels distributed throughout the entire stratigraphy. The various extensional phases of faulting and subsequent compressional events and incision, in combination with the presence of intra-formational seal units, have developed a myriad of proven trapping configurations in the basin.

3.2 Surrounding Wells

Well Name	Permit	Operator	Date Completed	TD (mRT)	Status
Tuna-2	VIC/L4	Esso Aust. Ltd.	09/12/1968	2761	P & A*, Successful gas & oil confirmation test
Turrum-1	VIC/L3	Esso Aust. Ltd.	27/06/1969	3057	P & A*, Gas Well
Sunfish-1	VIC/P1	Esso Aust. Ltd.	03/03/1974	2492	P & A*, Oil & Gas Well
Sunfish-2	VIC/P1	Esso Aust. Ltd.	14/10/1983	2647	P & A*, Oil Well
Tuna-4	VIC/L4	Esso Aust. Ltd.	31/08/1984	3321	P & A*, Oil & Gas Well
Remora-1	VIC/P1	Esso Aust. Ltd.	29/05/1987	2961	P & A*, Gas & Oil Discovery
Longtom-1	VIC/P1	BHP Petroleum	14/06/1995	2242	Abandoned Gas Well

P & A*- Plugged & Abandoned

3.3 Structure

The Longtom feature is a three-way dip-closed buttress closure formed by the juxtaposition of the Emperor Sub-group sandstones and shales on the southern downthrown side against the Strzelecki Group on the northern upthrown side, along a major WNW-ESE trending fault (Figures 2 & 4). This fault is one of several similarly oriented faults within the Rosedale Fault System that defines the northern edge of the Central Deep. Faulting along the WNW-ESE of the Rosedale Fault System commenced in the Santonian to Campanian. The structure lies along the same NE-SW anticlinal trend as Barracouta, Snapper and Sun fish to the south-west, and Sperm Whale, Patricia and Baleen to the north-east. This trend was formed in the Late to Middle Miocene in response to compressional tectonics.

3.4 Stratigraphy

The stratigraphic section penetrated in Longtom-2 is described below and summarised in Figure 5; delineation of age units is based on log correlation with nearby wells together with palynological data (Appendix 1). Detailed lithological descriptions are included in the cuttings descriptions, daily geological reports, core chip descriptions and mudlog section of the Longtom-2 & ST1 Basic Data Well Completion Report. Age, lithology and drilling data have been collated on the composite well log accompanying this report (Enclosure 1). No cuttings were recovered from spud to -987.4 mTVDAHD (1009.0 mMDRT).

Longtom-2: Northern Fields 3D tie line

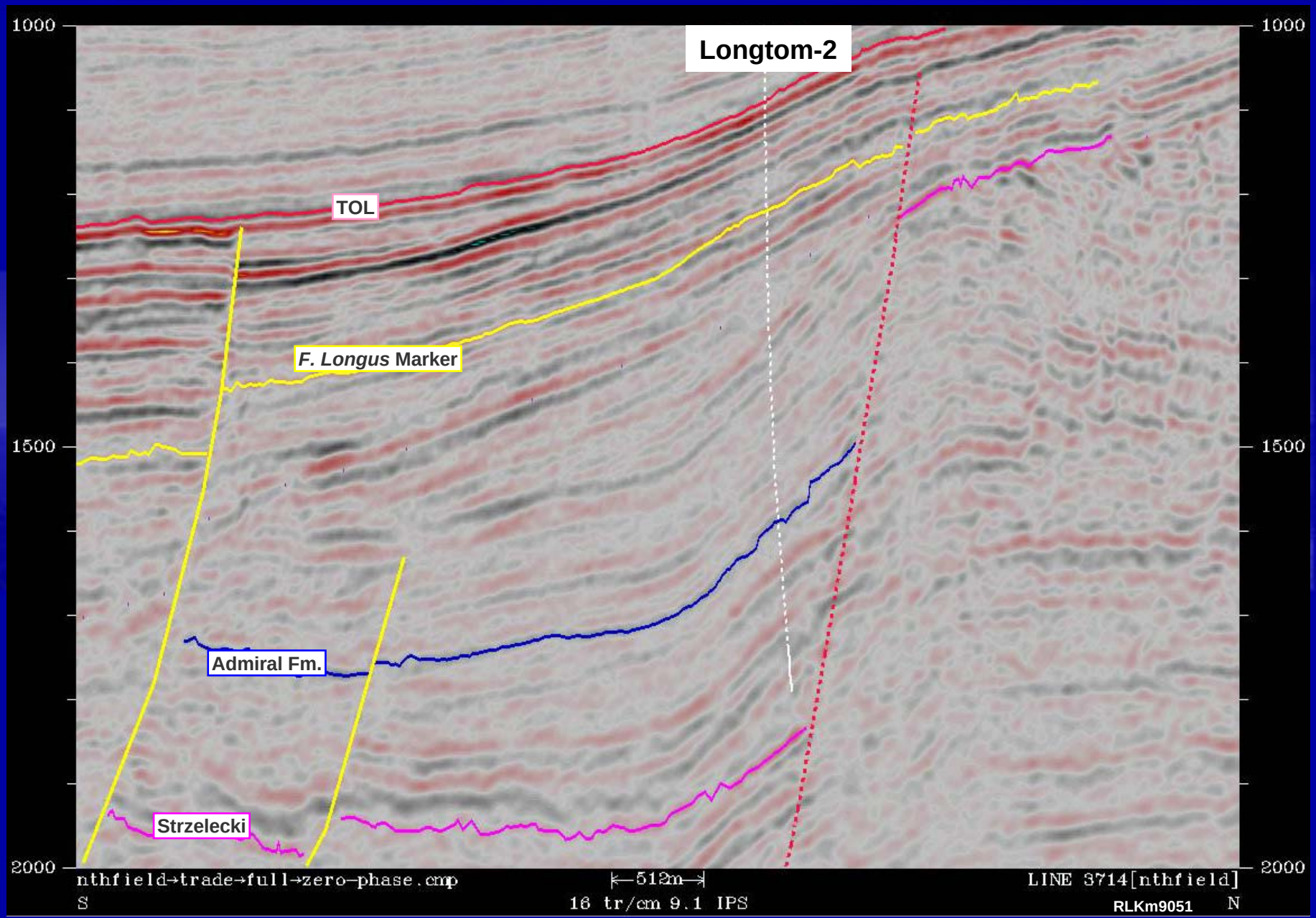

Figure 4

LONGTOM-2

STRATIGRAPHY

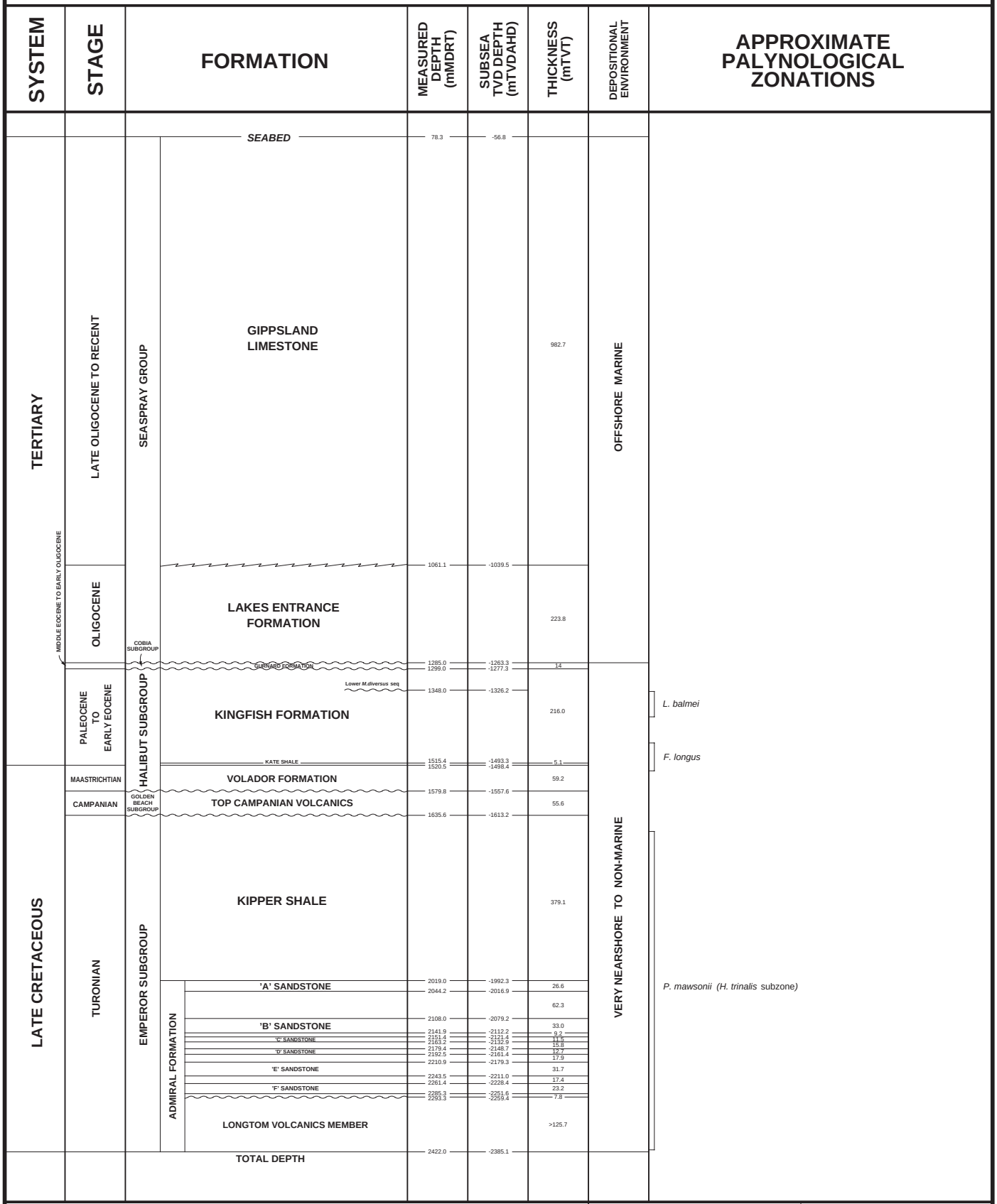

LONGTOM-2 ST1
KOP : -1934.5 mTVDAHD (1960.0 mMDRT)
TD : -2118.1 mTVDAHD (2148.0 mMDRT)

AUTHOR: WCR	DATED: September 2005
DRAWN: Perth Drafting Dept.	PLAN No. : STRu8938

Figure 5

Gippsland Limestone

Depth: -56.8 (Seabed) to -1309.5 mTVDAHD (78.3 to 1061.1 mMDRT)
Thickness: 982.7 mTVT
Age: Late Oligocene to Recent

The Gippsland Limestone sediments were not sampled above -987.5 mTVDAHD (1009.0 mMDRT) as returns were circulated to the seafloor. Below this level the lithology consists of predominantly calcisiltite, with minor silty marl seen below -1008.4 mTVDAHD (1030.0 mMDRT). Regionally, the Gippsland Limestone is interpreted to have been deposited in an offshore marine environment.

Lakes Entrance Formation

Depth: -1039.5 to -1263.3 mTVDAHD (1061.1 to 1285.0 mMDRT)
Thickness: 223.8 mTVT
Age: Oligocene

The Lakes Entrance Formation lies disconformably below the Gippsland Limestone and has been interpreted from LWD logs by correlation with offset well data. The lithology comprises interbedded calcarenite and argillaceous calcisiltite, which grades to silty marl in part. Regionally, the Lakes Entrance Formation is interpreted to have been deposited in an offshore marine environment.

Gurnard Formation

Depth: -1263.3 to -1277.3 mTVDAHD (1285.0 to 1299.0 mMDRT)
Thickness: 14.0 mTVT
Age: Early Oligocene to Middle Eocene

The Gurnard Formation lies unconformably below the Lakes Entrance Formation. It is interpreted from LWD logs by an increase in gamma ray, compressional sonic and neutron porosity logs which correspond to a minimum resistivity reading and a decrease in ROP. The lithology comprises interbedded sandstone and argillaceous calcisiltite, with minor calcarenite. The sandstone has very fine to very coarse-sized quartz grains that are angular to sub-rounded and moderately sorted. Other components include trace silica and pyrite cement, common argillaceous matrix and trace nodular pyrite. Inferred porosity is poor to fair and no hydrocarbon shows were observed.

Regionally, the Gurnard Formation is interpreted to be Middle Eocene to Early Oligocene in age, spanning the Upper to Lower *N. asperus* biozones, deposited in a shallow to open, offshore marine environment.

Kingfish Formation

Depth: -1277.3 to -1493.3 mTVDAHD (1299.0 to 1515.4 mMDRT)
Thickness: 216.0 mTVT
Age: Early Eocene to Middle Paleocene

The Kingfish Formation lies unconformably below the Gurnard Formation and is interpreted from LWD logs by a marked decrease in gamma ray response and

resistivity. The lithology comprises interbedded sandstone, silty claystone and coal seams. The sandstone (up to 90% of the lithology) is similar to that seen in the Gurnard Formation above. Poor to fair inferred porosity is noted and no hydrocarbon shows were observed.

Regionally, these sediments are interpreted to be Early Eocene to Middle Paleocene in age, spanning the *P. asperopolus, M. diversus* and *L. balmei* biozones. The Lower *M. diversus* sequence boundary has been interpreted from LWD logs in Longtom-2 at -1326.2 mTVDAHD (1348.0 mMDRT). Deposition is interpreted to have been in a non-marine to marginal marine environment.

Kate Shale

Depth: -1493.3 to -1498.4 mTVDAHD (1515.4 to 1520.5 mMDRT)
Thickness: 5.1 mTVT
Age: Maastrichtian

The Kate Shale lies conformably below the Kingfish Formation and is interpreted from LWD logs by an increase in gamma ray and resistivity values. The lithology comprises interbedded sandstone (up to 60%), silty claystone and coal seams. The sandstone is quartzose with dominantly medium-sized, sub-rounded to rounded grains that are moderately well sorted. Fair to good inferred porosity is noted but no hydrocarbon shows were observed.

Palynological analysis (Appendix 1) has interpreted these sediments to be Maastrichtian in age, deposited within the *F. longus* biozone, in a non-marine environment.

Volador Formation

Depth: -1498.4 to -1557.6 mTVDAHD (1520.5 to 1579.8 mMDRT)
Thickness: 59.2 mTVT
Age: Maastrichtian

The Volador Formation lies conformably below the Kate Shale and is interpreted from LWD logs by an increase in gamma ray and resistivity. The lithology comprises interbedded sandstone, silty claystone and coal seams (up to 80%). The sandstone is similar to that seen in the Kate Shale section above. No hydrocarbon shows were observed.

Palynological analysis has interpreted these sediments to be Maastrichtian in age, deposited within the *F. longus* biozone, in a non-marine environment.

Top Campanian Volcanics

Depth: -1557.6 to -1613.2 mTVDAHD (1579.8 to 1635.6 mMDRT)
Thickness: 55.6 mTVT
Age: Campanian

The Top Campanian Volcanics lie unconformably below the Volador Formation and are interpreted from LWD logs by a sharp decrease in gamma ray and resistivity. The lithology comprises interbedded weathered volcanics, sandstone

and silty claystone. Minor coal seams are present. The volcanics are white to greenish grey with 10 to 20% silt, aggregates of feldspar lathes (some show signs of alteration) and minor amounts of chlorite and pyrite. The sandstone is dominantly medium-sized grains that are sub-angular to sub-rounded and moderately sorted. Common argillaceous matrix is present as well as minor amounts of pyrite. Poor inferred porosity is noted and no hydrocarbon shows were observed.

No palynological analysis has been carried out on samples from this formation. Regionally, there is some variation in weathering of these volcanics and the clay content is directly correlated to this.

Kipper Shale

Depth: -1613.2 to -1992.3 mTVDAHD (1635.6 to 2019.0 mMDRT)
Thickness: 379.1 mTVT
Age: Turonian

The Kipper Shale lies unconformably below the Top Campanian Volcanics and has been interpreted from LWD logs by a marked increase in gamma ray response and a bulk shift in resistivity. The lithology comprises predominantly silty claystone with minor interbedded sandstone. The sandstone is grains that are dominantly fine-sized, sub-angular to sub-rounded and moderately sorted. Minor amounts of argillaceous matrix and calcite and siliceous cements were seen. Good inferred porosity was noted although no hydrocarbon shows were observed.

Palynological analysis has interpreted these sediments to be Turonian in age, deposited within the *P. mawsonii* biozones (*H. trinalis* subzone). Deposition is interpreted to have been in a non-marine to very nearshore marine environment. Traditionally the depositional environment of the Kipper Shale is interpreted as lacustrine, deposited within a lake basin of fluctuating water depth.

Admiral Formation

Depth: -1992.3 to -2259.4 mTVDAHD (2019.0 to 2293.3 mMDRT)
Thickness: 267.1 mTVT
Age: Turonian

The Admiral Formation lies conformably below the Kipper Shale and has been interpreted from LWD logs by a decrease in gamma ray response and an increase in resistivity. This corresponds to a decrease in both neutron porosity and compressional sonic. The lithology comprises interbedded sandstones and claystones with minor silty sandstone. Volcanoclastic content is described as increasing with depth.

Within the Admiral Formation the sandstones have been grouped into subdivisions, identified as ‘A’ to ‘F’ Sands (Figure 6). The sandstones all comprise very fine to fine-grained, angular to sub-angular, well sorted grains. Subordinate grains include red and black lithic grains, as well as minor argillaceous matrix. Poor inferred porosity is noted and no fluorescence was observed.

The ‘A’ Sand, intersected at -1992.3 mTVDAHD (2019.0 mMDRT), is a 26.6 m thick package of interbedded sandstone and claystone which correlates to the

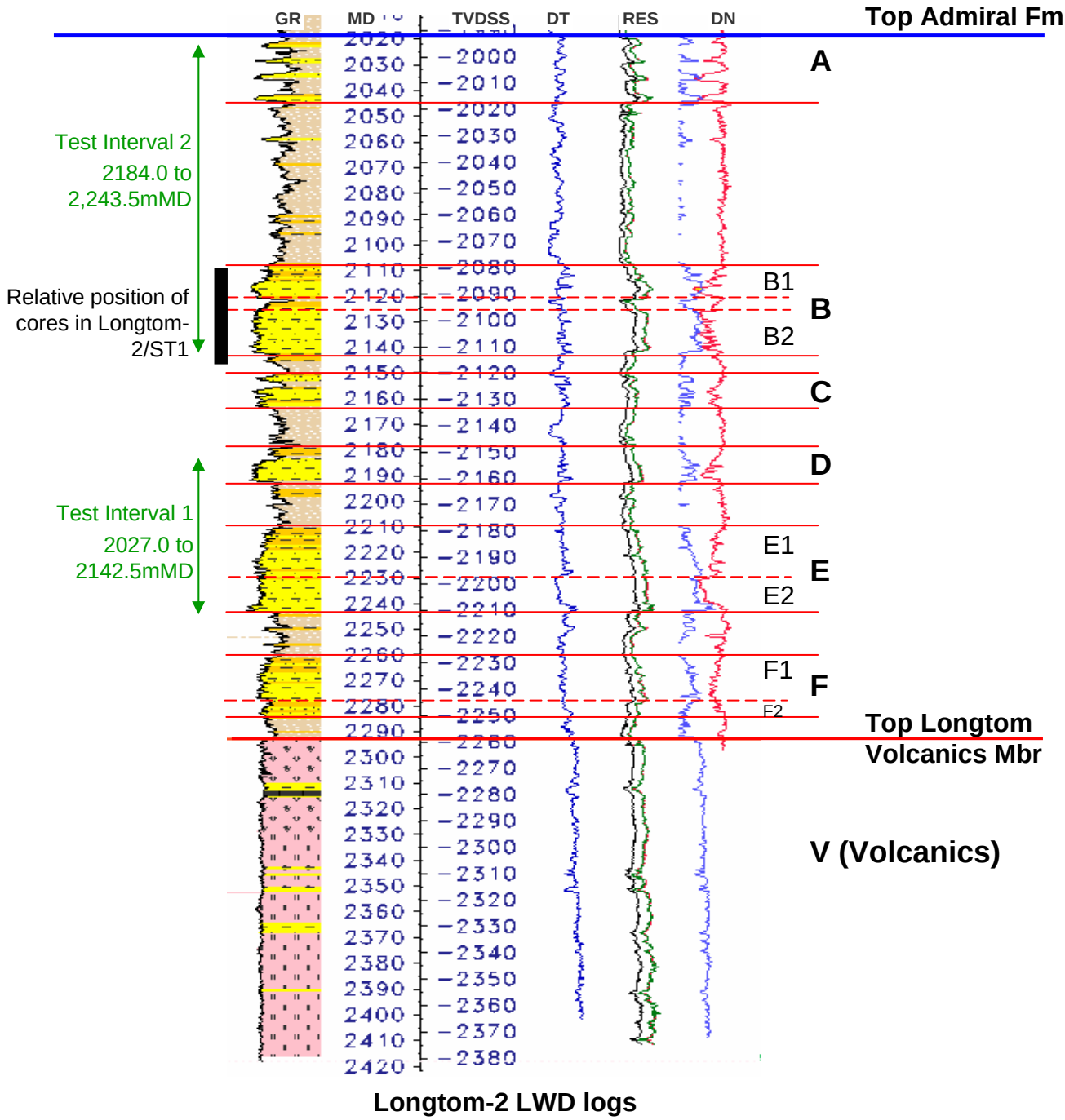

Figure 6. Longtom-2 Admiral Formation sandstone nomenclature and sub-division and relative positions of the two test zones and cores in Longtom-2/ST1.

Admiral Formation section drilled in Longtom-1/ST1 (based on the presence of the *C. parva* alga acme in both wells) (Figure 7).

The 'B' Sandstone was cored after failure of this sandstone and the overlying 'A' Sandstone to flow in DST2. Thirty six metres of core was cut in Longtom-2 ST1 with 35.6 m recovered. The lithology, from core chip samples, is predominantly lithic sandstone which contains quartz, vari-coloured lithic grains, common feldspar and weathered feldspar grains, trace chloritised grains, trace mica, common argillaceous matrix and minor siliceous cement. The sandstones range from very fine to medium in grain size. Minor coaly siltstone, claystone and argillaceous siltstone was seen. Routine core analysis (Appendix 2) has determined an average porosity, permeability and grain density to be 16.6%, 14.8 mD and 2.681 g/cc, respectively, although stress-release fracturing may have raised these. Eleven core plug samples were sent for special core analysis and results can be found in Appendix 3. Thin section analysis shows sandstones from the core comprised mostly feldspathic litharenites or litharenites composed of quartz, very common volcanic rock fragments, common plagioclase and alkali feldspar, clay-replaced grains, sandstone rock fragments, other lithics and localised carbonaceous fragments.

Total clay within the sandstones ranges from 15 to 23%, dominated by chlorite and kaolinite, with common illite/mica and rare mixed-layer illite and smectite. Roughly 50 to 70% of the clay is present as structural clay in the form of clay-replaced grains. Authigenic chlorite and kaolinite present as cements account for the rest of the clays. Other cements include common to abundant ferroan calcite, quartz overgrowths and pyrite. The potential for formation damage within such a formation is viewed as high and includes possible capillary water-block, ferric hydroxide precipitations, fines migration and sand production.

Palynological analysis has interpreted these sediments to be Turonian in age, deposited within the *P. mawsonii* biozone (*H. trinalis* sub-zone). The sandstones are interpreted to be fluvial in nature, mainly braided fluvial but with some evidence of meandering fluvial channels. Such fluvial channels may be located within a channel belt of less than 700 m wide and disconnected based on observations from sandstone bed thickness, channel depth and channel belt width. The intervening shales are interpreted as lacustrine in nature. The sharp-based nature of the two cored sandstone packages (B1 and B2) is testament to rapidity of drops in base-level in the lake basin.

<u>Longtom Volcanics Member</u>

Depth: -2259.4 to -2385.1 mTVDAHD (2293.3 to 2422.0 mMDRT)
Thickness: >125.7 mTVT
Age: Turonian

Below the 'A' to 'F' Sandstones and intervening claystones is a succession of volcanoclastics, sandy siltstones and claystone and is here called the Longtom Volcanics Member. The nature of the contact between the volcanics and the overlying sandstones and claystones is not clear, although probably represents a short duration unconformity. No hydrocarbon shows were observed although several significant gas peaks were recorded in this interval (Section 3.5).

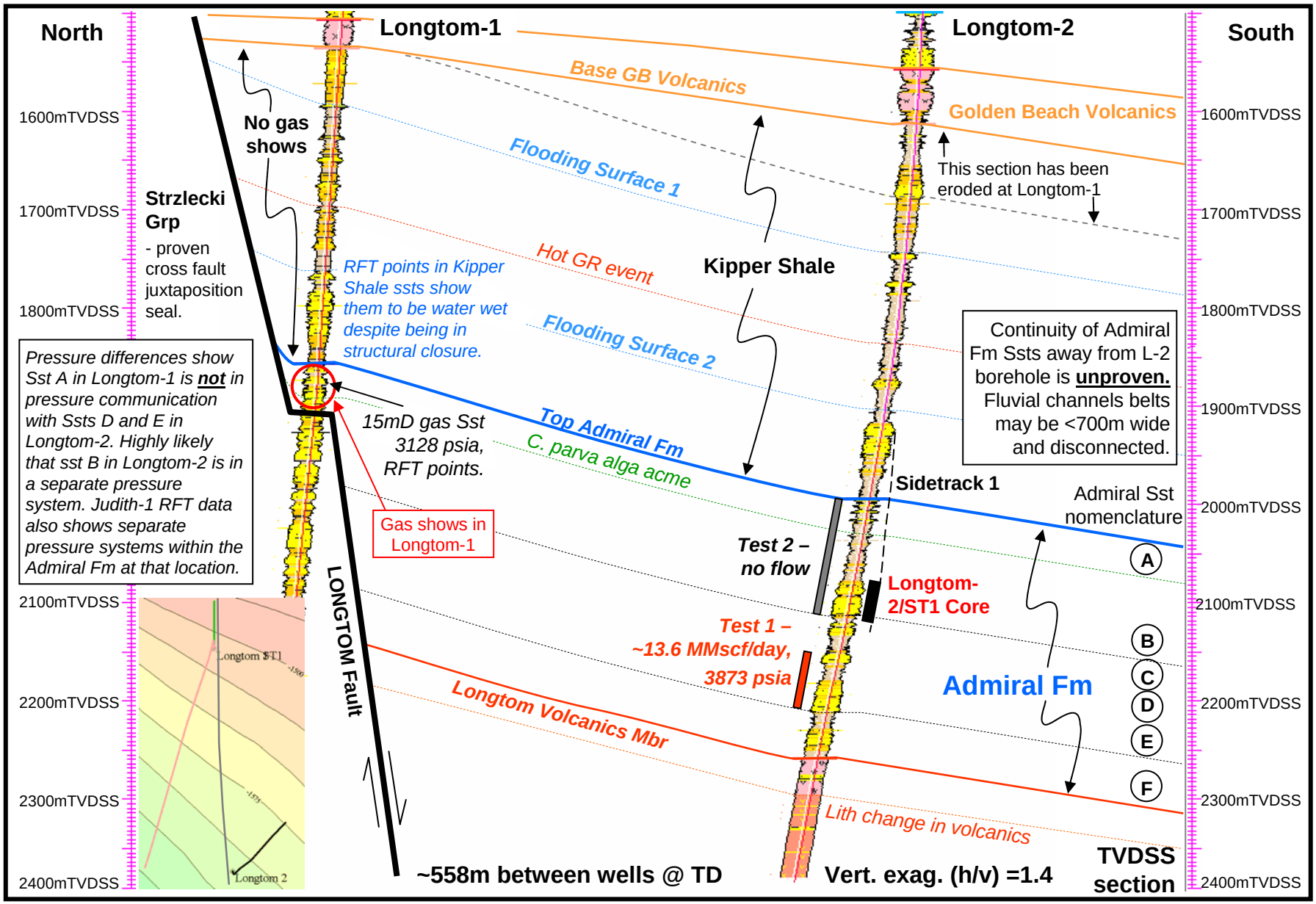

Figure 7. Longtom structural cross section, showing approximate location of the test intervals and Longtom-2/ST1 core relative to the Longtom-1 well. Sandstone A in Longtom-2 correlates to the Admiral Fm section drilled in Longtom-1/ST1 based on the presence of the *C. parva* alga acme. Note: erosion of Top Kipper Shale at the base of the Golden Beach Volcanics.

Palynological analysis has interpreted these sediments to be Turonian in age, deposited within the *P. mawsonii* biozone (*H. trinalis* sub-zone). The depositional environment is uncertain.

This volcanics unit has not been penetrated in the basin before and is a new subdivision of the Emperor Sub-group.

3.5 Hydrocarbon Occurrences

No gas-water contact was intersected in the well, however from post-well seismic inversion and fluid index studies gas-water contacts are definable for the 'B' and 'E' sandstones of the Admiral Formation and these contacts correspond to buttress structural closure against the fault to the north.

No hydrocarbon shows were observed in cuttings samples throughout Longtom-2 or the sidetrack, Longtom-2 ST1.

Several attempts were made to run a formation evaluation tool (RCI) but were unsuccessful due to the tool becoming hung up (greatest depth reached was -1894.2 mTVDAHD (1919.0 mMDRT)).

Longtom-2 drilled through new section of the Admiral Formation. The correlation of the Longtom-1 and Longtom-2 is shown in Figure 7. Petrophysical analysis (Appendix 4) has interpreted the Longtom-2 well intersected a 259.3 m gross gas column that contained 94.9 m net pay. Average porosity and calculated water saturations are 18.9% and 39.9%, respectively. No gas-water contact was evident on log analysis and the base of the sandstone unit represents a 'gas-down-to' level.

Drill stem testing was carried out at two levels within the Admiral Formation. DST #1, in the Lower Admiral Formation, resulted in a final gas flow rate of 19.1mmscf/d (unstabilised, at the end of the test). DST #2, in the Upper Admiral Formation, failed to flow to surface due to severe formation damage. As noted in section 3.4 the formation has high potential for formation damage.

Vitrinite reflectance values obtained from shales within the Admiral Formation indicate that the rocks are in the middle of the main oil generation window (0.73 to 0.81) (Appendix 5). There is no marked change in vitrinite levels at the contact between the sandstones and the Longtom Volcanics Member possibly indicating this boundary is not a major unconformity. Total organic carbon (TOC) ranged from 0.22 to 1.5%. With Hydrogen Index values ranging from 89 to 129 the section is deemed to only have potential for gas generation.

3.6 Contributions to Geological Knowledge and Conclusions

Longtom-2 was designed as an exploration well to appraise the gas column encountered within the Admiral Formation 'A' Sandstone in the Longtom-1/ST1

well, and the deeper and undrilled sandstones of the same formation that were not explored by Longtom-1/ST1.

The well intersected a 259.3 m gross gas column (94.9 m net pay) within the Admiral Formation with gas-down-to -2251.6 mTVDAHD (2285.3 mMDRT). This corresponds to the base of the 'F' Sandstone.

The Admiral Formation Sandstones were seen to be fluvial in origin, deposited within a lacustrine basin. The sandstones vary from feldspathic litharenites to litharenites. The Longtom Volcanics Member has not been penetrated before in any wells in the basin and Longtom-2 provided the first evidence of such a volcanic unit in either the Admiral Formation or the Emperor Sub-group.

The well identified the presence of a 259.3 m gross gas column with a gas-down-to contact. DST #1 in Longtom-2 is the first time hydrocarbons have been flowed to surface in the Gippsland Basin from the Emperor Sub-group and its subdivisions after 20 plus well penetrations in the basin.

Longtom-2/ST1, a gas discovery, was plugged and abandoned and the rig was released at 14:30 hrs on December 22, 2004 when 1 km from location.

APPENDIX 1

Palynology Report

PALYNOLOGY OF

LONGTOM-2

GIPPSLAND BASIN, AUSTRALIA

by

ROGER MORGAN

Prepared for
APACHE ENERGY **March 2005**

REF: GIP.LONGTOM-2 REPORT

PALYNOLOGY OF

LONGTOM-2

GIPPSLAND BASIN, AUSTRALIA

CONTENTS **PAGE**

1 SUMMARY

1350 m (cutts) – 1420 m (cutts) : *L. balmei* Zone : Paleocene : marginal marine : immature

1490 m (cutts) – 1530 m (cutts) : *F. longus* Zone, upper subzone : Maastrichtian : non-marine : immature

1660 m (cutts) – 2420 m (cutts) : *P. mawsonii* Zone, *H. trinalis* subzone : Turonian : very nearshore marine to non-marine (marginal marine, brackish, swamp margin, floodplain) : marginally to early to mature

2 INTRODUCTION

This data set comprise 19 samples studied on an urgent basis in a temporary laboratory in Sale, onshore eastern Victoria, and 25 followup samples processed by CORELABS in Perth and studied in Maitland, South Australia. The work was requested and supervised by Steve Moss of Apache Energy.

The overall zonation framework of Helby, Morgan and Partridge (1987) is shown in Figure 1. Sub-zonation and extra correlative events within the formal zones and subzones for the Gippsland Basin are under development.

The *P. mawsonii* Zone has also been restudied recently, particularly in the Otway Basin where Morgan (1992) and Partridge (1998) have introduced new subzones. Usuage in the Gippsland Basin was recently reviewed (Morgan 2004a, b) incorporating the work of Alan Partridge with possible refinements and some tentative microplankton subzones suggested using the mostly algal assemblages, as in Figure 2 herein. These algae were described by Marshall (1989). These tentative subzones are currently being tested. Further possible correlative events and subzones for the local Longtom area were also suggested in Morgan (2004b) using the data of Partridge (1995) as in Figure 3 but the data herein does not support correlation at this level.

All depths are given in metres and are recorded drillers depths. No corrections or conversions have been applied as some (such as core corrections), involve assumptions and interpretations.

Palaeoenvironmental assessments are based on specimen counts of 100 specimens, also providing a percentage content of all species. Criterea for the palaeo-environmental subdivisions are given on Table 1. In running text, rare = <1-3%, frequent = 4-10%, common = 11-30%, abundant = 31-50% and superabundant = 51-100%. Where dinoflagellates are present, marine environments are assigned as in the box on Table 1, although the assemblages are very low diversity and might reflect lowered salinity. Where only spiny acritarchs are present, brackish environments are assigned as in the box on Table 1. *Amosopollis cruciformis* is considered a spiny acritarch for this purpose, although in the past it has sometimes been considered a freshwater alga. The raw data for the environmental interpretations are shown in Table 2

Confidence ratings include the factor of sample type, and distinctiveness of the fossil event, according to the scheme shown on Figure 3 (Figure 3 shows key datum and suggested zones for Longtom-1). This is the STRATDAT scheme used by Esso.

TABLE 1

SUMMARY OF PALYNOLOGICAL DATA :LONGTOM-2

DEPTH (m)	SAMPLE TYPE	MICROFOSSIL YIELD	PERCENTAGE				DIVERSITY *1		SPORE-POLLEN ZONE	CR *2	MICROPLANKTON ZONE	CR *2	ENVIRONMENT *3
			MICROPLANKTON			SPORE-POLLEN-	SALINE MICROPLANKTON	SPORE-POLLEN					
			DINOFLAG	SPINY AC.	FRESH ALGAE								
1350	CUTTS	EX LOW	(15)	0	2	83	LOW	MODERATE	L. BALMEI	D2			?NON-MARINE
1420	CUTTS	LOW	(1)	0	2	97	LOW	MODERATE	L. BALMEI	D2			?NON-MARINE
1490	CUTTS	LOW	(2)	1	5	92	LOW	HIGH	F. LONGUS, UPPER	D3			?NON-MARINE
1530	CUTTS	LOW	0	0	3	97	NIL	HIGH	F. LONGUS, UPPER	D3			NON-MARINE
1660	CUTTS	EX LOW	0	0	5	95	EX LOW	MODERATE	P. MAWSONII, H. TRINALIS	D2			NON-MARINE
1760	CUTTS	LOW	5	0	24	71	EX LOW	MODERATE	P. MAWSONII, H. TRINALIS	D2			MARGINAL MARINE
1790	CUTTS	MODERATE	2	2	8	88	EX LOW	HIGH	P. MAWSONII, H. TRINALIS	D2			MARGINAL MARINE
1820	CUTTS	MODERATE	0	0	6	94	EX LOW	MODERATE	P. MAWSONII, H. TRINALIS	D2			NON-MARINE
1860	CUTTS	MODERATE	<1	3	8	89	EX LOW	HIGH	P. MAWSONII, H. TRINALIS	D2			MARGINAL AMRINE
1920	CUTTS	MODERATE	11	1	0	88	EX LOW	HIGH	P. MAWSONII, H. TRINALIS	D2			NEARSHORE MARINE
1940	CUTTS	MODERATE	<1	1	1	98	EX LOW	HIGH	P. MAWSONII, H. TIRNALIS	D2			MARGINAL AMRINE
2005	CUTTS	LOW	0	0	1	99	NIL	MODERATE	P. MAWSONII, H. TRINALIS	D2			NON-MARINE
2045	CUTTS	MODERATE	(1)	2	8	89	EX LOW	MODERATE	P. MAWSONII, H. TRINALIS	D2			BRACKISH MARINE
2055	CUTTS	MODERATE	0	0	6	94	EX LOW	MODERATE	P. MAWSONII, H. TRINALIS	D2			NON-MARINE
2080	CUTTS	MODERATE	0	0	8	92	EX LOW	HIGH	P. MAWSONII, H. TRINALIS	D2			NON-MARINE
2100	CUTTS	MODERATE	1	0	1	98	EX LOW	HIGH	P. MAWSONII, H. TRINALIS	D2			MARGINAL MARINE
2112.43	CORE	LOW	0	0	4	96	NIL	MODERATE	P. MAWSONII	D5			BRACKISH
2112.70	CORE	EX LOW	0	0	0	100	NIL	MODERATE	INDETERMINATE				NON-MARINE
2113.0	CORE	MODERATE	0	0	2	98	NIL	HIGH	P. MAWSONII, H. TRINALIS	D5			NON-MARINE
2123.0	CORE	MODERATE	<1	1	5	94	EX LOW	HIGH	P. MAWSONII, H. TRINALIS	D2			MARGINAL MARINE
2123.5	CORE	MODERATE	<1	3	5	92	EX LOW	HIGH	P. MAWSONII, H. TRINALIS	D2			MARGINAL MARINE
2124.5	CORE	LOW	0	1	1	98	EX LOW	HIGH	P. MAWSONII, H. TRINALIS	D2			BRACKISH MARINE
2144.61	CORE	LOW	0	0	4	96	NIL	MODERATE	P. MAWSONII	D5			NON-MARINE
2146.0	CORE	LOW	0	0	2	98	NIL	HIGH	P. MAWSONII, H. TRINALIS	D2			NON-MARINE
2146.61	CORE	MODERATE	0	0	4	96	NIL	HIGH	P. MAWSONII	D5			NON-MARINE
2147.0	CORE	MODERATE	0	0	5	95	NIL	HIGH	P. MAWSONII	D5			NON-MARINE
2148.0	CORE	MODERATE	0	0	5	95	NIL	HIGH	P. MAWSONII, H. TRINALIS	D2			NON-MARINE
2150	CUTTS	MODERATE	0	0	5	95	NIL	HIGH	P. MAWSONII, H. TRINALIS	D2			NON-MARINE
2160	CUTTS	MODERATE	0	0	5	95	NIL	HIGH	P. MAWSONII	D5			NON-MARINE
2180	CUTTS	MODERATE	<1	0	3	97	EX LOW	HIGH	P. MAWSONII, H. TRINALIS	D2			MARGINAL MARINE
2195	CUTTS	MODERATE	0	1	0	99	EX LOW	HIGH	P. MAWSONII	D5			BRACKISH
2200	CUTTS	MODERAE	5	1	3	91	EX LOW	HIGH	P. MAWSONII, H. TRINALIS	D2			MARGINAL MARINE
2205	CUTTS	MODERATE	0	0	6	94	EX LOW	HIGH	P. MAWSONII, H. TRINALIS	D2			NON-MARINE
2245	CUTTS	MODERATE	1	0	3	96	EX LOW	HIGH	P. MAWSONII, H. TRINALIS	D2			MARGINAL MARINE
2255	CUTTS	MODERATE	2	0	1	97	EX LOW	HIGH	P. MAWSONII, H. TRINALIS	D2			MARGINAL MARINE
2260	CUTTS	MODERATE	1	0	3	96	EX LOW	HIGH	P. MAWSONII, H. TRINALIS	D2			MARGINAL MARINE
2290	CUTTS	MODERATE	1	0	3	96	EX LOW	HIGH	P. MAWSONII, H. TRINALIS	D2			MARGINAL MARINE
2345	CUTTS	EX LOW	-	-	-	-	-	-	-	-			-
2360	CUTTS	EX LOW	(2)	0	<1	98	CAVED	MODERATE	P. MAWSONII, H. TRINALIS	D2			NON-MARINE
2370	CUTTS	MODERATE	1	0	0	99	EX LOW	HIGH	P. MAWSONII	D5			MARGINAL MARINE

2390	CUTTS	EX LEAN	-	-	-	-	-	-	-	-			-
2400	CUTTS	LEAN	0	0	4	96	EX LOW	HIGH	P. MAWSONII, H. TRINALIS	D2			NON-MARINE
2410	CUTTS	EX LEAN	-	-	-	-	-	-	-	-			-
2420	CUTTS	MODERATE	1	<1	5	94	EX LOW	HIGH	P. MAWSONII, H. TRINALIS	D2			MARGINAL MARINE

***1 DIVERSITY**	
V HIGH	30+ SPECIES
HIGH	20-29 SPECIES
MOD	10-19 SPECIES
LOW	5-9 SPECIES
EX LOW	1-4 SPECIES

***2 CONFIDENCE RATINGS**	
A = Core	1 = Excellent Confidence High diversity with key species
Bp = Sidewall core (percussion)	
Br = Sidewall core (rotary/mechanical)	2 = Good Confidence Moderate diversity with key species
C = Coal cuttings	
D = Ditch cuttings	3 = Fair Confidence Low diversity with key species
E = Junk basket	
F = Miscellaneous/unknown	4 = Poor Confidence Moderate to high diversity without key species
G = Outcrop	
	5 = Very Low Confidence Low diversity without key species

***3 ENVIRONMENTS**	**DINOFLAGELLATE CONTENT%**	**DINOFLAGELLATE DIVERSITY**	**FRESHWATER ALGAE CONTENT%**
OFFSHORE MARINE	67 to 100	VERY HIGH	LOW
SHELFAL MARINE	34 to 66	HIGH	"
NEARSHORE MARINE	11 to 33	MODERATE	"
VERY NEARSHORE MARINE	5 to 10	MODERATE-LOW	"
MARGINAL MARINE	<1 to 4	LOW-VERY LOW	"
BRACKISH	0, SPINY ACRITARCHS ONLY	EXTREMELY LOW	"
NON-MARINE (UNDIFF)	0, NO SPINY ACRITARCHS	NIL	LOW
NON-MARINE (LACUSTRINE)	0, NO SPINY ACRITARCHS	NIL	MODERATE 10%+

TABLE 2 ENVIRONMENTAL RAW DATA : LONGTOM-2

Depths (m)	Type	Total Marine MP	Total Fresh MP	Total Angiosperm Pollen	Total Gymnosperm Pollen	Total Spores	Total Other (mostly fungal)	Environments
1350	CUTTS	(15)	2	5	32	46	0	?non-marine-?swamp margin
1420	CUTTS	(1)	2	28	54	15	0	?non-marine, floodplain
1490	CUTTS	3	5	14	47	31	0	?non-marine, swamp margin
1530	CUTTS	0	3	43	19	35	1	non-marine, swamp
1660	CUTTS	0	5	3	76	16	0	wet floodplain
1760	CUTTS	5	24	3	59	8	1	nearshore marine
1790	CUTTS	4	8	8	64	15	1	nearshore marine
1820	CUTTS	0	6	2	69	23	0	wet floodplain
1860	CUTTS	4	8	1	46	41	1	marginal marine
1920	CUTTS	12	0	1	69	18	0	nearshore marine
1940	CUTTS	1	1	13	63	22	0	marginal marine
2005	CUTTS	0	1	3	77	18	1	non-marine, floodplain
2045	CUTTS	2	8	1	72	17	0	brackish marine
2055	CUTTS	0	6	2	54	38	0	swamp margin
2080	CUTTS	0	8	2	60	29	0	wet floodplain
2100	CUTTS	1	1	2	71	24	1	marginal marine
2112.43	CORE	<1	4	1	65	29	1	brackish marine
2112.70	CORE0	0	0	0	49	49	2	?non-marine
2113.0	CORE	0	2	0	56	42	0	swamp margin
2123.0	CORE	1	5	1	73	19	1	marginal marine
2123.5	CORE	1	5	2	80	12	0	marginal marine
2124.5	CORE	1	1	2	73	23	0	brackish marine
2144.61	CORE	0	0	4	53	42	1	swamp margin
2146.0	CORE	0	2	2	65	40	1	swamp margin
2146.61	CORE	0	4	0	68	28	0	floodplain
2147.0	CORE	0	5	<1	66	29	0	wet floodplain
2148.0	CORE	0	5	3	65	27	0	wet floodplain
2150	CUTTS	0	5	2	68	25	<1	wet floodplain
2160	CUTTS	0	5	1	67	26	0	wet floodplain
2180	CUTTS	<1	3	5	64	28	1	marginal marine
2195	CUTTS	1	0	4	74	21	0	brackish
2200	CUTTS	6	3	1	69	15	0	marginal marine
2205	CUTTS	1	5	10	56	27	1	wet floodplain
2245	CUTTS	1	3	2	69	25	<1	marginal marine
2255	CUTTS	2	1	<1	71	26	0	marginal marine
2260	CUTTS	1	3	5	65	25	1	marginal marine
2290	CUTTS	1	3	1	68	27	<1	marginal marine

2345	CUTTS	-	-	-	-	-	-	near barren
2360	CUTTS	(4) caved	<1	2	38	56	0	swamp margin
2370	CUTTS	1	0	<1	48	51	0	marginal marine
2390	CUTTS	-	-	-	-	-	-	near barren
2400	CUTTS	0	4	<1	57	39	0	swamp margin
2410	CUTTS	-	-	-	-	-	-	near barren
2420	CUTTS	1	5	2	52	40	0	marginal marine

THE NON-MARINE ENVIRONMENTS ARE RECOGNISED ON BINT & MARSHALL & HELBY (1988) CRITERA, NAMELY	
FLUVIAL:	LEAN, SANDY, POLLEN DOMINANT
FLOODPLAIN:	RICH, POLLEN DOMINANT, SPORES SUBORDINATE AND DIVERSE, NO OR VERY FEW FRESHWATER ALGAE
SWAMP MARGIN:	RICH, POLLEN AND SPORES CO-DOMINANT, SPORES VERY DIVERSE, MINOR FRESHWATER ALGAE <10%
SWAMP:	RICH, SPORES DOMINANT AND LOW DIVESITY, MINOR FRESHWATER ALGAE <10%
LACUSTRINE:	RICH, FRESHWATER ALGAE 10%+, POLLEN USUALLY DOMINANT, SPORES SUBORDINATE WITH USUALLY MODERATE TO LOW DIVERSITY

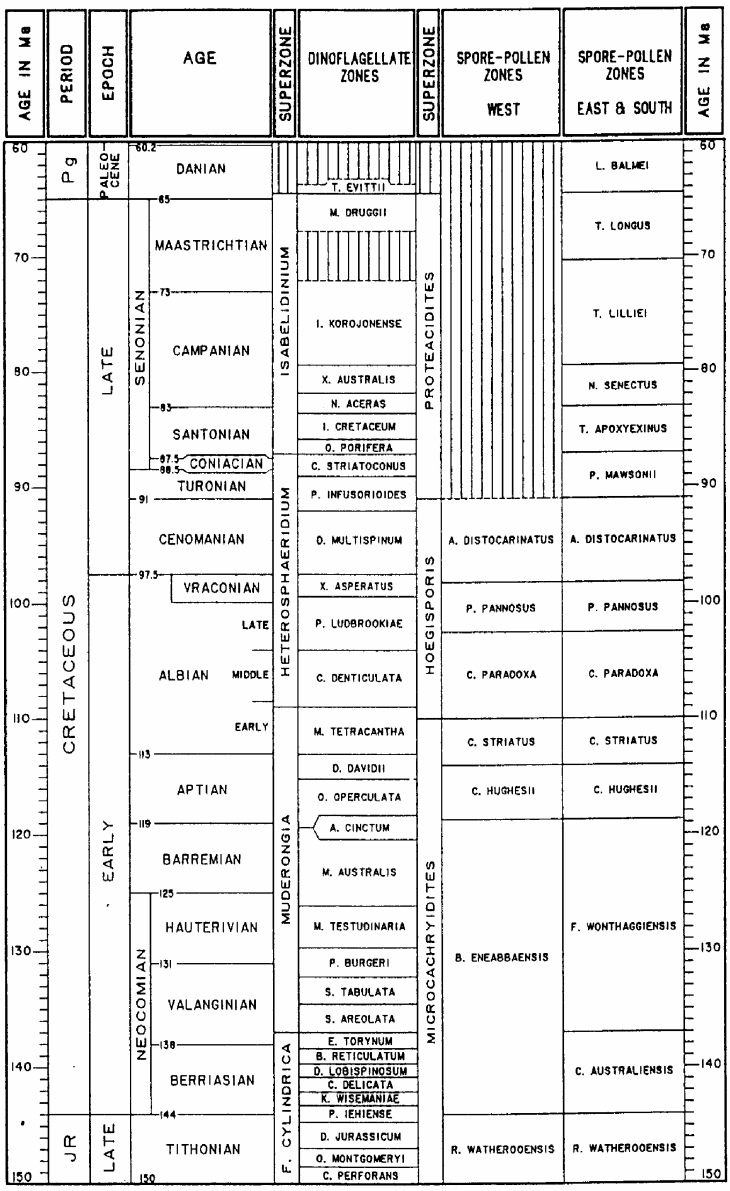

Figure 1a ZONATION FRAMEWORK - LATEST JURASSIC TO PALEOCENE

(from Helby et al, 1987)

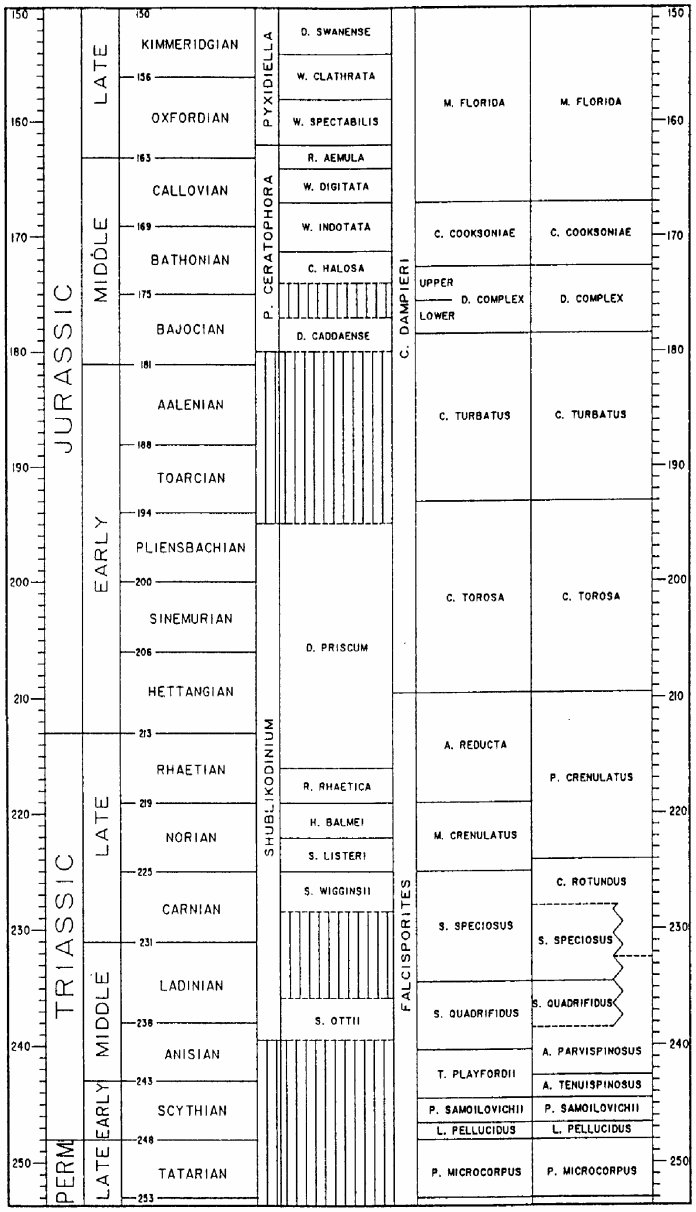

Figure 1b ZONATION FRAMEWORK - LATE PERMIAN TO LATE JURASSIC
(from Helby et al, 1987)

SPORE POLLEN					MICROPLANKTON			
Zones	**Subzones**		**Key Events**		**Zones**	**Subzones**	**Key Events**	
P. mawsonii	*G. ancorus*		top	*A. distocarinatus* *R. admiralis*	*Rimosicysta*	*Limbicysta*	top top base	*R. aspera* freq. *Limbicysta* *Limbicysta*
						R. cucullatum	top base	freq. *R. cucullatum* freq. *R. cucullatum*
	L. musa	upper	top	*L. musa* *C. "pileosa"*		*R. kipperi*	top	*R. kipperi*
			base	*A. obscurus*				
		lower	top	*C. tectifera*				
			top	*I. intraverrucatus*		*A. cruciformis*	top	abund. *A. cruciformis*
			top	*D. "pusillum"*				
						R."robusta"	top base base	*R. "robusta"* abund. *A. cruciformis* *Wuroia* spp.
			base	*C. "pileosa"*				
	H. trinalis	upper	top	*H. "trinalis"* abund. *Dilwynites*		*Luxadinium* sp. B	top acme base	consist. *Micrhystridium* abund. *Luxadinium* sp. B *Luxadinium* spp.
						Sigmopollis	abund	*Sigmopollis* spp.
			base	*Dilwynites* >10%			base	*Rimosicysta* spp.
		lower	base	*P. mawsonii*		*C. parvus*	top	freq. *C. parvus*
			base	*H. "trinalis"*			base	*C. parvus*
H. uniforma			top	*H. uniforma*				

Figure 2 Suggested subzonation of the *P. mawsonii* Zone, Gippsland Basin

Depth Scale (m)	Sample Depth	Sample Type	Spore pollen Events	Spore pollen Subzones		Microplankton Events	Micro-plankton Subzones		Possible Longtom-1 Sub-Subzones
	1567.0	swc	top *H. "trinalis"* top *L. "musa"*	*H. rinalis"*	upper	base *Micrhystridium* sp. A top *R. kipperi*	*Rimosicysta*	*Luxadinium* sp. B	*Micrhystridium* sp. A
1600									
	1615.0	swc	acme *D. "pusillum"* 55%			abt. *A. cruciformis* abt. *Luxadinium* sp. B top *R. "robusta"* rare *C. edwardsii*			abt *Luxadinium* sp. B
1700									
	1721.0	swc				base com *A. cruciformis*			com. *A. cruciformis* below *Luxadinium*
	1778.0	swc	acme *Dilwynites* 50%			base *"R. robusta"*			rare *"R. robusta"*
1800									
	1860.0	swc				base *Luxadinium* sp. B			rare *Luxadinium* sp. B
		swc	base abt. *Dilwynites* abt. *Araucariacites*			com. *R. kipperi* abt. *Rimosicysta* spp.		*Sigmo-pollis*	abt. *Rimosicysta* inc. *R. kipperi*
1900			acme *Cyath., Gleichen*		lower				
	1922.0	swc	base *P. mawsonii*			abt. *C. parvus*		*C. parvus*	abt. *C. parvus*
	1925/50	cutts							
	1931.0	swc	+ *A. distocarinatus*						
	1933.8	swc	abt. *Laevigatato* 45%			base freq. *C. parvus*			
	1934.0	swc	top *P. "eunuchus"* base *H. "trinalis"* *L. "musa"* *R. "admirabilis"*			base *R. kipperi* (?caved)			?rare *R. kipperi*
2000									

FIGURE 3 KEY DATUM AND SUGGESTED SUBZONES FOR LONGTOM-1

3 PALYNOSTRATIGRAPHY

3.1 1350 m (cutts) – 1420 m (cutts) : *L. balmei* Zone

Assignment is indicated at the top by youngest *Lygistepollenites balmei* and at the base by the absence of older markers. At 1360 m in a very poor yield, common is *Falcisporites similis* with frequent *Cyathidites australis, Cyathidites minor* and *Cyathidites spendens*. Rare elements include *L. balmei, Periporopollenites polyoratus, Proteacidites* spp., *Spinozonocolpites prominatus* and *Tricolpites phillipsii*. At 1420 m, common are *Australopollis obscurus, Phyllocladidites mawsonii* and *Vitreisporites pallidus* with frequent *C. minor, Dilwynites granulatus, F. similis, Gleicheniidites, L. balmei, Microcachryidites antarcticus* and *Proteacidites* spp. Rare elements include *Nothofagidites endurus* and *P. polyoratus*.

Dinoflagellates are frequent at 1350 m but are probably mostly caved. *Cordosphaeridium* spp. are frequent with a single *Ceratiopsis speciosus* probably in place, but not zone diagnostic. At 1420 m, dinoflagellates are very scarce and probably also mostly caved. A single *Apteodinium homomorphum* suggests the latest Paleocene *A. homomorphum* dinoflagellate zone, but may be caved.

The presence of rare dinoflagellates considered in place suggests marginal marine environments. The palynofloras considered in situ are totally dominated by spores and pollen.

Light yellow spore colours suggests immaturity for hydrocarbons.

3.2 1490 m (cutts) – 1530 m (cutts) : *F. longus* Zone, upper subzone

Assignment is indicated at the top by youngest rare *Quadraplanus brossus*. It is unusual that the other markers are not seen in this sample which otherwise would be assigned to the *L. balmei* Zone. At 1530 m, common *Gambierina rudata* and rare *Tricolpites confessus* confirm the *F. longus* Zone, and are more consistent with equivalent section in Longtom-1. Assignment is indicated at the base by oldest common *G. rudata* and rare *Stereisporites "punctatum"*. Confirming the *F. longus* Zone is oldest *Tetracolporites verrucosus*.

At 1490 m, common are *P. mawsonii* and *Proteacidites* spp. with frequent *C. australis, Gleicheniidites, Lygistepollenites florinii* and *V. pallidus*. Rare elements

include *Aequitriradites spinulosus, A. obscurus, Camarozonosporites ohaiensis, G. rudata, L. balmei, Q. brossus* and *S. "punctatum*".

At 1530 m, abundant are *Proteacidites* spp. with common *G. rudata* and frequent *C. minor, F. similis, Laevigatosporites ovatus, P. mawsonii, Stereisporites antiquasporites* and *S. "punctatus"*. Rare elements include *C. ohaiensis* and *T. confessus.*

Very rare dinoflagellates at 1490 m only are considered caved, with the in situ environments probably non-marine. Co-dominance of spores with saccate pollen suggest swamp margin environments.

Yellow spore colours suggests immaturity for hydrocarbons.

3.3 1660 m (cutts) – 2420 m (cutts) : *P. mawsonii* Zone, *H. trinalis* subzone

Assignment is indicated by youngest *Hoegisporis "trinalis"* at the top confirmed by youngest *Rimosicysta kipperi* and oldest *H. "trinalis"* at the base. Within the interval, *H. "trinalis"* is consistent but *Laevigatosporites "musa"* is rare and intermittent. Common to very common are *Dilwynites* and *F. similis* with intermittently common *Cyathidites, M. antarcticus* and *V. pallidus*. Intermittently frequent are *A. australis, Gleicheniidites* and *Podosporites microsaccatus*. Rare elements include persistent *H. trinalis* seen in almost all samples, and intermittently *Appendicisporites distocarinatus, Balmeisporites holodictyus, Coptospora "pileosa"* and *L. "musa"*. Extremely rare is *Cyatheacidites tectifera*. At the base (2260 – 2420 m), *A. distocarinatus* is very consistent and at 2370 – 2420, *Cyathidites* spp. become very common. Within this data set, the events suggested by Morgan (2003a) to subdivide the *H. trinalis* subzone occur right to the interval base, suggesting that these events are not useful and therefore that the subzones do not work.

Microplankton are mostly rare to occasionally frequent. Of these, dinoflagellates are always rare, with *Luxadinium* sp. B down to 1940 m (cutts) and *Subtilisphaera* spp. intermittently to the base but possibly partly caved in the cuttings. An acme (11%) of *Subtilisphaera* occurs at 1920 m (cutts). Spiny acritarchs are very intermittent. Algal elements are mostly minor in many samples. *Rimosicysta kipperi* is frequent at the top (1790 – 1820 m) with a major acme at 1760 m. It is a rare element below in cuttings, but absent from the core (suggesting that the cuttings are caved). Other algal types include *Schizosporis, Sigmopollis, Circulisporites* and *Botryococcus* with a notable acme of *Circulisporites parvus* at 2055 m.

Depths of events with correlative potential in Longtom-2 and their possible equivalents in Longtom-1 are listed below.

Depth (Longtom-2)	event and possible Longtom-1 equivalent
1660 m (cutts)	: top *R. kipperi, H. "trinalis"*, common *Dilwynites*
1760 m (cutts)	: *Rimosicysta* very common (20%) major lake input
1790 m (cutts)	: *Rimosicysta* frequent (5%)
1820 m (cutts)	: *Rimosicysta* frequent (3%), top *C. pileosa*
1860 m (cutts)	: top intermittent *A. distocarinatus*
1920 m (cutts)	: *Subtilisphaera* spp. common (11%) nearshore marine
1940 m (cutts)	: base *Luxadinium* sp. B (1860.0 m in Longtom-1)
2005 m (cutts)	:
2045 m (cutts)	: base consistent *R. kipperi* (1862.0 m or 1925/50 m in Longtom-1)
2055 m (cutts)	: acme *C. parvus* 3% (1922.0 m in Longtom-1)
2080 m (cutts)	
2100 m (cutts)	
2112.43 m (core)	: trace spiny acritarchs, brackish marine
2112.70 m (core)	: lean non-marine swamp margin
2113.0 m (core)	: non-marine swamp margin
2123.0 m (core)	: top rich interval, trace saline, marginal marine
2123.5 m (core)	: base rich interval, trace saline, marginal marine
2124.5 m (core)	: trace spiny acritarchs, brackish marine
2144.61m (core)	: non-marine swamp margin
2146.0 m (core)	: non-marine swamp margin
2146.61 m (core)	: non-marine floodplain
2147.0 m (core)	: non-marine wet floodplain
2148.0 m (core)	: non-marine wet floodplain
2150 m (cutts)	
2160 m (cutts)	
2195 m (cutts)	
2200 m (cutts)	
2245 m (cutts)	
2255 m (cutts)	: top very common *M. antarcticus*
2260 m (cutts)	: top consistent *A. distocarinatus*
2290 m (cutts)	
2345 m (cutts)	
2360 m (cutts)	
2370 m (cutts)	: top influx *Cyathidites*
2390 m (cutts)	
2400 m (cutts)	

2410 m (cutts)
2420 m (cutts)

Detailed correlation to a sequence of distinctive microplankton events seen in the swc-based Longtom-1 data set of Partridge (1995) and shown herein in Figure 3, is not possible with the existing data set. Failure to see these acme events may be because.

- the events do not carry laterally (facies restricted)
- events are very thin and although distinctive in swcs, they are diluted beyound recognition in cuttings
- cuttings samples have missed the events

Restudy of Longtom-1 using cuttings might produce a tighter correlation.

Within this data set, oldest *Luxadinium* sp. B (1940 m) and oldest consistent *R. kipperi* (2045 m, possibly caved beneath) suggest the subzones of Morgan (2003a) might be
1660 m (cutts) – 1940 m (cutts) : *Luxadinium* sp. B subzone
2005 m (cutts) – 2045 m (cutts) : *Sigmopollis* subzone
2055 m (cutts) – 2420 m (cutts) : *C. parvus* subzone

However, the lack of the acme horizons reduces confidence in these subzone assignments.

Environments are variable, and summarized in Table 2. About half contain low diversity dinoflagellates (1 or 2 species) are assigned to marginal marine, although such low diversity might indicate lowered salinity lagoons, lakes or estuaries. Some contain very rare spiny acritarchs and are assigned to brackish marine, implying lowered salinity lagoons or lakes. Many lack saline markers entirely and swamp margin and wet floodplain environments are indicated. Freshwater algae are significant components of many assemblages.

Light brown spore colours at the top indicate marginal maturity for oil, while light to mid brown spore colours at the base indicate early maturity for oil.

4 REFERENCES

Helby, R.J. Morgan, R.P. and Partridge, A.D. (1987) A palynological zonation of the Australian Mesozoic In : Studies in Australian Mesozoic Palynology, Assoc. Australias, Palaeontols. Mem. 4 1-94

Marshall, N.G. (1989) An unusual assemblage of algal cysts from the Late Cretaceous of the Gippsland Basin, southeastern Australia Palynology 13 : 21-56

Morgan, R.P., (1992) Overview of new cuttings based Late Cretaceous correlations, Otway Basin, Australia. Unpubl. rept. for BHPP

Morgan, R.P. (2004a) Status of P. mawsonii Zone palynology, Gippsland Basin with subzone intervals unpubl. rept. for Esso Australia

Morgan, R.P. (2004b) Subdivision of the *P. mawsonii* Zone at Longtom-1, Gippsland Basin, Austrlaia unpubl. rept. for BHP Billiton

Partridge, A.D. (1995) Palynological analysis of Longtom-1 and sidetrack Gippsland Basin unpubl. rept for Esso Biostrata Report 1995/13

Partridge, A.D. (1998) Biostratigraphy and interpreted stratigraphy of Champion-1 and Conan-1 from open file basic data unpubl. rept. Biostrata Rept. 1998/02

Well Name : LONGTOM-2

Operator : APACHE ENERGY

Interval : 1330m - 2440m — **Palynological Data Chart : BASIC DATA**

Scale : 1:5000 — **% Abundance histogram : Highest occurrence**

Chart date: 25 March 2005 — **Roger Morgan**

LONGTOM-2

Morgan Palaeo Associates
Maitland, South Australia

Enclosure 1

Sampling
Cutting
Core
Sidewall core

Text Keys
*1 % within discipline (40mm=100%)
*2 In-Situ occurrences

Depth | **Samples** (Samples in Discipline(s) - Paly)

Dinoflagellate Cysts (% within discipline (40mm=100%); In-Situ occurrences)
Ceratiopsis speciosa
Cleistosphaeridium spp.
Cordosphaeridium multispinosum
Cordosphaeridium spp.
Fibrocysta vectensis
Membraniarnacia sp.
Operculodinium spp.
Spiniferites ramosus
Apectodinium homomorphum (short spines)
Areoligera senonensis
Deflandrea spp.
Impagidinium sp.
Opercuiodinium centrocarpum
Belodinium nereidis
Corobsphaeridium fibrospinosum
Corrudinium spp.
Fibrocysta bipolaris
Paleocystodinium australinum
Leptospheridia spp.
Subtilisphaera spp.
Wurroia tubiformis
Fibrocysta spp. B
Luxadinium sp.
Apteodinium "spongy"
Heterosphaeridium heterocanthum
Subtilisphaera "minutum"
Cribroperidinium edwardsii

AC (*1, *2)
Micrhystridium spp.
Amosopollis cruciformis
Veryhachium spp.
Microforams .

FT (*1, *2)
Schizosporis psilatus
Rimosicysta kipperii

Algae (% within discipline (40mm=100%); In-Situ occurrences)
Rimosicysta aspera (sensu lato)
Rimosicysta ovata
Rimosicysta eversa
Sigmopollis hispidus
Circulisporites parvus
Rimosicysta spp.

ALBO (*1, *2)
Botryococcus spp.

MP (*1, *2)
Pediastrum paleogeneites
Quadraplanus brossus
Reworking - Triassic
Reworking - Permian

Spores And Pollen (% within discipline (40mm=100%); In-Situ occurrences)
Araucariacites australis
Cyathidites asper
Cyathidites australis
Cyathidites minor
Cyathidites splendens
Dilwynites granulatus
Falcisporites similis
Gleicheniidites spp.
Lygistepollenites balmei
Osmundacidites wellmanii
Periporopollenites polyoratus
Proteacidites grandis
Proteacidites pseudomoides
Proteacidites spp.
Spinozonocolpites prominatus
Tricolpites phillipsii
Vitreisporites pallidus
Australopollis obscuris
Ceratosporites equalis
Contignisporites glebulentus
Microcachryidites antarcticus
Nothofagidites brachyspinulosus
Nothofagidites endurus
Phyllocladidites mawsonii
Podosporites microsaccatus
Stereisporites antiquasporites
Aequitriradites spinulosus
Cameronzonosporites ohaiensis
Dictyophyllidites spp.
Dilwynites "pusillum"
Forcipites longus
Gambierina rudata
Laevigatosporites ovatus
Lygistepollenites florinii
Proteacidites reticuloconcavus ms
Retitriletes austroclavatidites
Stereisporites punctatus
Stereisporites regium
Laevigatosporites "musa"
Proteacidites annularis
Tetracolporites verrucosus
Tricolpites confessus
Cupressiacites spp.
Hoegisporis "trinalis"
Tricolpites sp.
Triporoletes reticulatus
Dilwynites tuberculatus
Falcisporites grandis
Perinopollenites elatoides
Balmeisporites holodictyus
Coptospora "pilosa"
Lycopodiacidites asperatus
Neoraistrickia spp.
Triporoletes radiatus
Appendicisporites distocarinatus
Clavifera triplex
Perotriletes "baldii"
Cicatricosisporites australiensis
Pertriletes jubatus/margarii
Cycadopites follicularis
Phimopollenites pannosus
Tricolporites apoxyexinus
Phyllocladidites "eunuchus"
Cicatricosisporites ludbrookiae
Schizosporis parvus
Cicatricosisporites spp.
Convolutispora "magnifica"
Corollina torosa
Foraminisporis dailyi
Annulispores follicutosa
Crybelosporites cf. brenneri
Cyatheacidites tecitfera
Senectotetradites fistulosus
Callialaspories dampieri
Triletes tuberculiformis
Appendicisporites tricomitatus
Foraminisporis caelatus
Trilobosporites trioreticulosus
Tricolpites waiparaensis
Fungae .

FU (*1, *2)

Samples (Samples in Discipline(s) - Paly)

Total Count — Total count: Total Count (In-Situ occurrences)

% Category — Category %: % Category (In-Situ occurrences)
FT
AL
MP
AC
FU
DC
ALBO
SP

Well Name : LONGTOM-2

Operator : APACHE ENERGY

Interval : 1330m - 2440m

Scale : 1:5000

Chart date: 25 March 2005

Palynological Data Chart : BASIC DATA

% Abundance histogram : Highest occurrence

Roger Morgan

LONGTOM-2

Morgan Palaeo Associates
Maitland, South Australia

Enclosure 1

Sampling
Cutting
Core
Sidewall core

Text Keys
*1 % within discipline (40mm=100%)
*2 In-Situ occurrences

APPENDIX 2

Routine Core Analysis

CORE LABORATORIES AUSTRALIA PTY LTD

447-449 Belmont Ave, Kewdale, Perth WA 6105
Tel : (61 8) 9353 3944 Fax : (61 8) 9353 1369
Email : corelab.australia@corelab.com

Routine Core Analysis
Well Longtom – 2 ST1
Offshore
Australia

Prepared for
Apache Energy Ltd.

March 2005

File: PRP-04110

Rock Properties
Core Laboratories
Perth
Australia

CORE LABORATORIES AUSTRALIA PTY LTD

4th March 2005

Apache Energy Ltd.
Level 3
256 St. George's Tce.
Perth, WA 6005

Attention : Dr. Steve Moss

Subject : Routine Core Analysis
Well : Longtom - 2 ST1
File : PRP-04110

Dear Steve,

Presented herein is the final report of a routine core analysis study conducted on two cores from the above well that arrived at our laboratory on December 21st 2004.

We appreciate the opportunity to present this service to Apache Energy Ltd. Please contact us should you require any further information or assistance.

Yours sincerely,
Core Laboratories Australia Pty Ltd

James Brown
Senior Core Analyst

ABN. 67 065 540 838
P.O Box 785 Cloverdale, WA 6105 Australia Tel : (61-8) 9353 3944 Fax : (61-8) 9353 1369
Email : corelab.australia@corelab.com

TABLE OF CONTENTS

INTRODUCTION

Fourteen inner core barrels (core 1, seven fibreglass barrels; core 2, seven aluminium barrels), containing two and one half inch diameter core were delivered to Core Laboratories' premises in Kewdale, on the 21st December 2004.

Services performed and presented in the report include:

- Total surface core gamma
- Spectral core gamma
- Profile permeametry on slabbed core
- Core photography on slabbed core - white light (large and small format on a CD-Rom)
- Horizontal Permeability, porosity, (at NOBP) and grain density measurements on plugs
- Residual fluid saturations
- Core description

The reported data for the above services are presented digitally on a CD-Rom, whilst the digital core photographs are on a CD-Rom. The core description and photographs were sent under separate covers.

SUMMARY

Porosity and permeability measurements were determined at a net confining stress of 1800psi for all routine core analysis samples.

	Minimum	Maximum	Average
Core Plugs:			
Net Confining Pressure of 1800psig.			
Porosity (%)	7.1	26.1	16.6
Permeability, Kinf, (md)	0.002	132	14.8
Grain Density (g/cc)	2.631	2.819	2.681

Note: Permeability data from fractured samples was not used in the above table.

As can be seen from the core photographs and inspection of the core, much of the core material contained stress release fracturing/parting. These partings may have been exacerbated by drying out of the core with time. In many cases, these partings are so closely spaced it was impossible to avoid them while drilling core plugs for porosity/permeability analyses. These core plugs containing partings/fractures have been flagged both in the tabular data on pages 6 through 8, and in the porosity/permeability cross-plot on page 16. The permeabilities within zones affected by stress-release fracturing may be unrepresentatively high and should be treated with caution.

Some of the profile permeability data tabulated on pages 10 through 15 are similarly flagged where stress fractures may have led to unrepresentatively high permeability values.

Since stress fractures are too closely spaced at some depths to obtain reservoir representative core plugs, alternate procedures for obtaining permeability values (such as rock-typing from thin section to obtain analog values from a data-base) should be considered.

LABORATORY PROCEDURES

Initial Inventory:

After the arrival of the cores on the 21st December 2004, the inner core barrels were unloaded, laid out in order and the barrel depths recorded on an in-house inventory (fourteen barrels). The barrels on arrival were approximately in three-metre lengths.

Core Preparation:

Total surface core gamma was run along the cores while still in the inner core barrels. The core was unloaded from the barrels, fitted together, cleaned of drilling fluids, and marked with a continuous slab line and core depths. Some sections of the core were frozen under dry ice due to the unconsolidated nature of the rock (2117.67-2121.38m, 2127.2-2130.00m, 2134.14-3135.14m and 2136.52-2138.45m). The cores were then plugged, slabbed into two half sections, and described by Duncan Barr. Surface spectral core gamma was then run prior to profile permeability measurements being taken and the core photographed.

Surface Core Gamma:

The cores were logged while still in the core barrels. A zero base-line was established, and a standard calibration tube logged prior to running the core. During the logging of the cores, one observer verified that each barrel passing the detector was in its correct sequence and orientation, whilst two people loaded and offloaded the barrels. As each barrel cleared the detector it was replaced in sequence on the lay out benches. The preliminary digitised surface gamma trace was sent by e-mail to Apache Energy Ltd once the core had been run.

Core Slabbing:

The competent sections of core were slabbed into two half sections using a 2% potassium chloride brine solution as the blade lubricant. The frozen sections of core were cut dry.

Spectral Core Gamma:

The cores were logged after they had been removed from their inner core barrels. The spectral core gamma was calibrated using known standards prior to the cores being run. A sample spacing of 2cm was used during measurement. The spectral core gamma has a higher resolution and compensates for the small diameter of the cores. The total core gamma trace is plotted on the integrated core log.

Profile Permeametry:

Profile permeametry was conducted on the cut face of the cores using the PDPK™300 profile permeameter. Measurements were made approximately every ten centimetres down the cores as requested. A total of 354 point measurements were attempted.

Core Photography:

After slabbing, the half section of the core was cleaned, then photographed under white light using a digital camera. The large format images were annotated with the routine core analysis data. A CD-Rom containing both large and small format images were forwarded under a separate cover.

Sample Preparation:

Before slabbing two sets of one inch diameter core plugs were drilled. The first set (set A, consisting of twenty-one plugs) were cut and trimmed using air. Six of the samples were mounted in nickel sleeves with screens, as they were unconsolidated. Set A core plugs were cut for Dean-Stark / tracer analysis. Ninety-seven core plugs were attempted for the second set of plugs (for porosity, permeability and grain density measurements), of which one failed and thirty-one were mounted in nickel sleeves. Set B core plugs were attempted at every 30 cms intervals after advice from the Apache Energy Ltd. Sampling depths were adjusted accordingly to avoid core breaks and/or shale sections. The plugs were cut and trimmed using a 2% potassium chloride brine. The plugs cut in the frozen core were drilled and trimmed using air, then mounted. All plugs (except set A) were placed in cool refluxing toluene to remove any residual hydrocarbons. Once cleaned, the plugs were removed from the soxhlet, air-dried to expel the excess toluene, then placed in cool refluxing methanol to remove residual salts. When cleaned of salts, the plugs were removed from the soxhlet, air-dried to expel the excess methanol, and dried in a controlled humidity oven at 60°C and 45% humidity. The plugs were then removed from the oven, placed into individual snap lock plastic bags and allowed to cool to room temperature.

Residual Fluid Saturations, Dean-Stark:

A subset of ten plugs from set A were selected, then individually placed into dried, pre-weighed thimbles, weighed and loaded into individual Dean-Stark distillation units. Boiling toluene was used to drive water out of the sample and to extract any hydrocarbons present. The distillation process was monitored until the water volume produced from each sample had stabilised. Following the Dean-Stark distillation, each plug with thimble was then dried in a convection oven at 95ºC for an initial twenty-four hour period. The plugs were removed from the convection oven, cooled in a moisture-free environment and weighed. The water saturation was computed directly from the water recovered and the helium pore volume. The oil saturation was calculated based on the non-water weight loss during the Dean-Stark procedure. The core plugs were not extracted of residual salts. Following cleaning, the plugs were dried in a convection oven at 95ºC for a twenty-four hour period. Eleven samples were not run. These samples remained sealed and stored for future possible analysis.

Corrected Residual Fluid Saturations:

Brine volumes of the plugs were determined by Dean-Stark analysis. The plugs were not cleaned in methanol and so retained salts originally dissolved in the water contained in the sample and any tracer that entered the core via mud filtrate (only distilled water emanates from the core samples during Dean-Stark analysis). Porosity, permeability and grain density were determined prior to the samples been crushed and a known volume of distilled water added to redissolve the salts and the

tracer. This brine was then analysed. Knowing the original volume of brine in the samples, the amount of distilled water added later and the sample weights, concentrations of the ions and tracer in the sample brine were then calculated. Knowing the concentration of the tracer in the mud system, the volume of mud filtrate that had invaded the sample was calculated, then subtracted from the volume of water that was produced by the Dean-Stark analysis. The brine saturations were then recalculated.

Grain Volume and Grain Density:

The weight, diameter and length of all plug samples were measured before they were processed through the Ultrapore™ porosimeter to determine grain volume. As a standard quality control measure, a calibration check plug was run after every ten samples. Grain density data was calculated from grain volume and sample weight data.

Permeability and Porosity:

The core plugs were run at a confining stress of 1800psi. while determining porosity and permeability. The confining stress was supplied by Apache Energy Ltd. A standard check plug was run with every set plug samples. Klinkenberg permeability (K_{inf}) values are obtained directly from the CMS^{TM}300, since it operates by unsteady-state principles. Porosity data was obtained by combining pore volumes from the CMS^{TM}300 data with grain volumes from the Ultrapore porosimeter. For in-house QC and in preparation for subsequent SCAL work, all samples were routinely run at ambient conditions. Plug data at ambient conditions is contained with digital version of the spreadsheet on the CD-Rom.

Core Description:

Duncan Barr conducted a core description on the slabbed core, the results of which are presented in a separate report.

POROSITY, PERMEABILITY and GRAIN DENSITY (NOBP)

SAMPLE NUMBER	DEPTH (m)	NOBP 1800psi			GRAIN DENSITY (g/cc)	COMMENTS
		PERMEABILITY		POROSITY (%)		
		Kinf (md)	Kair (md)			
		Core 1				
1	2112.43	0.019	0.047	14.6	2.668	
2	2112.70	0.024	0.057	14.0	2.688	
3	2113.03	0.052	0.108	15.5	2.687	
4	2113.36	0.044	0.093	15.5	2.670	
5	2113.85	0.018	0.045	14.4	2.684	
6	2114.11	0.028	0.065	14.9	2.678	
7	2114.41	0.003	0.007	8.9	2.703	
8	2114.72	0.015	0.038	13.7	2.681	
9	2115.17	-	-	-	2.676	Sample failed
10	2115.95	0.005	0.012	10.6	2.691	
11	2116.24	-	-	-	-	No sample
12	2116.56	0.040	0.082	13.9	2.682	
13	2116.87	0.008	0.016	9.9	2.691	
14	2117.16	0.097	0.198	13.4	2.685	
15	2117.52	0.177	0.292	13.9	2.688	
16	2117.70	17.9	22.4	15.4	2.675	Mounted
17	2118.05	120	142	24.3	2.672	Mounted (Fractured)
18	2118.35	239	296	26.1	2.664	Mounted (Fractured)
19	2118.70	85.3	105	23.6	2.664	Mounted (Fractured)
20	2118.97	460	537	25.7	2.664	Mounted (Fractured)
21	2119.26	305	396	24.3	2.675	Mounted (Fractured)
22	2119.50	123	146	23.5	2.634	Mounted (Fractured)
23	2119.82	110	124	23.3	2.666	Mounted (Fractured)
24	2120.15	23.0	27.7	17.2	2.662	Mounted
25	2120.45	20.0	23.6	18.9	2.675	Mounted
26	2120.74	14.5	17.5	17.8	2.669	Mounted
27	2121.06	9.27	11.2	18.1	2.674	Mounted
28	2121.33	7.45	8.61	17.2	2.741	Mounted
29	2121.65	5.38	6.43	18.5	2.689	
30	2121.93	14.3	15.9	20.0	2.710	
31	2122.16	31.5	34.5	21.1	2.713	
32	2122.46	0.010	0.025	7.1	2.692	
33	2122.74	0.004	0.010	8.6	2.707	
34	2124.55	0.002	0.004	13.2	2.699	
35	2124.92	0.007	0.014	14.9	2.697	
36	2125.36	0.002	0.004	14.2	2.699	
37	2125.59	0.002	0.005	13.7	2.701	
38	2125.97	0.068	0.115	14.9	2.686	
39	2126.25	0.271	0.421	17.2	2.686	
40	2126.57	0.810	0.999	18.0	2.705	
41	2126.87	0.004	0.010	8.7	2.702	
42	2127.14	10.8	12.2	19.7	2.686	
43	2127.48	38.1	45.5	20.7	2.663	Mounted
44	2127.79	169	190	23.4	2.676	Mounted (Fractured)
45	2128.06	55.9	65.0	21.1	2.672	Mounted
46	2128.36	46.0	51.6	20.4	2.672	Mounted

POROSITY, PERMEABILITY and GRAIN DENSITY (NOBP)

SAMPLE NUMBER	DEPTH (m)	NOBP 1800psi			GRAIN DENSITY (g/cc)	COMMENTS
		PERMEABILITY		POROSITY (%)		
		Kinf (md)	Kair (md)			
47	2128.66	28.2	31.9	20.1	2.674	Mounted
48	2128.94	51.0	57.0	21.2	2.678	Mounted
49	2129.26	22.4	25.6	19.8	2.675	Mounted
50	2129.56	28.9	32.9	20.3	2.673	Mounted
51	2129.86	39.5	44.8	20.9	2.673	Mounted
		Core 2				
52	2130.26	0.005	0.014	9.0	2.697	
53	2130.59	8.88	10.2	19.5	2.688	
54	2130.79	0.162	0.265	14.2	2.694	
55	2131.13	6.81	7.79	18.3	2.687	
56	2131.43	35.0	37.6	20.3	2.681	
57	2131.73	20.7	22.6	19.4	2.678	
58	2132.06	7.62	8.71	18.7	2.678	
59	2132.37	3.52	4.12	17.4	2.679	
60	2132.63	13.2	14.7	19.4	2.674	
61	2132.94	15.1	16.9	19.5	2.672	
62	2133.24	14.3	16.0	19.7	2.678	
63	2133.55	22.3	24.5	20.0	2.668	
64	2133.89	20.9	22.8	20.5	2.696	
65	2134.10	22.7	24.6	19.7	2.684	
66	2134.45	169	209	24.2	2.670	Mounted (Fractured)
67	2134.75	56.4	62.3	21.9	2.673	Mounted
68	2135.14	6.21	7.27	18.3	2.679	Mounted
69	2135.30	0.005	0.011	10.2	2.690	
70	2135.59	6.52	7.90	16.7	2.676	
71	2135.91	0.044	0.084	12.2	2.680	
72	2136.19	0.107	0.189	14.5	2.674	
73	2136.44	7.93	9.06	19.0	2.666	
74	2136.82	39.9	44.5	21.3	2.819	Mounted
75	2137.04	21.6	25.1	19.5	2.675	Mounted
76	2137.38	16.0	19.3	18.8	2.677	Mounted
77	2137.72	25.4	28.3	20.0	2.679	Mounted
78	2137.95	17.0	19.1	17.9	2.685	Mounted
79	2138.31	15.2	17.5	19.7	2.678	Mounted
80	2138.59	63.4	66.7	21.9	2.680	
81	2138.88	36.2	38.7	20.6	2.669	
82	2139.18	0.981	1.13	15.7	2.677	
83	2139.48	0.007	0.016	10.1	2.687	
84	2139.80	9.66	10.7	19.1	2.667	
85	2140.10	38.9	42.0	20.4	2.659	
86	2140.40	52.3	55.5	20.7	2.662	
87	2140.71	132	139	22.3	2.659	
88	2141.05	73.5	77.7	21.5	2.675	
89	2141.35	0.101	0.175	12.2	2.689	
90	2141.70	0.168	0.271	11.9	2.674	
91	2142.03	0.061	0.108	11.0	2.658	
92	2142.34	0.064	0.118	11.8	2.691	

POROSITY, PERMEABILITY and GRAIN DENSITY (NOBP)

SAMPLE NUMBER	DEPTH (m)	NOBP 1800psi			GRAIN DENSITY (g/cc)	COMMENTS
		PERMEABILITY		POROSITY (%)		
		Kinf (md)	Kair (md)			
93	2142.64	0.007	0.016	7.9	2.695	
94	2144.61	0.011	0.030	13.5	2.690	
95	2145.63	0.030	0.056	12.9	2.631	
96	2145.84	0.015	0.033	12.6	2.650	
97	2146.61	0.007	0.015	10.5	2.680	

POROSITY, PERMEABILITY, GRAIN DENSITY and RESIDUAL FLUID SATURATIONS

SAMPLE NUMBER	DEPTH (m)	Ambient conditions			GRAIN DENSITY (g/cc)	RESIDUAL FLUID SATURATIONS				COMMENTS
		PERMEABILITY		POROSITY (%)		From Dean-Stark		Corrected*		
		Kinf (md)	Kair (md)			So (%)	Sw (%)	So (%)	Sw (%)	
14A	2117.10	-	-	-	-	-	-	-	-	Stored
18A	2118.56	-	-	-	-	-	-	-	-	Stored
20A	2118.92	713	836	25.8	2.654	0.0	70.7	0.0	56.0	Mounted
24A	2120.18	38.7	45.8	17.5	2.650	0.0	78.9	0.0	73.4	Mounted
30A	2121.87	-	-	20.4	2.685	0.0	68.5	0.0	63.6	Poor shape
33A	2122.70	-	-	-	-	-	-	-	-	Stored
41A	2126.84	-	-	-	-	-	-	-	-	Stored
46A	2128.40	19.1	22.2	19.6	2.696	0.0	72.0	0.0	66.6	Mounted
50A	2129.60	84.2	93.2	21.5	2.694	0.0	77.8	0.0	65.1	Mounted
54A	2130.86	-	-	-	-	-	-	-	-	Stored
59A	2132.28	12.6	14.0	19.7	2.689	0.0	68.3	0.0	64.7	
62A	2133.31	-	-	-	-	-	-	-	-	Stored
68A	2135.09	34.7	45.3	19.9	2.704	0.0	76.2	0.0	64.6	Mounted
70A	2135.67	-	-	-	-	-	-	-	-	Stored
73A	2136.48	-	-	-	-	-	-	-	-	Stored
78A	2137.91	25.4	29.8	17.8	2.707	0.0	96.0	0.0	74.6	Mounted
84A	2139.84	15.7	17.5	20.2	2.681	0.0	69.1	0.0	63.7	
87A	2140.75	282	296	23.8	2.683	0.0	56.8	0.0	49.5	
90A	2141.78	-	-	-	-	-	-	-	-	Stored
93A	2142.67	-	-	-	-	-	-	-	-	Stored
95A	2145.66	-	-	-	-	-	-	-	-	Stored

NOTE: **Corrected*** means mud filtrate taken into account, estimated by Thiocyanate Tracer found in the sample

PROFILE PERMEAMETRY

SAMPLE POINT	DEPTH (m)	PERMEABILITY Kinf (md)	PERMEABILITY Kair (md)	COMMENTS
	Core 1			
1	2112.46	0.330	0.527	
2	2112.55	0.024	0.062	Shaly sand
4	2112.65	1.45	1.96	
5	2112.75	0.017	0.047	Shaly sand
6	2112.85	0.039	0.089	Shaly sand
7	2112.95	1.91	2.52	
8	2113.07	1.97	2.59	
10	2113.17	0.030	0.073	
11	2113.25	0.293	0.475	
12	2113.34	0.924	1.31	
13	2113.46	3.23	4.10	
14	2113.56	0.599	0.888	
15	2113.67	0.089	0.175	
16	2113.75	0.022	0.058	Shaly sand
17	2113.89	0.549	0.819	
18	2113.96	0.843	1.20	
19	2114.05	0.564	0.839	
20	2114.15	0.137	0.249	
21	2114.26	0.079	0.158	
22	2114.36	0.024	0.062	
23	2114.46	0.156	0.278	
24	2114.56	0.179	0.312	
25	2114.66	2.00	2.63	
26	2114.75	0.401	0.624	
27	2114.88	-	-	2114.9-2115.3 Rubble
28	2115.06	2.54	3.28	
30	2115.23	-	-	Fracture
31	2115.34	0.619	0.914	
32	2115.45	-	-	Poor seal
33	2115.53	0.195	0.336	
34	2115.65	0.176	0.308	
35	2115.74	0.236	0.394	
36	2115.84	0.420	0.650	Shaly sand
37	2115.98	0.091	0.178	
38	2116.04	0.574	0.852	
39	2116.17	-	-	Carbonaceous lamina
40	2116.33	5.06	6.26	
41	2116.44	3.96	4.98	
42	2116.53	0.522	0.785	
43	2116.62	-	-	Fracture
44	2116.75	0.971	1.37	
45	2116.83	0.105	0.200	
46	2116.95	0.093	0.181	
47	2117.05	1.47	1.99	
48	2117.20	1.12	1.56	
49	2117.25	1.39	1.89	
50	2117.34	1.82	2.43	
51	2117.45	-	-	Fracture
52	2117.55	0.485	0.734	
53	2117.64	1.25	1.72	
54	2117.75	6.45	7.85	
55	2117.95	-	-	Carbonaceous parting
57	2118.08	-	-	Fracture
58	2118.17	58.8	64.3	Possible fracture
59	2118.25	-	-	Fracture
60	2118.38	-	-	Fracture
61	2118.49	-	-	Soft core
62	2118.60	-	-	Carbonaceous parting
63	2118.64	115	124	Possible fracture

PROFILE PERMEAMETRY

SAMPLE POINT	DEPTH (m)	PERMEABILITY Kinf (md)	PERMEABILITY Kair (md)	COMMENTS
64	2118.77	-	-	Fracture
65	2118.84	-	-	Fracture
66	2118.99	-	-	Fracture
67	2119.07	44.3	49.0	
68	2119.15	5.48	6.74	
69	2119.29	174	185	Fracture?
70	2119.35	-	-	Fracture
71	2119.46	-	-	Fracture
72	2119.55	415	434	
73	2119.63	160	170	
74	2119.76	-	-	Fracture
75	2119.88	-	-	Fracture
76	2119.94	-	-	Fracture
77	2120.06	61.9	67.6	
78	2120.15	2.82	3.61	
79	2120.25	3.68	4.64	
80	2120.36	3.81	4.79	
81	2120.44	65.1	70.9	Possible fracture
82	2120.54	12.8	14.9	
83	2120.65	19.7	22.5	
84	2120.73	16.3	18.8	
85	2120.84	-	-	Carbonaceous parting
86	2120.95	3.63	4.56	
87	2121.03	10.0	11.9	
88	2121.15	8.67	10.3	
89	2121.25	2.22	2.90	
90	2121.36	2.95	3.77	
91	2121.45	6.05	7.39	
92	2121.55	4.94	6.13	
93	2121.70	6.21	7.57	
94	2121.75	7.61	9.16	
95	2121.90	24.7	27.9	
96	2121.96	52.3	57.4	
97	2122.03	25.0	28.3	
98	2122.14	20.9	23.8	
99	2122.25	0.233	0.392	
100	2122.35	0.181	0.316	
101	2122.44	0.063	0.131	
102	2122.54	-	-	Fracture
103	2122.65	0.151	0.271	
104	2122.78	0.616	0.912	
105	2122.85	0.685	1.00	
106	2122.96	-	-	Shale parting
107	2123.06	0.124	0.230	
108	2123.15	0.519	0.781	2122.9-2124.3 Shale
109	2123.24	0.224	0.378	
110	2123.34	-	-	Fracture
111	2123.45	0.165	0.291	
112	2123.55	0.266	0.438	
113	2123.66	0.204	0.349	
114	2123.74	0.376	0.590	
115	2123.83	0.088	0.172	
116	2123.93	0.111	0.210	
117	2124.04	0.038	0.089	
118	2124.15	0.115	0.215	
119	2124.25	-	-	Shale parting
120	2124.35	0.126	0.233	
121	2124.46	0.503	0.760	
122	2124.58	0.149	0.268	
123	2124.65	0.078	0.156	

PROFILE PERMEAMETRY

SAMPLE POINT	DEPTH (m)	PERMEABILITY Kinf (md)	PERMEABILITY Kair (md)	COMMENTS
124	2124.76	0.037	0.085	
125	2124.83	0.182	0.318	
126	2124.95	0.078	0.157	
127	2125.05	0.012	0.036	
128	2125.15	0.022	0.058	
129	2125.25	0.008	0.028	
130	2125.33	0.144	0.260	
131	2125.45	0.039	0.091	
132	2125.56	0.046	0.103	
133	2125.66	-	-	Poor seal
134	2125.75	0.362	0.571	
135	2125.85	0.484	0.736	
136	2125.93	0.289	0.471	
137	2126.05	2.71	3.49	
138	2126.12	0.155	0.277	
139	2126.24	1.11	1.54	
140	2126.33	2.91	3.73	
141	2126.44	9.80	11.6	
142	2126.56	7.21	8.72	
143	2126.64	2.91	3.73	
144	2126.75	0.050	0.110	
145	2126.81	0.555	0.829	
146	2126.94	1.19	1.64	2127-2129m Soft fragile core
147	2127.05	38.1	42.3	
148	2127.17	13.3	15.5	
149	2127.25	22.5	25.5	
150	2127.36	25.7	29.0	
151	2127.44	105	113	
152	2127.56	-	-	Fracture
153	2127.68	-	-	Fracture
154	2127.74	146	156	
155	2127.88	246	260	Fracture ?
156	2127.96	217	229	Fracture ?
157	2128.08	64.9	70.7	
158	2128.16	62.0	67.8	
159	2128.25	46.9	51.7	
160	2128.33	116	124	
161	2128.44	0.584	0.864	
162	2128.55	113	121	
163	2128.63	24.6	27.8	
164	2128.75	98.7	106	
165	2128.85	164	174	
166	2128.93	223	236	
167	2129.05	32.2	36.0	
168	2129.16	8.32	9.97	
169	2129.28	28.4	31.9	
170	2129.36	36.6	40.7	
171	2129.45	47.9	52.8	
172	2129.62	32.3	36.1	
173	2129.67	18.5	21.2	
174	2129.74	24.6	27.8	
175	2129.88	9.06	10.8	
176	2129.95	-	-	Poor seal
		Core 2		
177	2130.06	33.7	37.7	
178	2130.14	1.07	1.50	
179	2130.23	0.204	0.355	
180	2130.42	19.5	22.3	2130.33-60 Rubble
181	2130.51	15.4	17.8	
182	2130.65	2.42	3.17	

PROFILE PERMEAMETRY

SAMPLE POINT	DEPTH (m)	PERMEABILITY Kinf (md)	PERMEABILITY Kair (md)	COMMENTS
183	2130.75	0.805	1.17	
184	2130.88	1.96	2.61	
185	2130.95	3.46	4.39	
186	2131.05	9.52	11.3	
187	2131.16	7.44	8.98	
188	2131.24	10.7	12.7	
189	2131.34	5.13	6.36	
190	2131.46	44.5	49.1	
191	2131.56	28.5	32.0	
192	2131.66	3.75	4.74	
193	2131.76	8.98	10.7	
194	2131.87	10.0	11.9	
195	2131.95	19.9	22.8	
196	2132.11	40.0	44.4	
197	2132.15	13.9	16.1	
198	2132.25	11.7	13.7	
199	2132.39	4.06	5.11	
200	2132.45	6.17	7.55	
201	2132.57	11.0	13.0	2132.6-2133.0 Rubble
202	2132.73	-	-	Fracture
203	2132.83	6.25	7.63	
204	2132.98	61.8	67.3	
205	2133.05	7.85	9.43	
206	2133.16	9.19	11.0	
207	2133.36	2.45	3.17	
208	2133.46	6.82	8.29	
209	2133.59	48.1	53.0	
210	2133.67	45.7	50.4	
211	2133.76	8.10	9.70	
212	2133.84	29.0	32.5	
213	2133.96	21.4	24.3	
214	2134.05	5.37	6.62	
215	2134.14	18.8	21.5	
216	2134.24	35.4	39.4	
217	2134.37	-	-	Fracture
218	2134.48	23.3	26.4	
219	2134.57	58.2	63.7	
220	2134.65	39.3	43.6	
221	2134.78	52.1	57.2	
222	2134.86	50.6	55.6	
223	2134.96	53.9	59.1	
224	2135.05	2.73	3.51	
225	2135.17	1.62	2.17	
226	2135.25	1.19	1.64	
227	2135.35	2.19	2.86	
228	2135.45	0.332	0.529	
229	2135.56	1.23	1.69	
230	2135.64	7.82	9.41	
231	2135.75	13.5	15.7	
232	2135.85	9.35	11.1	
233	2135.94	1.05	1.47	
234	2136.05	0.846	1.21	
235	2136.14	4.79	5.95	
236	2136.24	1.84	2.44	
238	2136.34	-	-	Poor seal
239	2136.41	9.24	11.0	
240	2136.55	31.1	34.8	
241	2136.66	22.4	25.4	
242	2136.75	29.7	33.3	
243	2136.88	44.3	49.0	

PROFILE PERMEAMETRY

SAMPLE POINT	DEPTH (m)	PERMEABILITY Kinf (md)	PERMEABILITY Kair (md)	COMMENTS
244	2136.95	12.3	14.4	
245	2137.03	-	-	Carbonaceous parting
246	2137.15	9.07	10.8	
247	2137.25	9.78	11.6	
248	2137.36	8.15	9.77	
249	2137.45	4.85	6.01	
250	2137.56	-	-	Fracture
251	2137.69	91.0	98.2	
252	2137.79	27.3	30.7	
253	2137.86	2.61	3.36	
254	2137.90	9.12	10.8	
255	2138.05	8.84	10.5	
256	2138.15	15.9	18.3	
257	2138.27	42.4	46.9	
258	2138.36	9.61	11.4	
259	2138.45	50.5	55.5	
260	2138.56	16.2	18.7	
261	2138.65	49.4	54.3	
262	2138.75	66.1	72.0	
263	2138.84	85.7	92.6	
264	2138.92	73.1	79.4	
265	2139.09	12.0	14.1	
266	2139.15	3.37	4.26	
267	2139.25	0.240	0.400	
268	2139.35	0.430	0.661	
269	2139.44	0.194	0.334	
270	2139.55	1.07	1.49	
271	2139.65	7.25	8.75	
272	2139.75	14.3	16.6	
273	2139.86	23.2	26.2	
274	2139.96	-	-	Poor seal
275	2140.05	17.7	20.3	
276	2140.15	14.7	17.1	
277	2140.26	7.45	8.98	
278	2140.36	32.3	36.1	
279	2140.45	64.3	70.1	
280	2140.56	37.8	41.9	
281	2140.66	168	178	
282	2140.77	151	161	
283	2140.85	240	252	
284	2140.95	70.6	76.8	
285	2141.06	159	170	
286	2141.15	50.9	55.9	
287	2141.25	3.73	4.70	
288	2141.38	0.457	0.697	
289	2141.45	0.456	0.696	
290	2141.55	-	-	Carbonaceous parting
291	2141.65	4.05	5.07	
292	2141.75	1.09	1.51	
293	2141.84	2.50	3.23	
294	2141.96	5.38	6.62	
295	2142.06	0.317	0.508	
296	2142.14	-	-	Carbonaceous parting
297	2142.25	0.756	1.09	
298	2142.37	0.546	0.814	
299	2142.46	-	-	Poor seal
300	2142.55	0.391	0.610	
301	2142.69	0.637	0.937	
302	2142.75	1.00	1.41	
303	2142.86	4.14	5.18	

PROFILE PERMEAMETRY

SAMPLE POINT	DEPTH (m)	PERMEABILITY Kinf (md)	PERMEABILITY Kair (md)	COMMENTS
304	2142.95	0.043	0.097	2142.9-2144.0 Shaly sand
305	2143.05	1.53	2.06	
306	2143.15	0.011	0.034	
307	2143.25	1.44	1.95	
308	2143.35	0.123	0.227	
309	2143.45	0.143	0.257	
310	2143.55	0.258	0.426	
311	2143.65	0.039	0.090	
312	2143.76	0.005	0.020	
313	2143.85	0.156	0.278	
314	2143.95	0.020	0.052	
315	2144.05	0.593	0.880	
316	2144.15	0.276	0.451	
317	2144.25	0.017	0.046	
318	2144.36	0.010	0.032	
319	2144.45	0.081	0.161	
320	2144.56	0.891	1.27	
321	2144.65	-	-	Carbonaceous parting
322	2144.75	-	-	Carbonaceous parting
323	2144.85	0.046	0.102	
324	2144.95	0.757	1.09	
325	2145.05	-	-	Carbonaceous parting
326	2145.13	0.267	0.440	
327	2145.25	0.114	0.214	
328	2145.35	0.074	0.150	
329	2145.45	0.011	0.034	
330	2145.55	1.05	1.46	
331	2145.69	0.168	0.295	
332	2145.76	0.206	0.352	
333	2145.86	0.329	0.526	
334	2145.95	0.017	0.047	
335	2146.05	0.021	0.055	
336	2146.15	0.028	0.069	
337	2146.26	0.057	0.121	
338	2146.35	0.117	0.218	
339	2146.45	0.010	0.032	
340	2146.56	0.265	0.436	
341	2146.66	0.039	0.089	
342	2146.75	0.031	0.074	
343	2146.86	0.016	0.044	
344	2146.95	0.266	0.437	
345	2147.05	1.18	1.62	
346	2147.15	0.004	0.016	
347	2147.25	-	-	Micro fracture
348	2147.34	0.025	0.064	
349	2147.45	0.150	0.268	
350	2147.55	0.030	0.073	
351	2147.66	0.019	0.052	
352	2147.76	0.053	0.115	
353	2147.86	0.054	0.116	
354	2147.96	-	-	Micro fracture

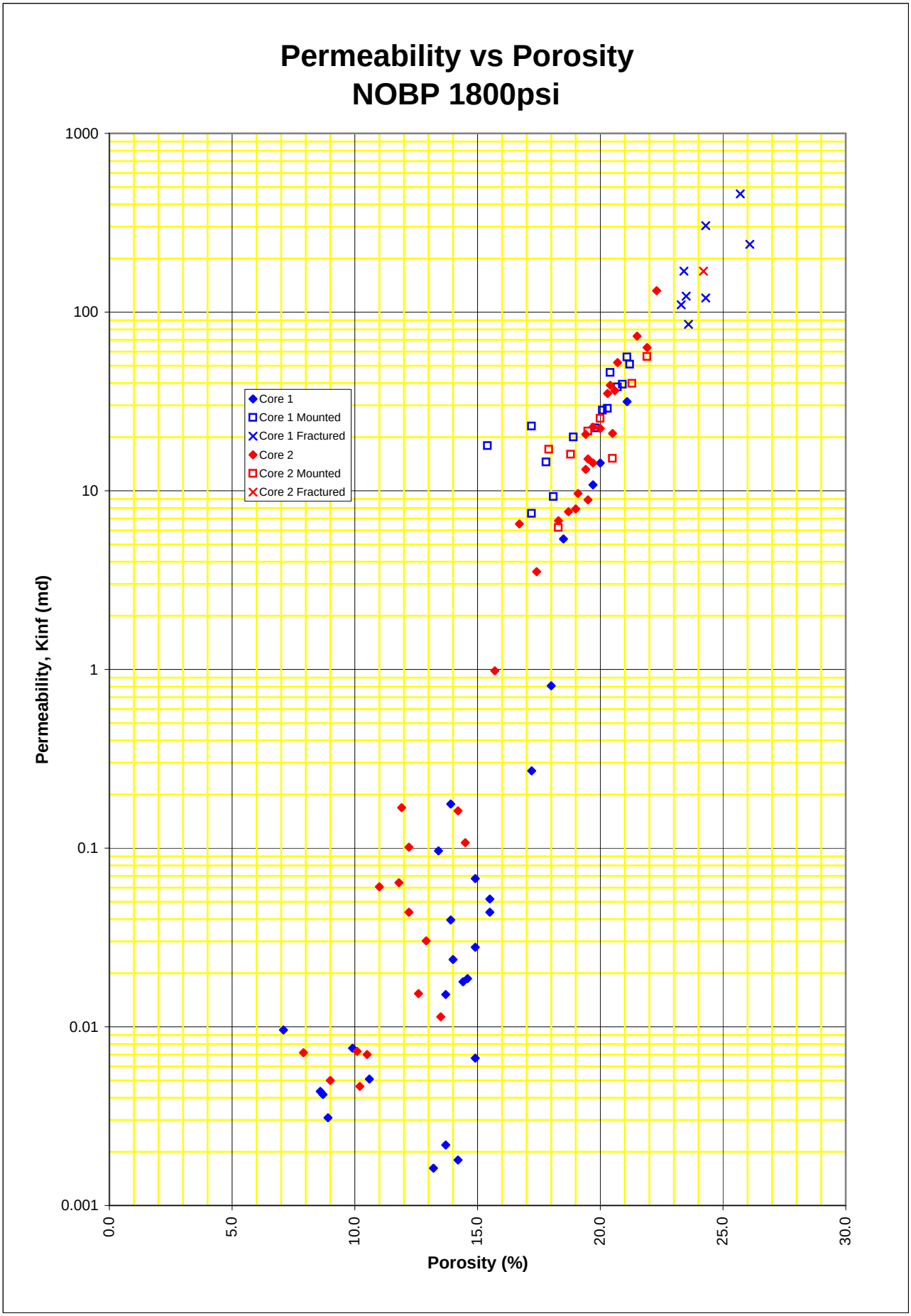
Permeability vs Porosity
NOBP 1800psi
Permeability, Kinf (md)
1000
100
10
1
0.1
0.01
0.001
0.0
5.0
10.0
15.0
20.0
25.0
30.0
Porosity (%)
Core 1
Core 1 Mounted
Core 1 Fractured
Core 2
Core 2 Mounted
Core 2 Fractured

COMPANY : APACHE ENERGY LTD
WELL : LONGTOM-2 ST1

INTEGRATED CORELOG

(Drillers Depths)

VERTICAL SCALE
1 : 200

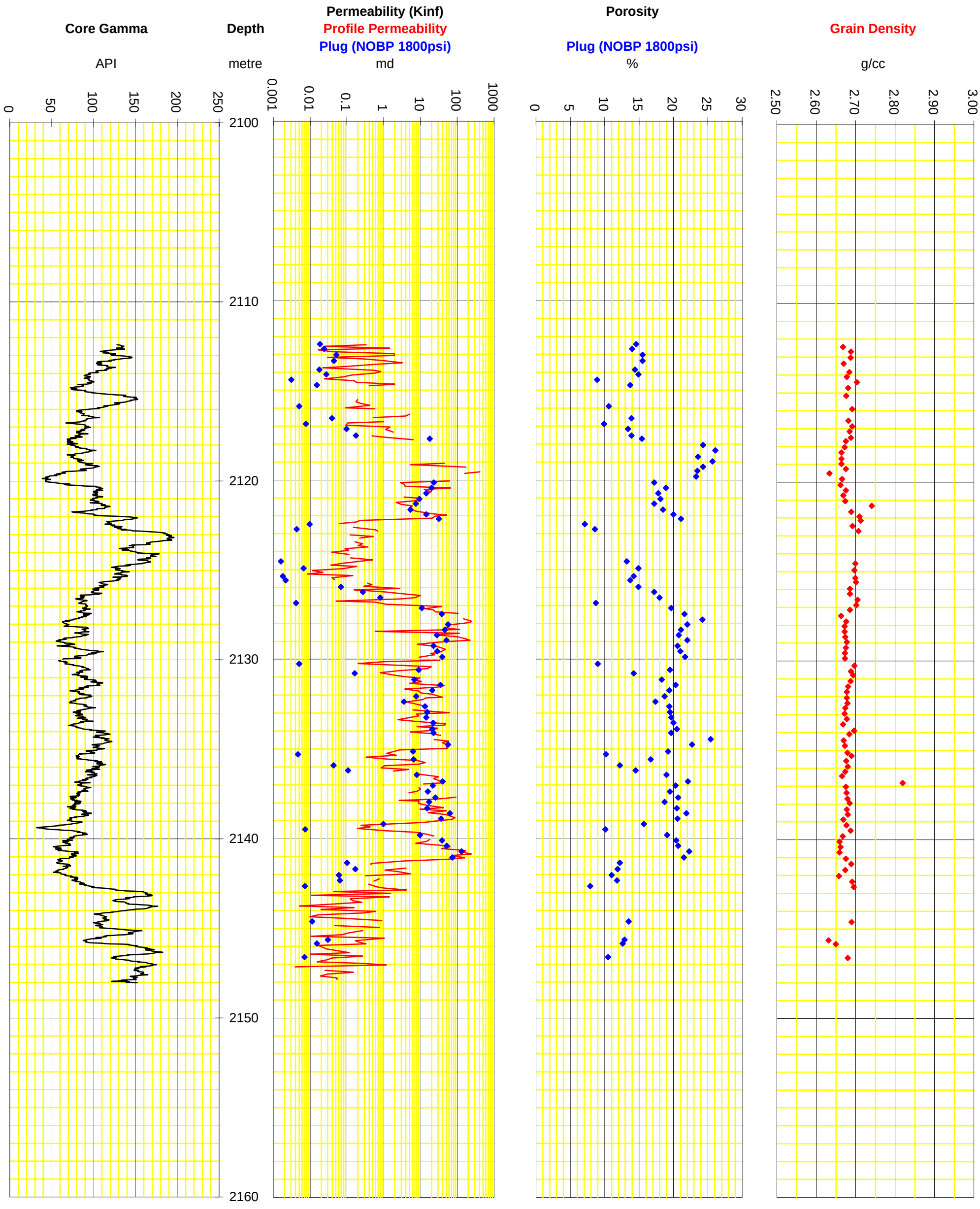

COMPANY : APACHE ENERGY LTD
WELL : LONGTOM-2 ST1

SPECTRAL CORE GAMMA

VERTICAL SCALE
1 : 200

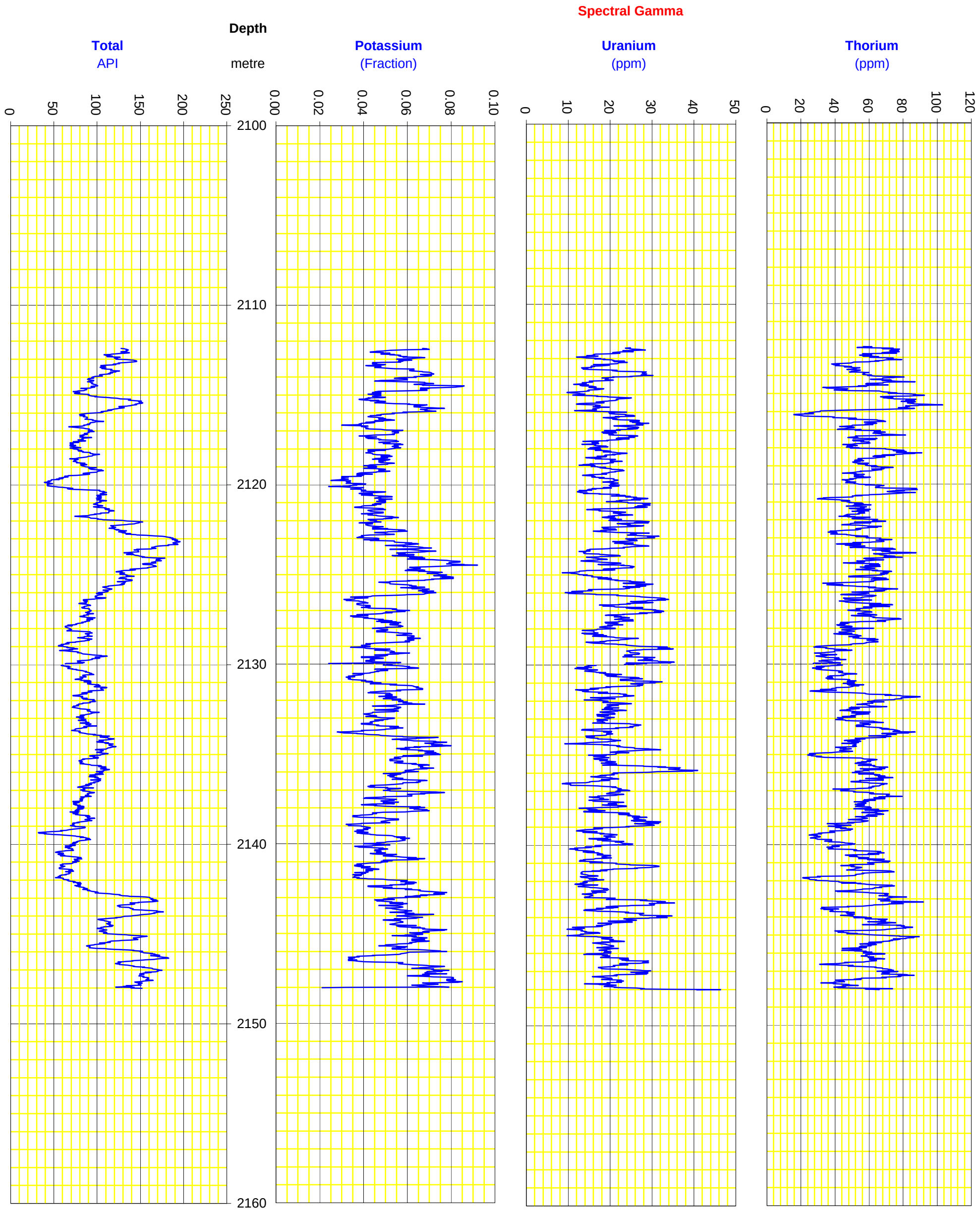

COMPANY : **APACHE ENERGY LTD**
WELL : **LONGTOM-2 ST1**

Core Inventory

TUBE	DEPTH (m) TOP	BOTTOM
	CORE 1	
7	2112.39	2115.00
6	2115.00	2117.60
5	2117.60	2120.37
4	2120.37	2121.60
3	2121.60	2124.40
2	2124.40	2127.20
1	2127.20	2130.00

TUBE	DEPTH (m) TOP	BOTTOM
	CORE 2	
	2130.00	2132.80
	2132.80	2135.60
	2135.60	2138.45
	2138.45	2139.60
	2139.60	2142.40
	2142.40	2145.20
	2145.20	2148.00

POROSITY, PERMEABILITY and GRAIN DENSITY (AMBIENT)

SAMPLE NUMBER	DEPTH (m)	AMBIENT CONDITIONS			GRAIN DENSITY (g/cc)	COMMENTS
		PERMEABILITY		POROSITY (%)		
		Kinf (md)	Kair (md)			
		Core 1				
1	2112.43	0.043	0.089	14.7	2.668	
2	2112.70	0.044	0.098	14.1	2.688	
3	2113.03	0.081	0.164	16.0	2.687	
4	2113.36	0.069	0.142	15.9	2.670	
5	2113.85	0.031	0.076	14.7	2.684	
6	2114.11	0.048	0.108	15.1	2.678	
7	2114.41	0.008	0.017	9.4	2.703	
8	2114.72	0.035	0.077	13.9	2.681	
9	2115.17	-	-	-	2.676	Sample failed
10	2115.95	0.011	0.022	11.0	2.691	
11	2116.24	-	-	-	-	No sample
12	2116.56	0.069	0.135	14.2	2.682	
13	2116.87	0.015	0.033	10.4	2.691	
14	2117.16	0.226	0.402	13.8	2.685	
15	2117.52	0.509	0.766	14.0	2.688	
16	2117.70	42.6	54.9	16.3	2.675	Mounted
17	2118.05	191	240	25.4	2.672	Mounted (Fractured)
18	2118.35	400	501	27.3	2.664	Mounted (Fractured)
19	2118.70	159	205	25.0	2.664	Mounted (Fractured)
20	2118.97	623	752	26.6	2.664	Mounted (Fractured)
21	2119.26	497	656	25.4	2.675	Mounted (Fractured)
22	2119.50	209	256	24.8	2.634	Mounted (Fractured)
23	2119.82	167	197	24.3	2.666	Mounted (Fractured)
24	2120.15	60.8	77.1	18.1	2.662	Mounted
25	2120.45	47.4	57.4	19.8	2.675	Mounted
26	2120.74	35.0	43.7	18.6	2.669	Mounted
27	2121.06	23.7	29.2	18.9	2.674	Mounted
28	2121.33	20.3	23.5	18.0	2.741	Mounted
29	2121.65	6.15	7.34	19.0	2.689	
30	2121.93	15.6	17.4	20.5	2.710	
31	2122.16	34.5	37.7	21.7	2.713	
32	2122.46	0.030	0.056	7.5	2.692	
33	2122.74	0.008	0.020	9.1	2.707	
34	2124.55	0.003	0.008	14.2	2.699	
35	2124.92	0.009	0.019	15.6	2.697	
36	2125.36	0.003	0.008	14.8	2.699	
37	2125.59	0.004	0.009	14.3	2.701	
38	2125.97	0.091	0.154	15.4	2.686	
39	2126.25	0.507	0.733	17.8	2.686	
40	2126.57	0.960	1.190	18.4	2.705	
41	2126.87	0.008	0.019	8.9	2.702	
42	2127.14	11.9	13.4	20.2	2.686	
43	2127.48	76.2	97.5	21.6	2.663	Mounted
44	2127.79	229	273	24.2	2.676	Mounted (Fractured)
45	2128.06	103	126	22.0	2.672	Mounted
46	2128.36	67.6	78.2	21.1	2.672	Mounted
47	2128.66	45.8	53.7	20.8	2.674	Mounted

POROSITY, PERMEABILITY and GRAIN DENSITY (AMBIENT)

SAMPLE NUMBER	DEPTH (m)	AMBIENT CONDITIONS			GRAIN DENSITY (g/cc)	COMMENTS
		PERMEABILITY		POROSITY (%)		
		Kinf (md)	Kair (md)			
48	2128.94	73.2	84.8	22.0	2.678	Mounted
49	2129.26	42.3	49.3	20.6	2.675	Mounted
50	2129.56	47.4	56.7	21.0	2.673	Mounted
51	2129.86	57.1	67.3	21.7	2.673	Mounted
		Core 2				
52	2130.26	0.017	0.033	8.9	2.697	
53	2130.59	16.7	18.9	20.2	2.688	
54	2130.79	0.260	0.399	14.8	2.694	
55	2131.13	7.86	9.00	18.8	2.687	
56	2131.43	39.3	42.2	20.9	2.681	
57	2131.73	22.4	24.4	19.9	2.678	
58	2132.06	8.35	9.57	19.2	2.678	
59	2132.37	3.94	4.64	17.9	2.679	
60	2132.63	14.7	16.4	20.0	2.674	
61	2132.94	16.8	18.8	20.1	2.672	
62	2133.24	16.3	18.2	20.3	2.678	
63	2133.55	24.5	27.0	20.5	2.668	
64	2133.89	27.5	29.8	21.1	2.696	
65	2134.10	24.2	26.3	20.2	2.684	
66	2134.45	303	379	25.4	2.670	Mounted (Fractured)
67	2134.75	83.0	95.6	22.7	2.673	Mounted
68	2135.14	17.0	19.6	19.2	2.679	Mounted
69	2135.30	0.008	0.021	10.6	2.690	
70	2135.59	10.9	13.9	17.3	2.676	
71	2135.91	0.086	0.149	12.3	2.680	
72	2136.19	0.192	0.312	15.0	2.674	
73	2136.44	9.20	10.5	19.5	2.666	
74	2136.82	58.3	67.0	22.1	2.819	Mounted
75	2137.04	36.7	43.7	20.3	2.675	Mounted
76	2137.38	33.4	41.4	19.5	2.677	Mounted
77	2137.72	39.7	45.6	20.7	2.679	Mounted
78	2137.95	37.0	42.5	18.7	2.685	Mounted
79	2138.31	27.7	32.3	20.5	2.678	Mounted
80	2138.59	67.4	70.8	22.4	2.680	
81	2138.88	38.7	41.4	21.1	2.669	
82	2139.18	0.859	1.15	16.1	2.677	
83	2139.48	0.011	0.029	10.5	2.687	
84	2139.80	10.5	11.7	19.7	2.667	
85	2140.10	41.8	45.1	20.9	2.659	
86	2140.40	55.9	59.3	21.2	2.662	
87	2140.71	140	148	22.9	2.659	
88	2141.05	78.5	82.9	22.1	2.675	
89	2141.35	0.168	0.275	12.7	2.689	
90	2141.70	0.306	0.456	12.4	2.674	
91	2142.03	0.157	0.240	11.0	2.658	
92	2142.34	0.129	0.213	11.9	2.691	
93	2142.64	0.023	0.039	8.3	2.695	
94	2144.61	0.019	0.052	14.0	2.690	

POROSITY, PERMEABILITY and GRAIN DENSITY (AMBIENT)

SAMPLE NUMBER	DEPTH (m)	AMBIENT CONDITIONS			GRAIN DENSITY (g/cc)	COMMENTS
		PERMEABILITY		POROSITY (%)		
		Kinf (md)	Kair (md)			
95	2145.63	0.077	0.123	13.2	2.631	
96	2145.84	0.039	0.073	13.2	2.650	
97	2146.61	0.010	0.027	11.0	2.680	

APPENDIX 3

Special Core Analysis

CORE LABORATORIES AUSTRALIA PTY LTD

447-449 Belmont Ave, Kewdale, Perth WA 6105
Tel : (61 8) 9353 3944 Fax : (61 8) 9353 1369
Email : corelab.australia@corelab.com

A Special Core Analysis Study of Selected Samples From Well : LONGTOM-2 ST1

Prepared for
Apache Energy Limited

June 2005

File: PRP-04110A

Rock Properties
Core Laboratories Australia Pty. Ltd.
Perth
Australia

CORE LABORATORIES
AUSTRALIA PTY LTD

June 15th, 2005

APACHE ENERGY LIMITED.
Level 3, 256 St. George's Terrace
Perth, WA 6000

Attention : Robert Benkovic

Subject: A Special Core Analysis Study
Well : Longtom-2 ST1
File : PRP-04110A

Dear Robert,

Presented herein is the final report of a Special Core Analysis study conducted on selected samples from the subject well.

Thank you for the opportunity to have been of service to Apache Energy Limited. If you have any questions regarding these results or if we can be of any further assistance please do not hesitate to contact us.

Yours sincerely,
Core Laboratories Australia Pty Ltd

Ajit Singh
Supervisor - Rock Properties Perth

ABN. 67 065 540 838
P.O Box 785 Cloverdale, WA 6105 Australia Tel : (61-8) 9353 3944 Fax : (61-8) 9353 1369
Email : corelab.australia@corelab.com

CONTENTS

SECTION 1
INTRODUCTION & SUMMARY

INTRODUCTION

Nineteen core plug samples, taken from the Longtom-2 ST1 well, were identified for the Special Core Analysis (SCAL) programme. These samples had previously undergone Routine Core Analysis (RCA) measurements (our file ref : PRP-04110).

On completion of visual and CT-screening, a sub-set of eleven samples was selected to undergo the following special core analyses :

- Formation resistivity factor at NOBP
- Formation resistivity index at NOBP
- Air-brine capillary pressure by centrifuge
- Capillary pressure by mercury injection analysis
- Pore size distribution from mercury injection analysis
- Centrifuge water-gas relative permeability (end-point) analysis

With the exception of sample 82, which was selected for mercury injection analysis only, the remaining ten samples underwent all of the above analyses.

Preliminary reporting of all SCAL results was completed on 18th April 2005.

Information on the brine salinity (35,000 ppm) was given by Apache in an e-mail dated 7th February 2005.

SUMMARY OF RESULTS

Routine Core Analysis

Eleven core plug samples taken from the Longtom-2 ST1 well were selected to undergo special core analysis testing. The selected samples' porosity values ranged from 15.7 to 21.9% whilst permeability (Kair) values range from 1.13 to 77.7 md. Grain density values ranged from 2.666 to 2.689 g/cc.

Electrical Measurements

Results from the formation resistivity factor measurements are presented in both tabular and graphical formats within SECTION 2 of this report. Assuming an intercept, "a", of 1.00, the composite plot exhibits an average value for the cementation exponent, "m" of 2.06.

Resistivity measurements taken of the partially saturated samples yielded values of resistivity index ranging from 1.52 to 11.11. Resistivity index results are presented both in tabular and graphical formats within pages 2-2 to 2-14. The composite resistivity index plot yields an average saturation exponent "n" of 2.12.

Air-Brine Capillary Pressure

At the maximum air-brine capillary pressure of 200 psi, the selected samples yielded immobile water saturation (Swi) values between 26.2 and 52.0% pore volume (pv). Graphical summary of air permeability versus Swi indicates the expected relationship of increasing Swi with decreasing permeability.

Air–brine capillary pressure data is presented within SECTION 3 of this report.

Pore Size Distribution from Mercury Injection Analysis

Capillary pressure by mercury injection analyses were conducted on eleven samples. At the maximum 2,000 psia injection pressure, mercury saturation in the pore spaces varied from 53.9% to 79.0% pore volume (pv).

From the calculated pore size distribution data, the median pore throat radii varied from approximately 0.071 to 0.53 microns.

Results from the pore size distribution analysis are presented within SECTION 3 of this report.

Centrifuge Water-Gas Relative Permeability (End-Point) Analysis

Residual gas saturations (Sgr) from water-displacing-gas relative permeability analysis ranged between 10.2 and 20.6 % pv (average – 16.0% pv). Gas recoveries ranged between 66.0 and 76.3 % initial gas-in-place (average – 72.6% IGIP).

Results from the centrifuge water-gas relative permeability tests are presented within SECTION 4 of this report.

Sample identification and base data

Sample no.	Depth (m)	At 1800 psi NOBP			Grain Density (g/cc)	CT (Pass/Fail)
		Kinf (md)	Kair (md)	Porosity (%)		
25*	2120.45	20.0	23.6	18.9	2.675	Pass
29*	2121.65	5.38	6.43	18.5	2.689	Pass
30	2121.93	14.3	15.9	20.0	2.710	Fail
45*	2128.06	55.9	65.0	21.2	2.672	Pass
47	2128.66	28.2	31.9	20.1	2.674	Pass
48	2128.94	51.0	57.0	21.2	2.678	Fail
50*	2129.56	28.9	32.9	20.3	2.673	Pass
55*	2131.13	6.81	7.79	18.3	2.687	Pass
58	2132.06	7.62	8.71	18.7	2.678	Pass
63	2133.55	22.3	24.5	20.0	2.668	Fail
64	2133.89	20.9	22.8	20.5	2.696	Fail
67*	2134.75	56.4	62.3	21.9	2.673	Pass
73*	2136.44	7.93	9.06	19.0	2.666	Pass
76*	2137.38	16.0	19.3	18.8	2.677	Pass
80	2138.59	63.4	66.7	21.9	2.680	Pass
81*	2138.88	36.2	38.7	20.6	2.669	Pass
82*	2139.18	0.981	1.13	15.7	2.677	NA
87	2140.71	132	139	22.3	2.659	Pass
88*	2141.05	73.5	77.7	21.5	2.675	Pass

* SCAL selected samples.

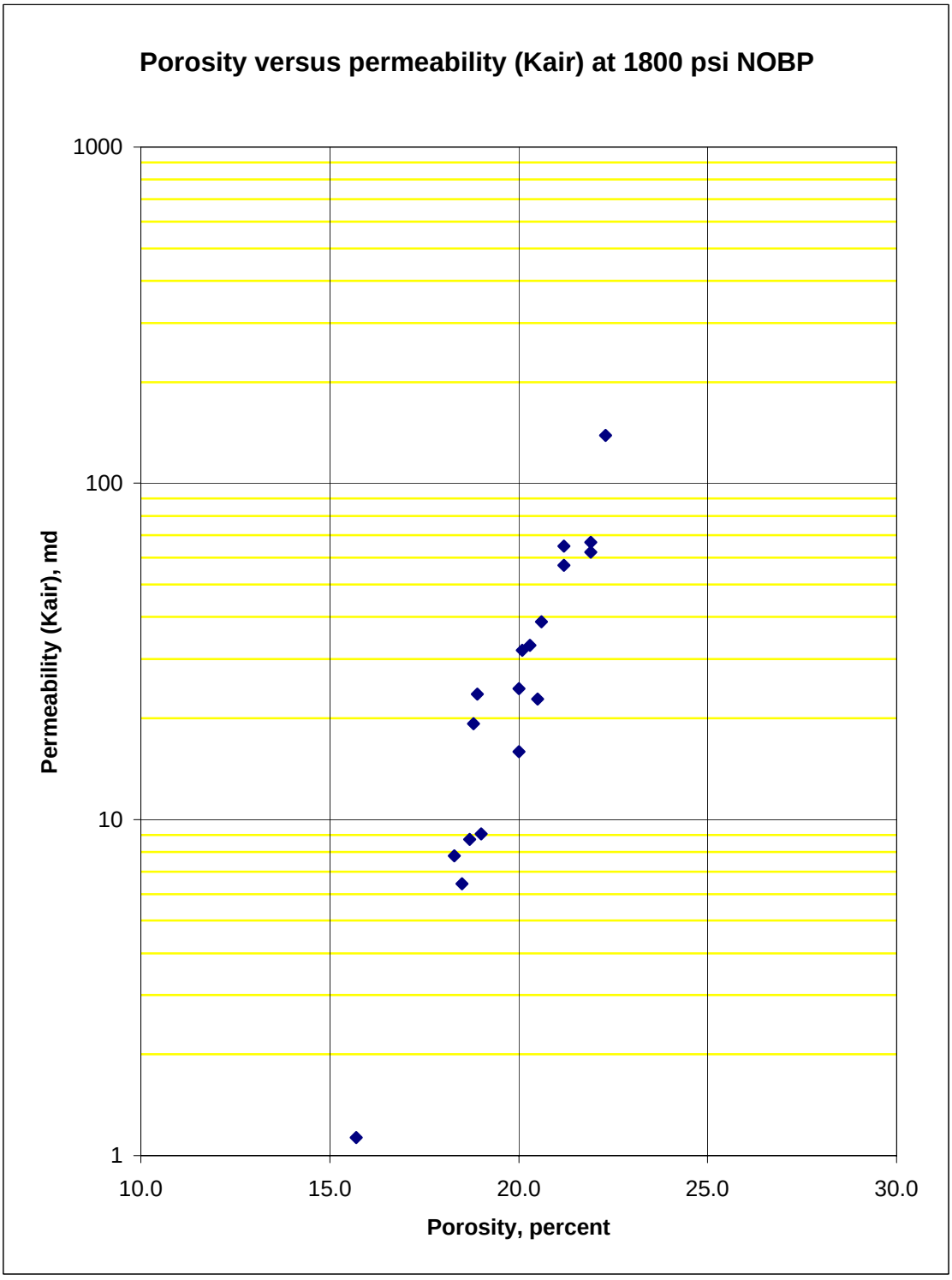
Porosity versus permeability (Kair) at 1800 psi NOBP
1000
100
10
1
Permeability (Kair), md
10.0
15.0
20.0
25.0
30.0
Porosity, percent

SECTION 2
ELECTRICAL PROPERTIES

Formation resistivity factor (FRF) at 1800 psi NOBP

Sample no.	Depth (metres)	Grain Density g/cc	At 1800 PSI NOBP				
			Kinf (%)	Kair (%)	Porosity (%)	FRF	m
25	2120.45	2.675	20.0	23.6	18.9	30.94	2.06
29	2121.65	2.689	5.38	6.43	18.5	30.68	2.03
45	2128.06	2.672	55.9	65.0	21.2	25.44	2.08
50	2129.56	2.673	28.9	32.9	20.3	29.43	2.12
55	2131.13	2.687	6.81	7.79	18.3	32.84	2.06
67	2134.75	2.673	56.4	62.3	21.9	22.33	2.05
73	2136.44	2.666	7.93	9.06	19.0	30.81	2.06
76	2137.38	2.677	16.0	19.3	18.8	35.40	2.13
81	2138.88	2.669	36.2	38.7	20.6	24.30	2.02
88	2141.05	2.675	73.5	77.7	21.5	22.52	2.03
			Average Cementation Exponent "m"				**2.06**

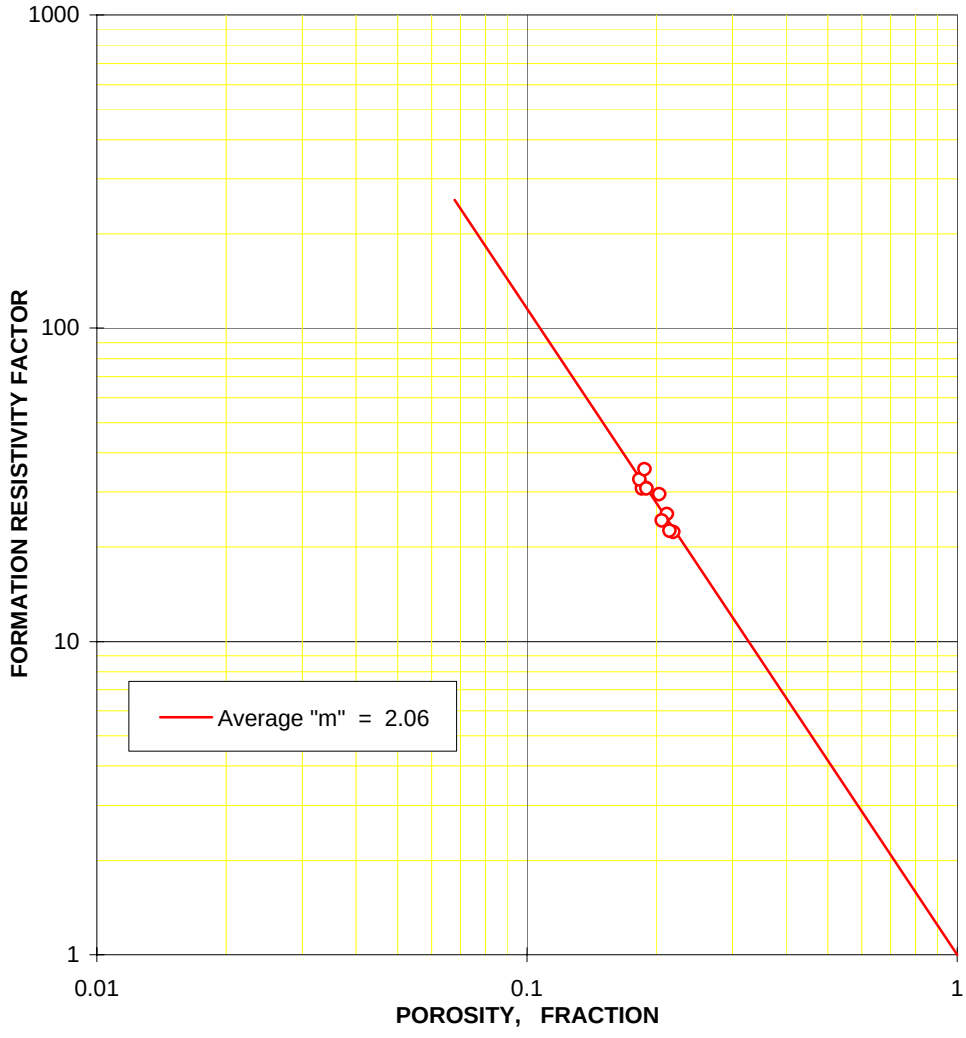

Formation resistivity index at 1800 psi NOBP - Composite Table

(with simulated formation brine)

Sample no.	Depth (metres)	Grain density (g/cc)	Determined at 1800 psi NOBP				
			Perm. to air (md)	Porosity (%)	Brine saturation (%pv)	Resistivity index	Sat. Exp. n
25	2120.45	2.675	23.6	18.9	100.0	1.00	-
					80.1	1.58	2.05
					73.9	1.92	2.15
					63.9	2.60	2.14
					56.5	3.52	2.20
					37.6	7.09	2.00
29	2121.65	2.689	6.43	18.5	100.0	1.00	-
					82.7	1.52	2.21
					73.0	2.06	2.30
					64.4	2.58	2.15
					56.7	3.22	2.06
					52.0	3.93	2.09
45	2128.06	2.672	65.0	21.2	100.0	1.00	-
					69.3	1.97	1.84
					61.4	2.59	1.96
					47.1	5.09	2.16
					34.1	7.78	1.91
					28.3	10.09	1.83
50	2129.56	2.673	32.9	20.3	100.0	1.00	-
					78.7	1.67	2.13
					70.7	2.08	2.12
					57.1	3.26	2.11
					45.8	5.30	2.13
					34.6	7.42	1.89
55	2131.13	2.687	7.79	18.3	100.0	1.00	-
					76.4	1.84	2.26
					71.0	2.18	2.27
					63.6	2.70	2.19
					59.8	3.43	2.40
					52.0	4.49	2.30
67	2134.75	2.673	62.3	21.9	100.0	1.00	-
					69.7	2.09	2.04
					59.6	2.99	2.12
					46.2	5.45	2.20
					38.3	7.88	2.15
					28.3	11.11	1.91

Formation resistivity index at 1800 psi NOBP - Composite Table

(with simulated formation brine)

Sample no.	Depth (metres)	Grain density (g/cc)	Determined at 1800 psi NOBP				
			Perm. to air (md)	Porosity (%)	Brine saturation (%pv)	Resistivity index	Sat. Exp. n
73	2136.44	2.666	9.06	19.0	100.0	1.00	-
					82.5	1.55	2.29
					74.5	1.90	2.18
					64.7	2.46	2.07
					58.4	3.20	2.16
					51.9	4.13	2.16
76	2137.38	2.677	19.3	18.8	100.0	1.00	-
					71.0	2.08	2.13
					61.8	2.83	2.16
					55.2	3.54	2.13
					45.7	4.95	2.04
					40.7	5.16	1.83
81	2138.88	2.669	38.7	20.6	100.0	1.00	-
					61.8	3.03	2.30
					53.7	3.99	2.23
					45.8	5.87	2.27
					40.7	6.67	2.11
					34.0	7.96	1.92
88	2141.05	2.675	77.7	21.5	100.0	1.00	-
					68.4	2.59	2.51
					58.9	3.44	2.33
					51.8	4.31	2.22
					44.7	5.05	2.01
					29.2	10.74	1.93
					Average Exponent		2.12

Composite Graph - Formation Resistivity Index at 1800 psi NOBP

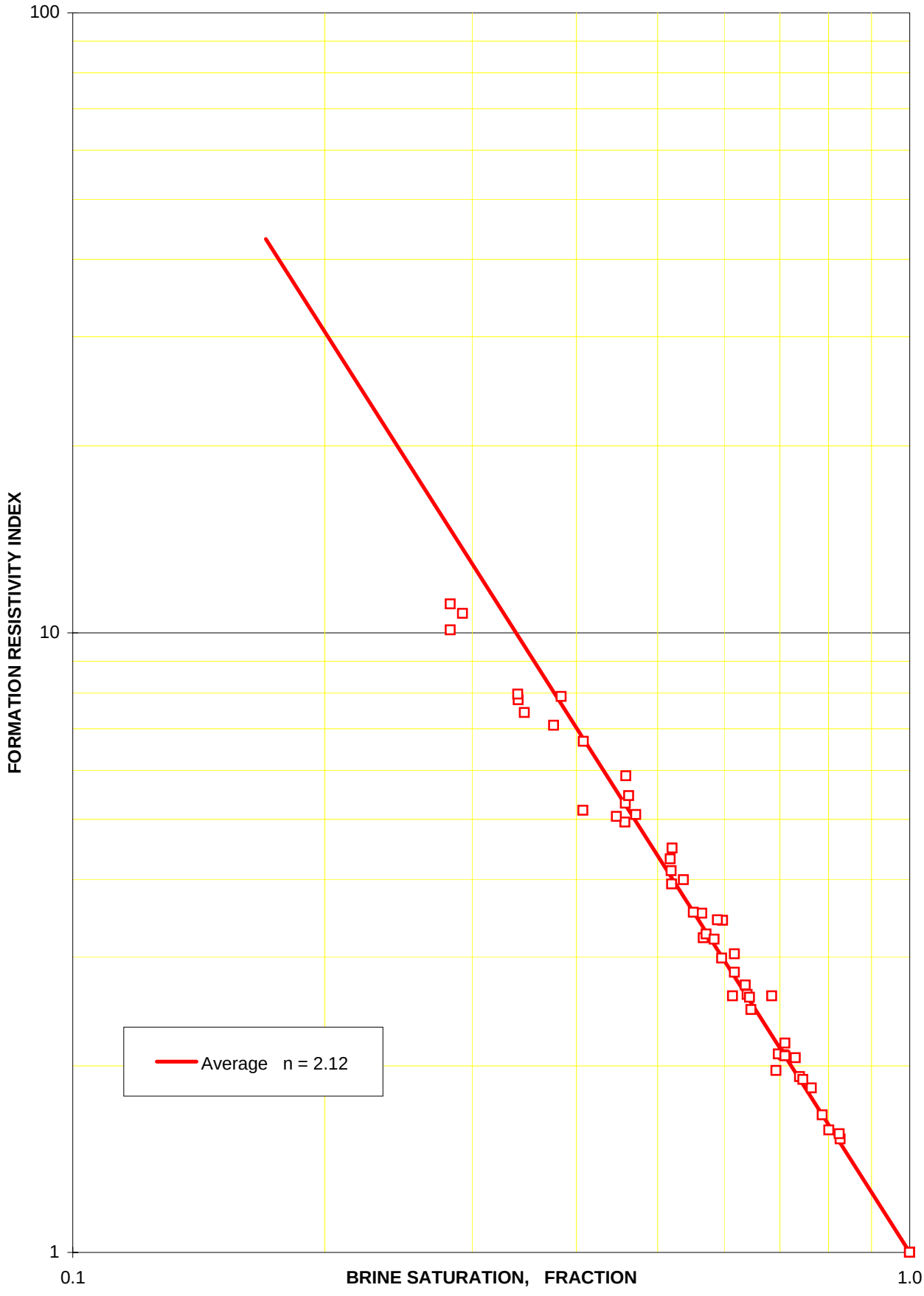

Formation resistivity index at 1800 psi NOBP

(with simulated formation brine)

Sample no.	Depth (metres)	Grain density (g/cc)	Determined at 1800 psi NOBP				
			Perm. to air (md)	Porosity (%)	Brine saturation (%pv)	Resistivity index	Sat. Exp. n
25	2120.45	2.675	23.6	18.9	100.0	1.00	-
					80.1	1.58	2.05
					73.9	1.92	2.15
					63.9	2.60	2.14
					56.5	3.52	2.20
					37.6	7.09	2.00

FRF at NOBP	30.94
Rw at 25°C, ohm-m	0.182

Average Exponent	2.11

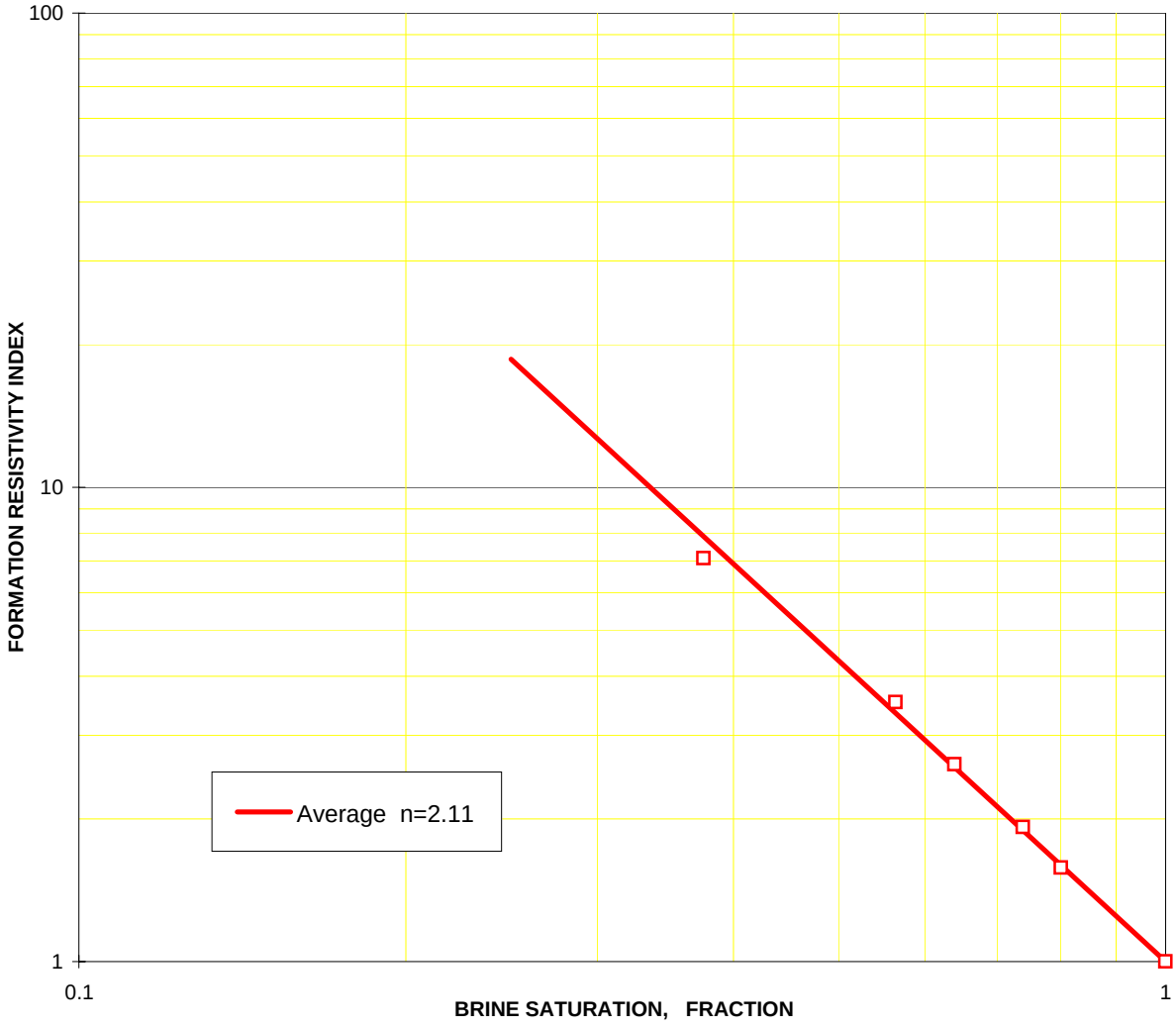

Formation resistivity index at 1800 psi NOBP

(with simulated formation brine)

Sample no.	Depth (metres)	Grain density (g/cc)	Determined at 1800 psi NOBP				
			Perm. to air (md)	Porosity (%)	Brine saturation (%pv)	Resistivity index	Sat. Exp. n
29	2121.65	2.689	6.43	18.5	100.0	1.00	-
					82.7	1.52	2.21
					73.0	2.06	2.30
					64.4	2.58	2.15
					56.7	3.22	2.06
					52.0	3.93	2.09

FRF at NOBP	30.68
Rw at 25°C, ohm-m	0.182

Average Exponent	2.16

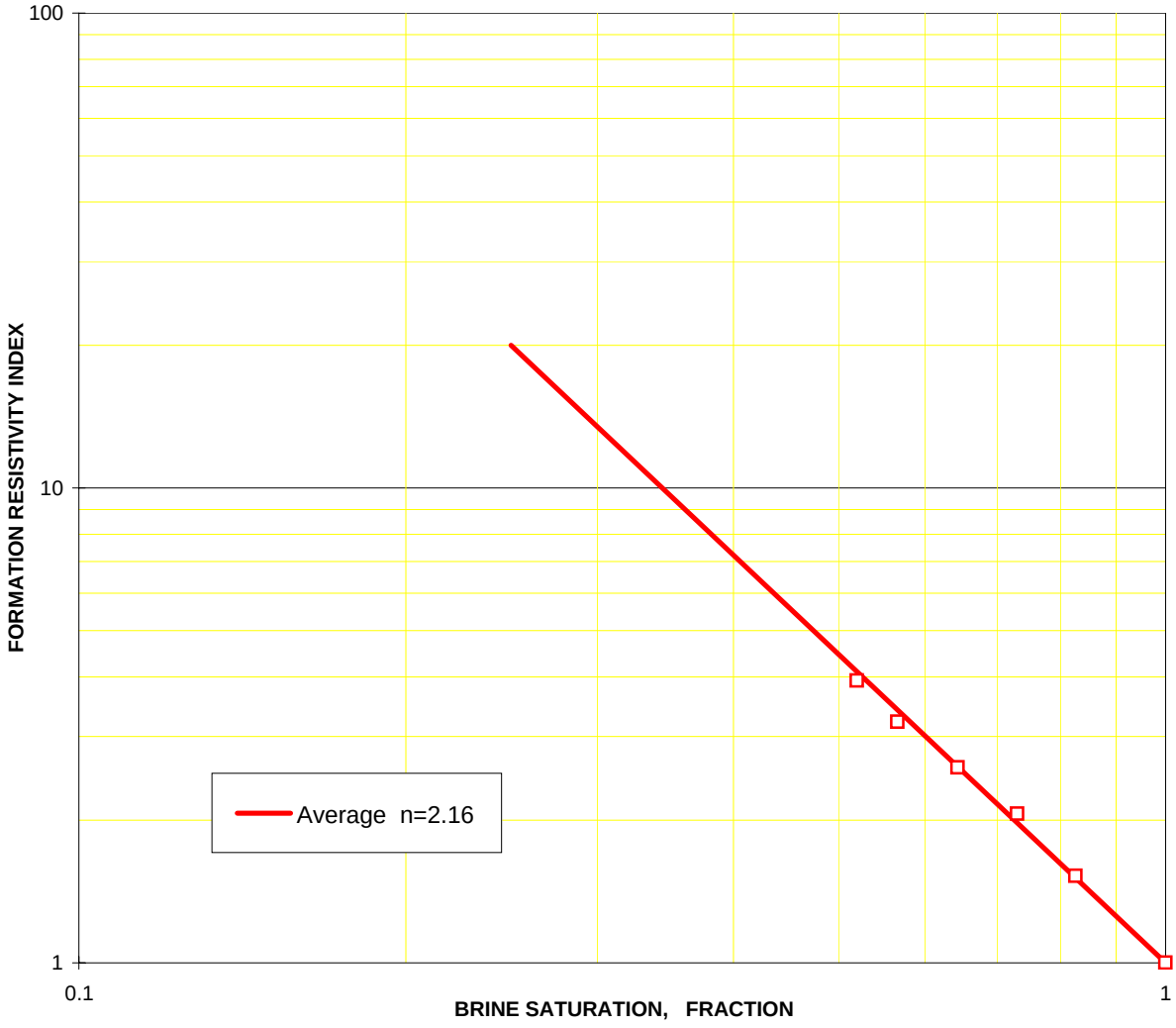

Formation resistivity index at 1800 psi NOBP

(with simulated formation brine)

Sample no.	Depth (metres)	Grain density (g/cc)	Determined at 1800 psi NOBP				
			Perm. to air (md)	Porosity (%)	Brine saturation (%pv)	Resistivity index	Sat. Exp. n
45	2128.06	2.672	65.0	21.2	100.0	1.00	-
					69.3	1.97	1.84
					61.4	2.59	1.96
					47.1	5.09	2.16
					34.1	7.78	1.91
					28.3	10.09	1.83

FRF at NOBP	25.44
Rw at 25°C, ohm-m	0.182

Average Exponent	1.94

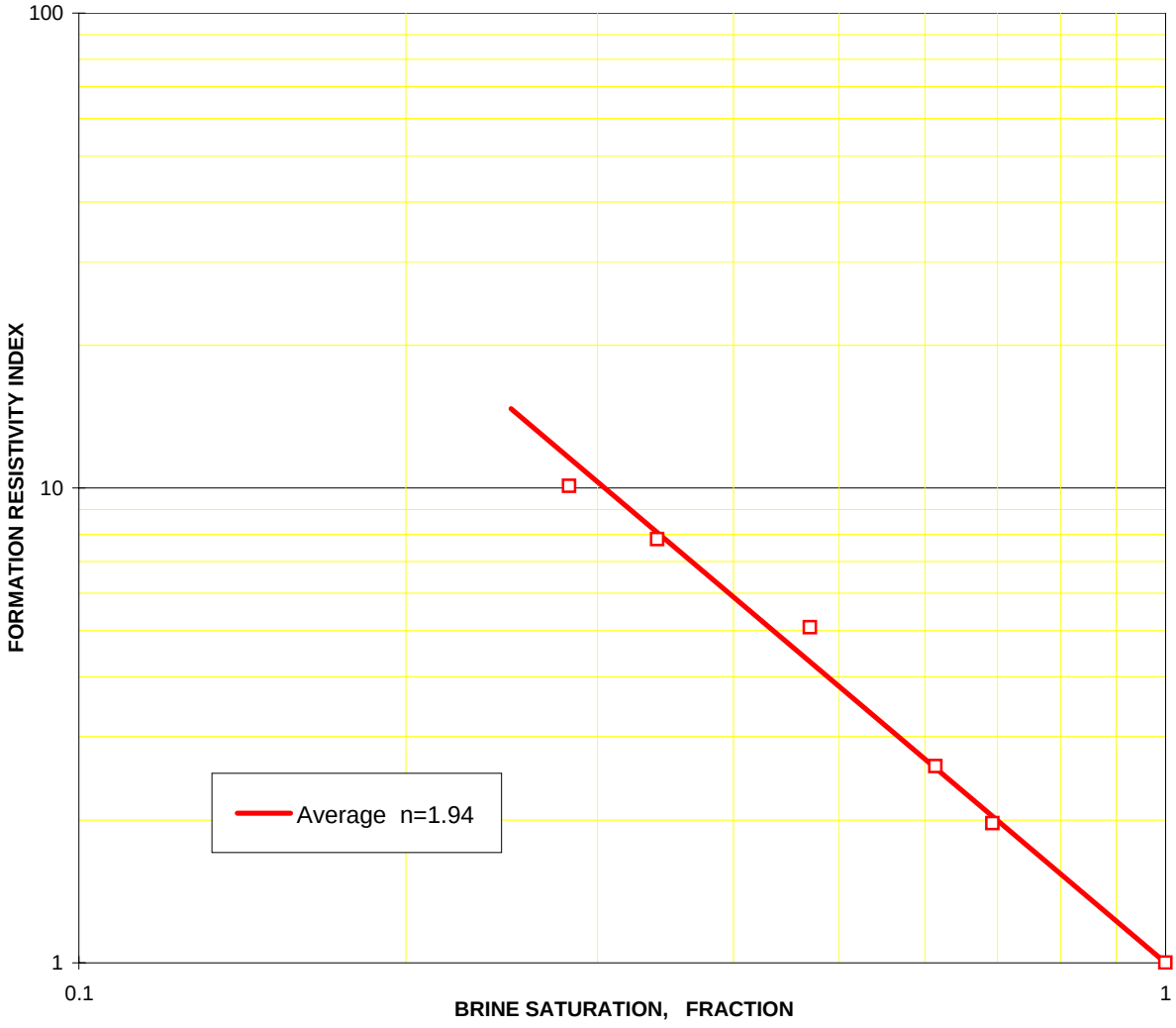

Formation resistivity index at 1800 psi NOBP

(with simulated formation brine)

Sample no.	Depth (metres)	Grain density (g/cc)	Determined at 1800 psi NOBP				
			Perm. to air (md)	Porosity (%)	Brine saturation (%pv)	Resistivity index	Sat. Exp. n
50	2129.56	2.673	32.9	20.3	100.0	1.00	-
					78.7	1.67	2.13
					70.7	2.08	2.12
					57.1	3.26	2.11
					45.8	5.30	2.13
					34.6	7.42	1.89

FRF at NOBP	29.43
Rw at 25°C, ohm-m	0.182

Average Exponent	2.08

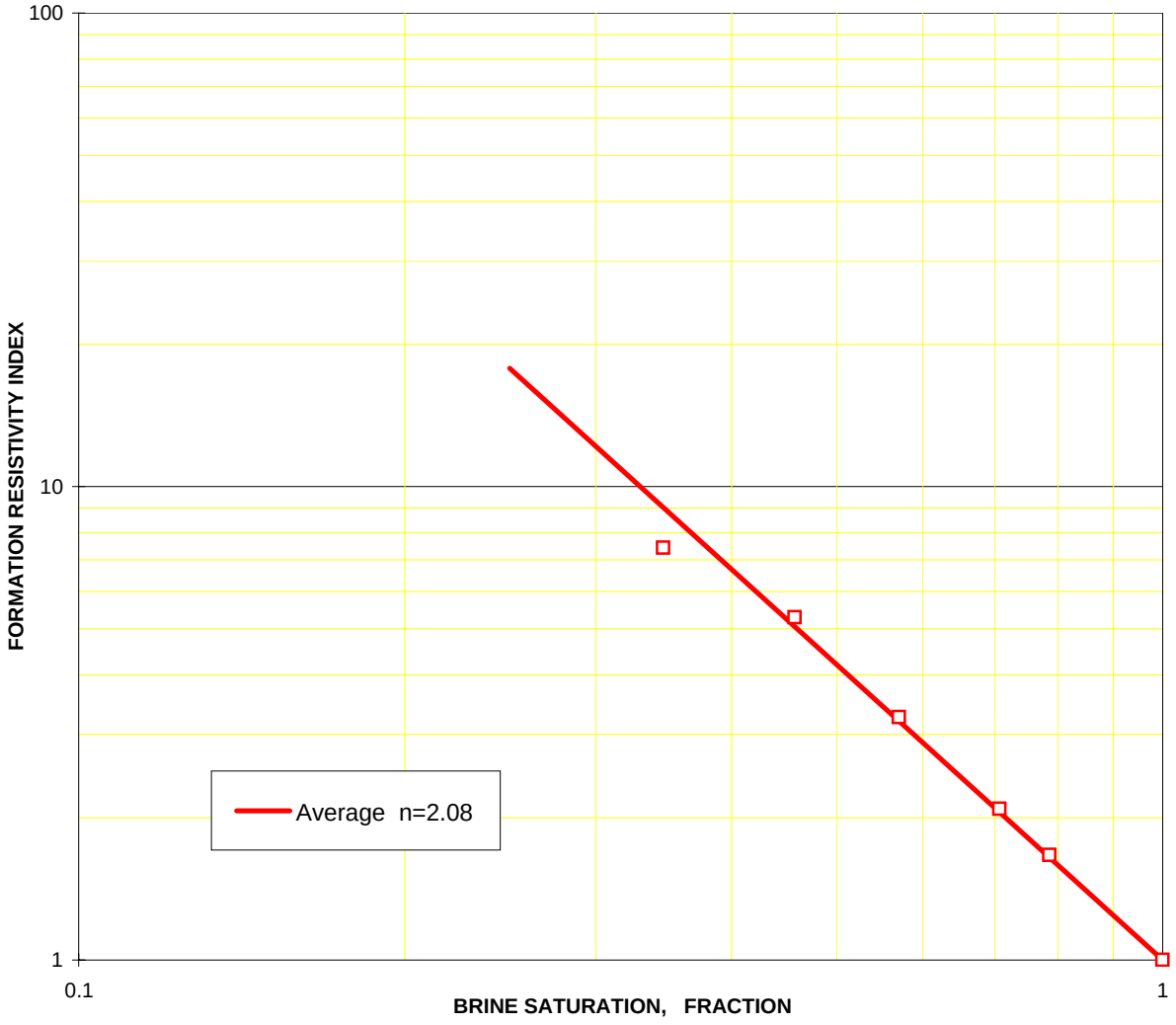

Formation resistivity index at 1800 psi NOBP

(with simulated formation brine)

Sample no.	Depth (metres)	Grain density (g/cc)	Determined at 1800 psi NOBP				
			Perm. to air (md)	Porosity (%)	Brine saturation (%pv)	Resistivity index	Sat. Exp. n
55	2131.13	2.687	7.79	18.3	100.0	1.00	-
					76.4	1.84	2.26
					71.0	2.18	2.27
					63.6	2.70	2.19
					59.8	3.43	2.40
					52.0	4.49	2.30

FRF at NOBP	32.84
Rw at 25°C, ohm-m	0.182

Average Exponent	2.28

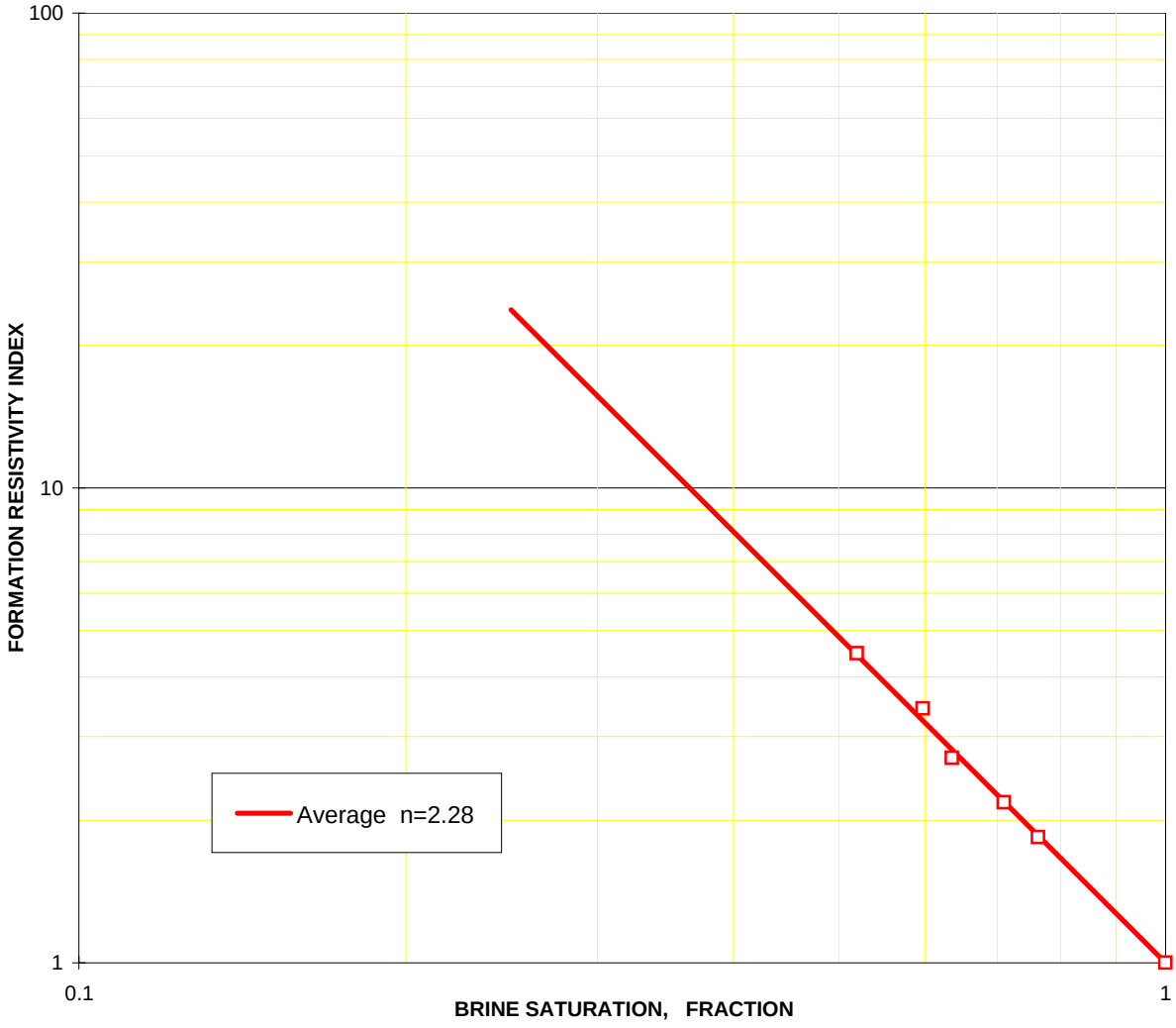

Formation resistivity index at 1800 psi NOBP

(with simulated formation brine)

Sample no.	Depth (metres)	Grain density (g/cc)	Determined at 1800 psi NOBP				
			Perm. to air (md)	Porosity (%)	Brine saturation (%pv)	Resistivity index	Sat. Exp. n
67	2134.75	2.673	62.3	21.9	100.0	1.00	-
					69.7	2.09	2.04
					59.6	2.99	2.12
					46.2	5.45	2.20
					38.3	7.88	2.15
					28.3	11.11	1.91

FRF at NOBP	22.33
Rw at 25°C, ohm-m	0.182

Average Exponent	2.08

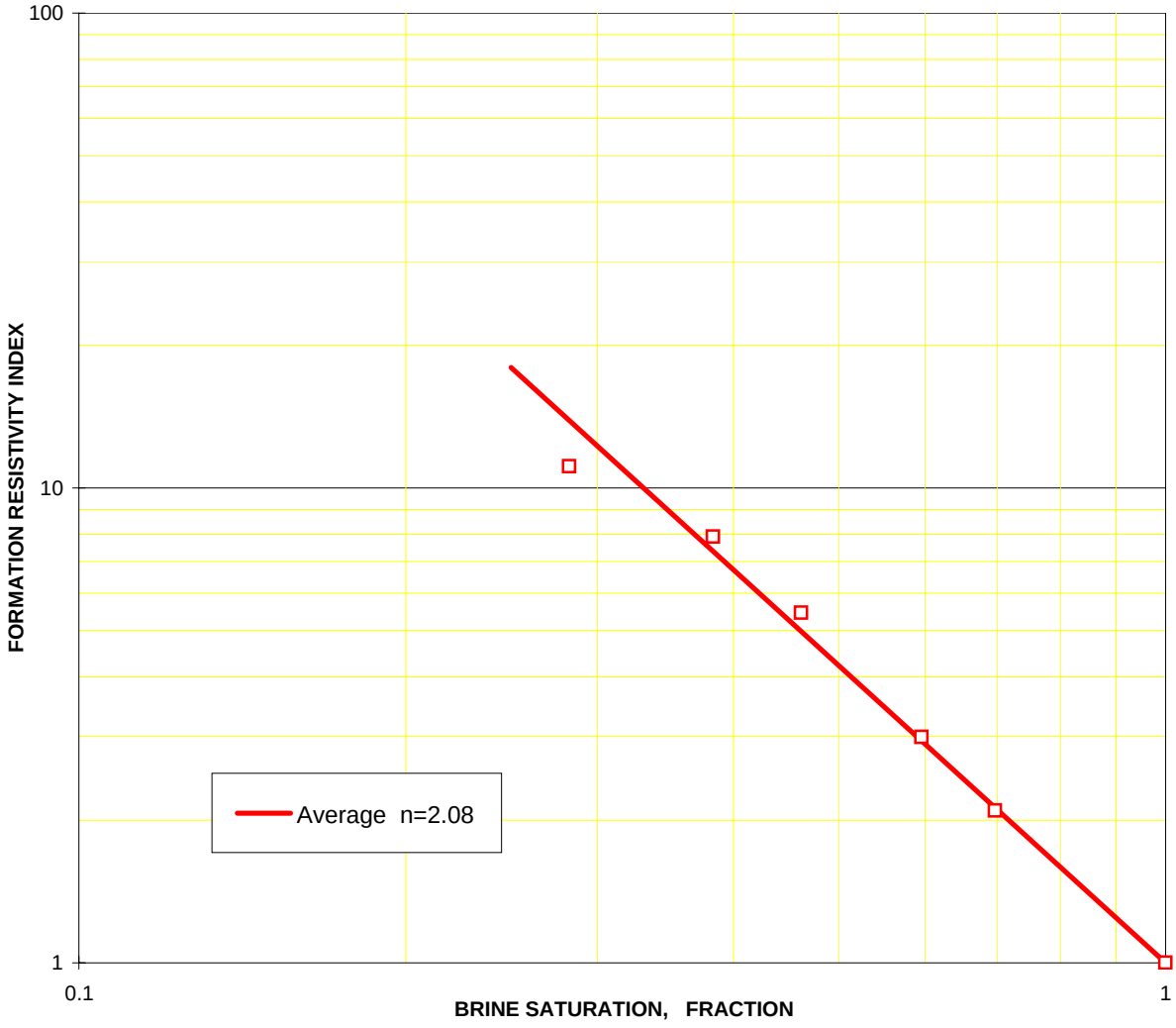

Formation resistivity index at 1800 psi NOBP

(with simulated formation brine)

Sample no.	Depth (metres)	Grain density (g/cc)	Determined at 1800 psi NOBP				
			Perm. to air (md)	Porosity (%)	Brine saturation (%pv)	Resistivity index	Sat. Exp. n
73	2136.44	2.666	9.06	19.0	100.0	1.00	-
					82.5	1.55	2.29
					74.5	1.90	2.18
					64.7	2.46	2.07
					58.4	3.20	2.16
					51.9	4.13	2.16

FRF at NOBP	30.81
Rw at 25°C, ohm-m	0.182

Average Exponent	2.17

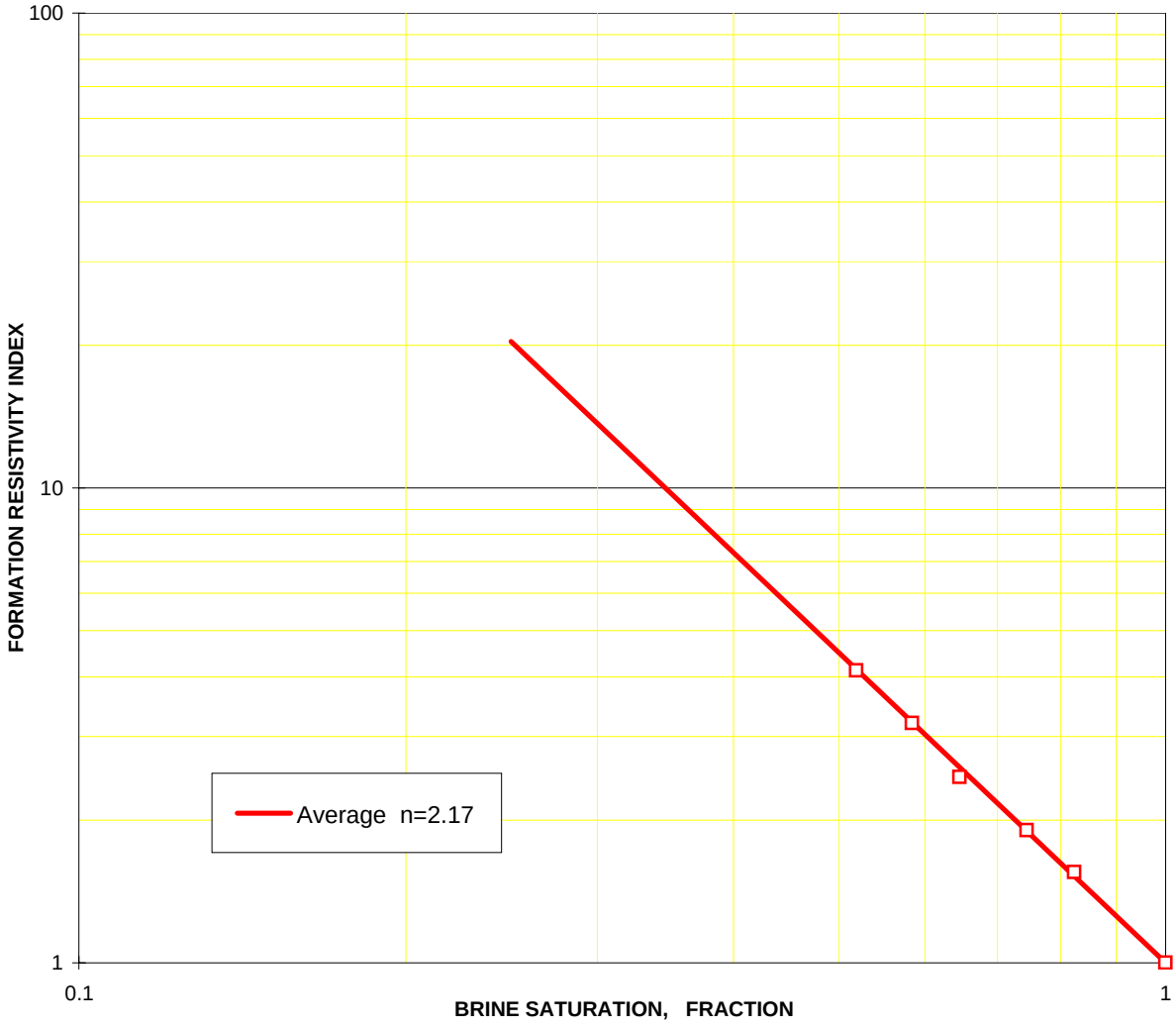

Formation resistivity index at 1800 psi NOBP

(with simulated formation brine)

Sample no.	Depth (metres)	Grain density (g/cc)	Determined at 1800 psi NOBP				
			Perm. to air (md)	Porosity (%)	Brine saturation (%pv)	Resistivity index	Sat. Exp. n
76	2137.38	2.677	19.3	18.8	100.0	1.00	-
					71.0	2.08	2.13
					61.8	2.83	2.16
					55.2	3.54	2.13
					45.7	4.95	2.04
					40.7	5.16	1.83

FRF at NOBP	35.40
Rw at 25°C, ohm-m	0.182

Average Exponent	2.06

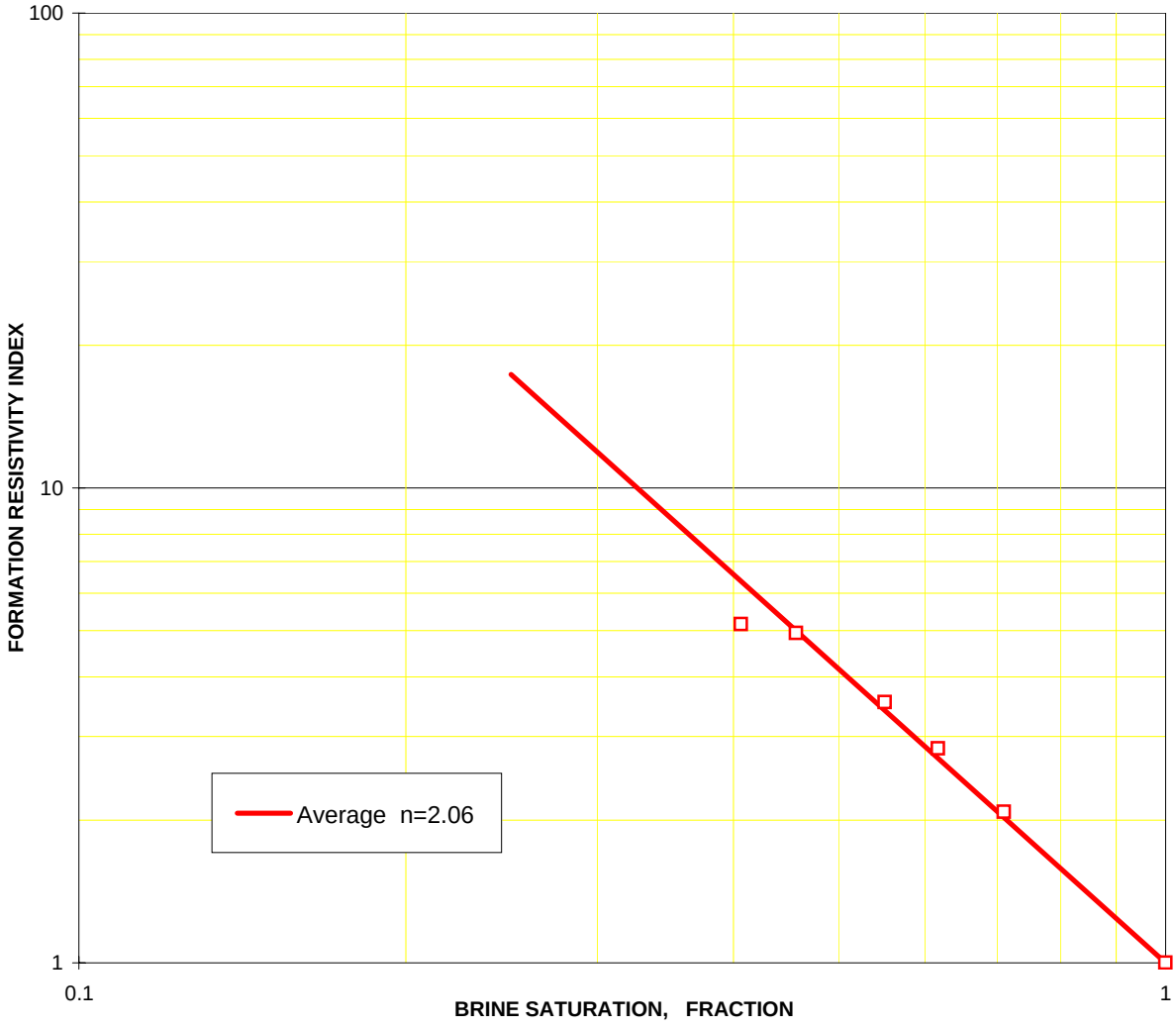

Formation resistivity index at 1800 psi NOBP

(with simulated formation brine)

Sample no.	Depth (metres)	Grain density (g/cc)	Determined at 1800 psi NOBP				
			Perm. to air (md)	Porosity (%)	Brine saturation (%pv)	Resistivity index	Sat. Exp. n
81	2138.88	2.669	38.7	20.6	100.0	1.00	-
					61.8	3.03	2.30
					53.7	3.99	2.23
					45.8	5.87	2.27
					40.7	6.67	2.11
					34.0	7.96	1.92

FRF at NOBP	24.30
Rw at 25°C, ohm-m	0.182

Average Exponent	2.17

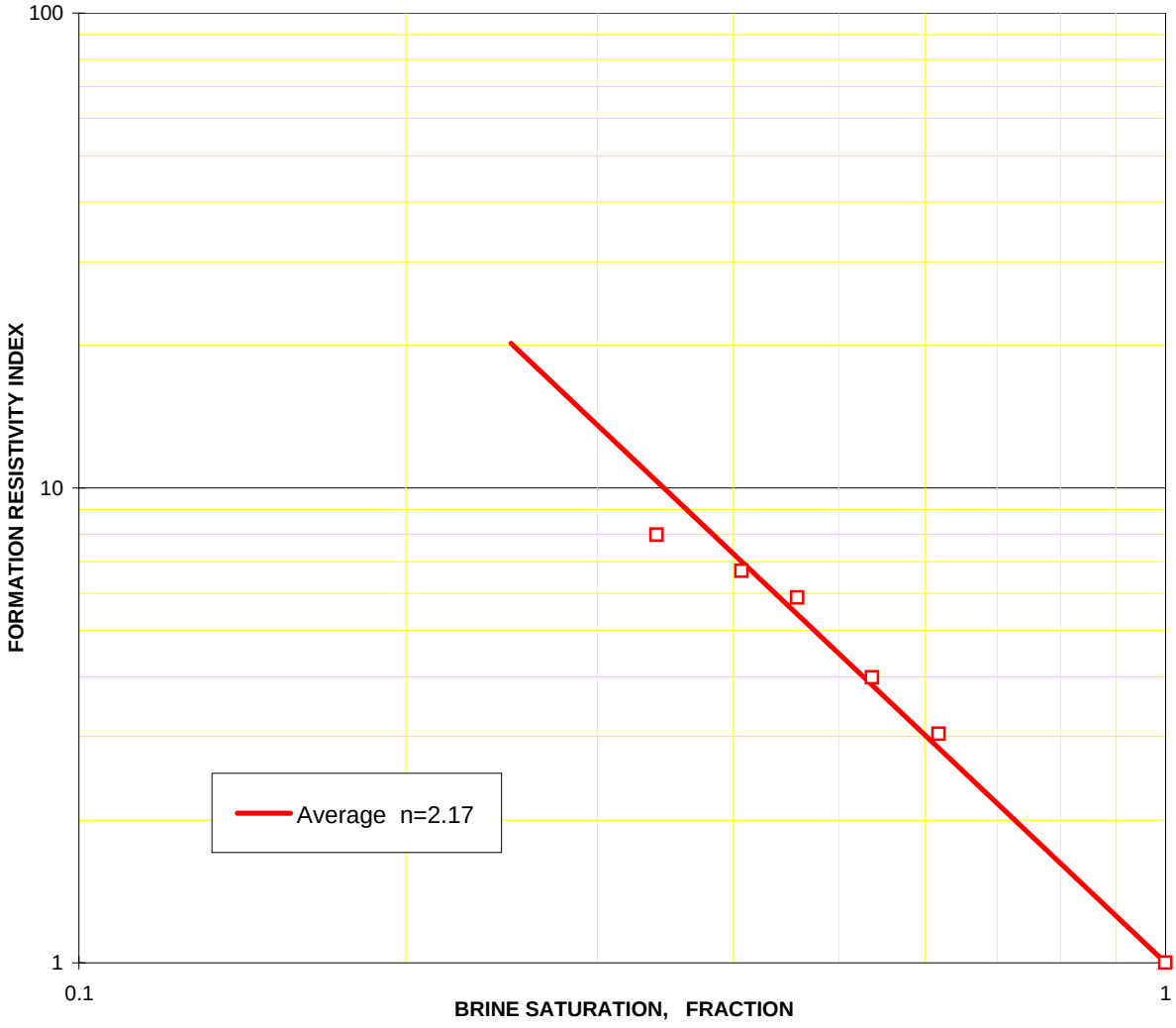

Formation resistivity index at 1800 psi NOBP

(with simulated formation brine)

Sample no.	Depth (metres)	Grain density (g/cc)	Determined at 1800 psi NOBP				
			Perm. to air (md)	Porosity (%)	Brine saturation (%pv)	Resistivity index	Sat. Exp. n
88	2141.05	2.675	77.7	21.5	100.0	1.00	-
					68.4	2.59	2.51
					58.9	3.44	2.33
					51.8	4.31	2.22
					44.7	5.05	2.01
					29.2	10.74	1.93

FRF at NOBP	22.52
Rw at 25°C, ohm-m	0.182

Average Exponent	2.20

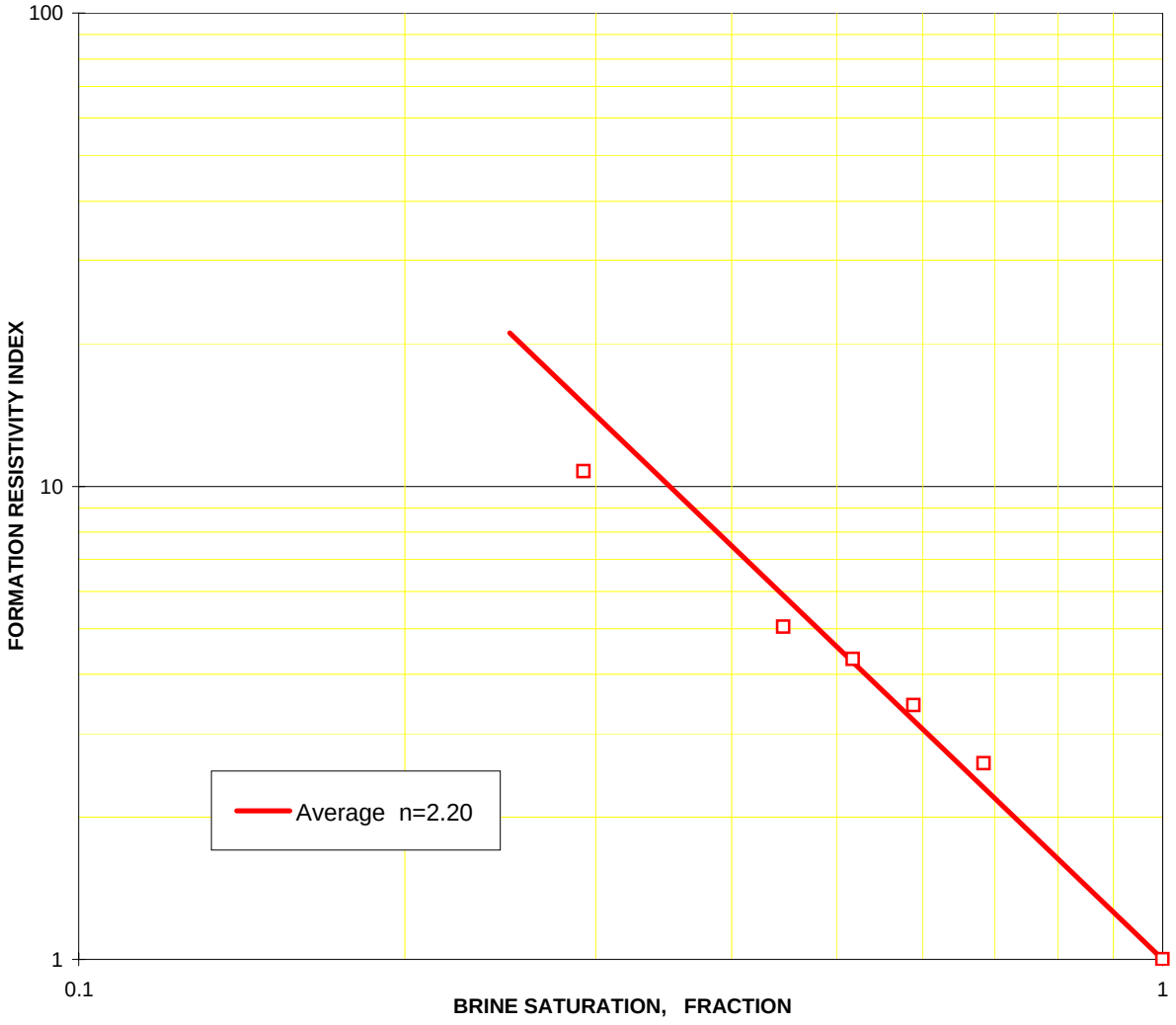

SECTION 3
CAPILLARY PRESSURE
AND
PORE SIZE DISTRIBUTION

COMPANY : APACHE ENERGY LIMITED
WELL : LONGTOM-2 ST1

Summary of air-brine centrifuge capillary pressure data at NOBP

Sample no.	Depth (m)	Kinf (md)	Kair (md)	Porosity (%)	AIR - BRINE CAPILLARY PRESSURE (PSI)								
					0 psi	2 psi	4 psi	8 psi	15 psi	30 psi	60 psi	100 psi	200 psi
					END FACE SATURATION Sw (%PV)								
25	2120.45	20.0	23.6	18.9	100	93.2	88.4	80.0	68.8	54.4	44.0	41.2	37.6
29	2121.65	5.38	6.43	18.5	100	100	93.8	85.2	75.6	66.3	60.1	58.2	52.0
45	2128.06	55.9	65.0	21.2	100	86.2	75.3	62.7	51.8	41.6	33.5	29.2	28.3
50	2129.56	28.9	32.9	20.3	100	100	83.1	68.8	58.2	48.6	40.7	35.9	32.4
55	2131.13	6.81	7.79	18.3	100	98.4	89.2	81.0	75.1	67.3	61.2	57.9	52.0
67	2134.75	56.4	62.3	21.9	100	89.4	78.4	65.5	53.5	41.5	32.2	27.1	26.2
73	2136.44	7.93	9.06	19.0	100	100	92.9	80.0	73.7	67.7	61.6	57.1	51.9
76	2137.38	16.0	19.3	18.8	100	100	86.2	76.0	68.6	59.1	48.2	42.9	40.7
81	2138.88	36.2	38.7	20.6	100	99.1	81.8	68.0	57.8	48.8	41.5	37.1	34.0
88	2141.05	73.5	77.7	21.5	100	79.6	56.4	47.0	40.9	35.3	31.4	29.4	28.1

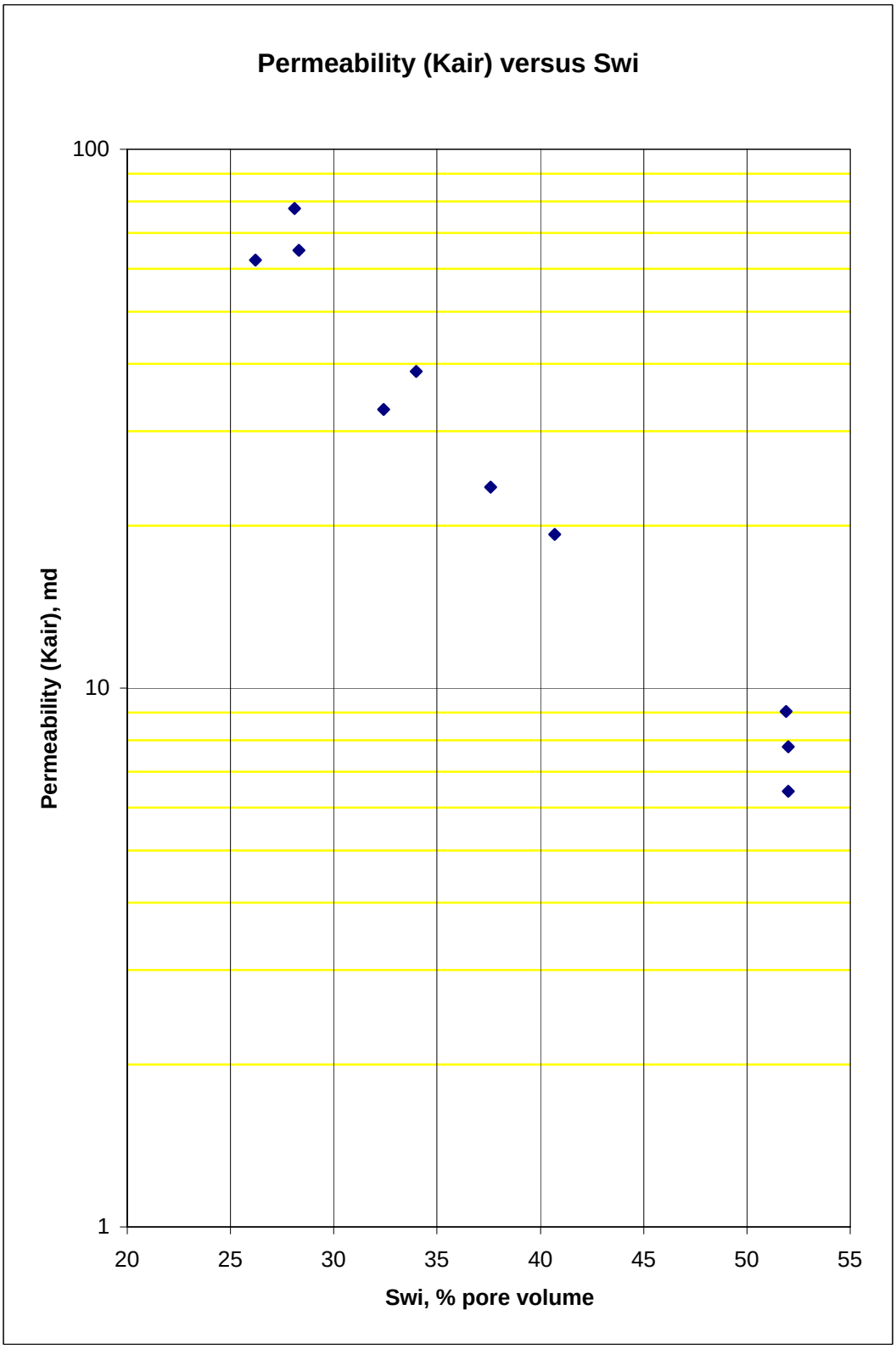
Permeability (Kair) versus Swi
100
10
1
Permeability (Kair), md
20
25
30
35
40
45
50
55
Swi, % pore volume

Air-brine capillary pressure by centrifuge at 1800 psi NOBP

Sample no.	Depth (m)	Determined at 1800 psi NOBP				
		Kinf (md)	Kair (md)	Porosity (%)	Capillary pressure (psi)	Brine saturation (%PV)
25	2120.45	20.0	23.6	18.9	0	100
					2	93.2
					4	88.4
					8	80.0
					15	68.8
					30	54.4
					60	44.0
					100	41.2
					200	37.6

The terminal capillary pressure (200 psi) was obtained by porous-plate desaturation.

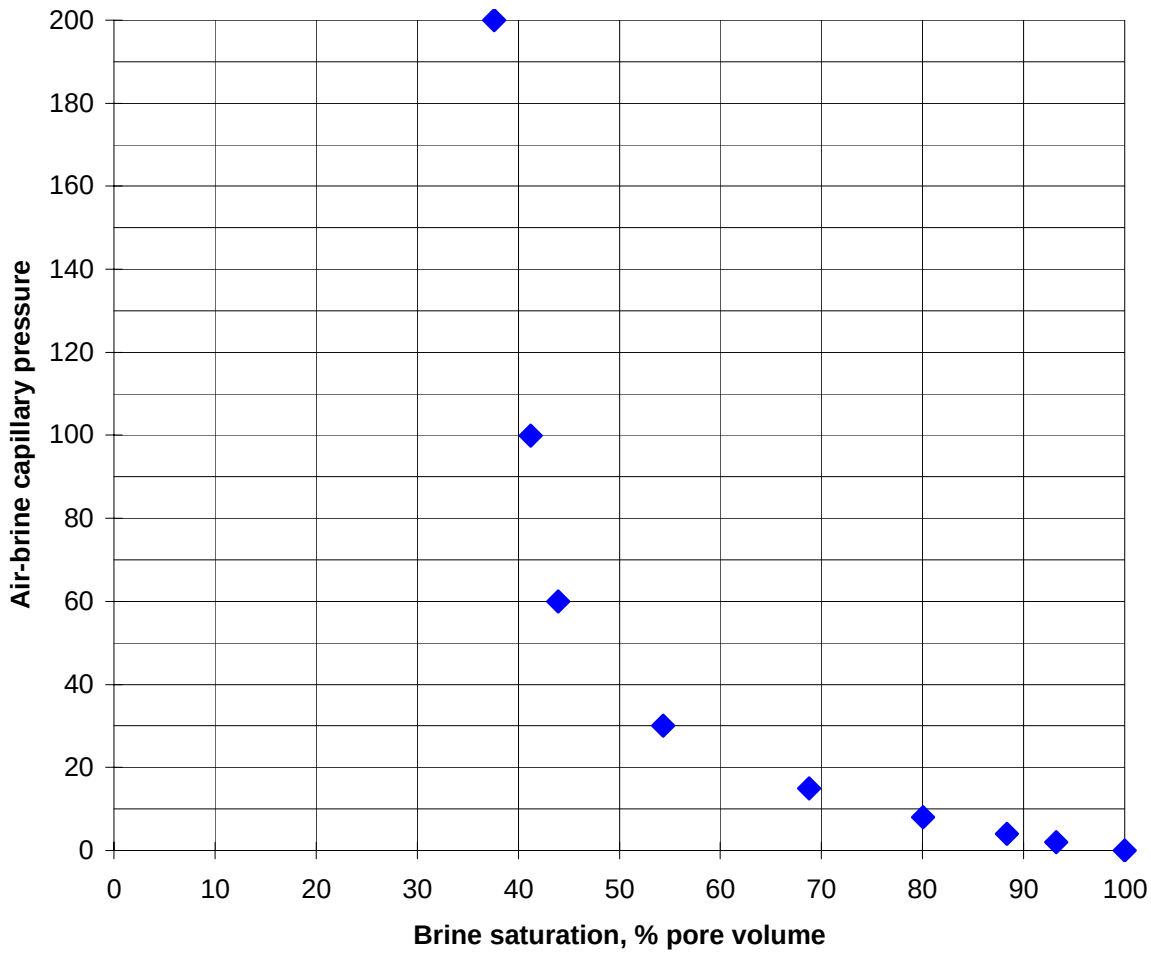

Air-brine capillary pressure by centrifuge at 1800 psi NOBP

Sample no.	Depth (m)	Determined at 1800 psi NOBP				
		Kinf (md)	Kair (md)	Porosity (%)	Capillary pressure (psi)	Brine saturation (%PV)
29	2121.65	5.38	6.43	18.5	0	100
					2	100
					4	93.8
					8	85.2
					15	75.6
					30	66.3
					60	60.1
					100	58.2
					200	52.0

The terminal capillary pressure (200 psi) was obtained by porous-plate desaturation.

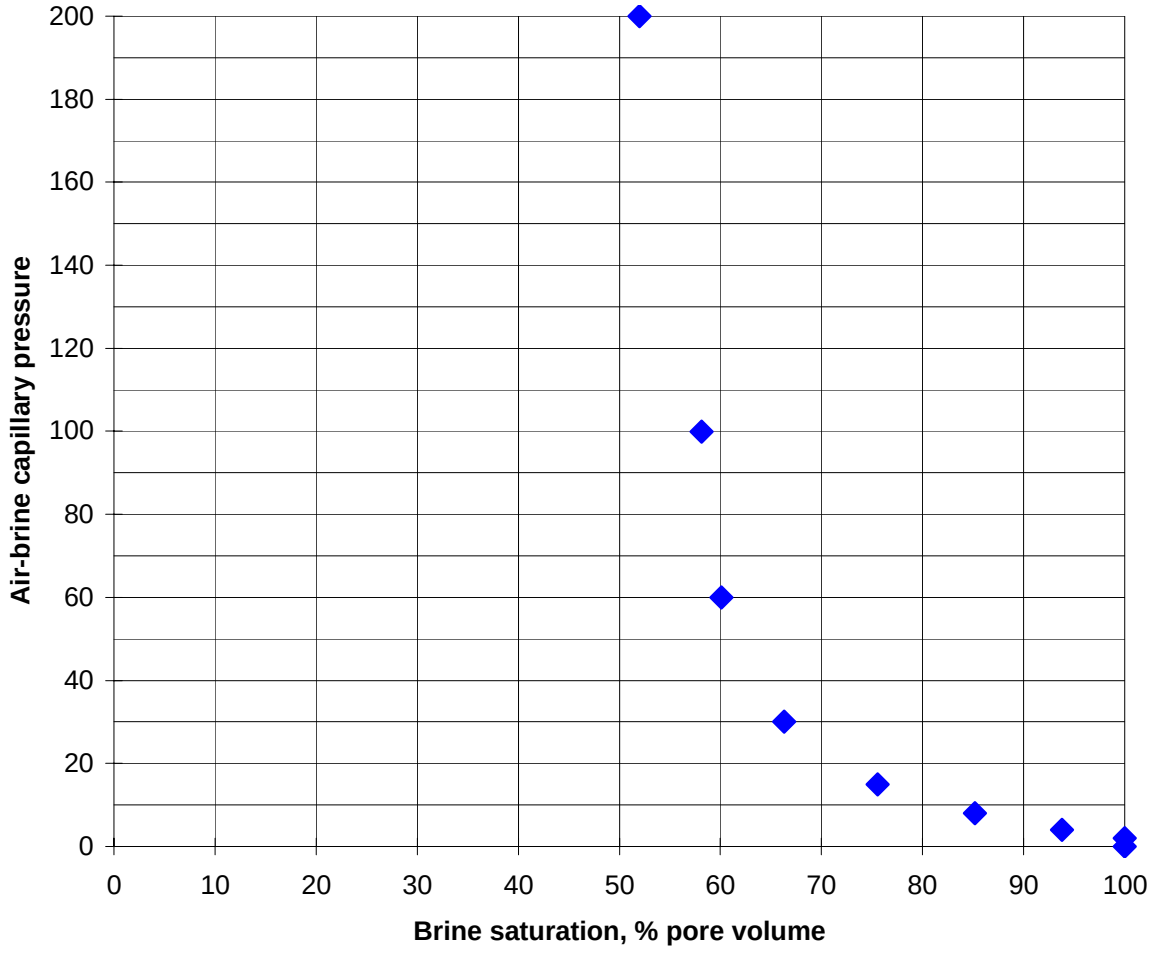

Air-brine capillary pressure by centrifuge at 1800 psi NOBP

Sample no.	Depth (m)	Determined at 1800 psi NOBP				
		Kinf (md)	Kair (md)	Porosity (%)	Capillary pressure (psi)	Brine saturation (%PV)
45	2128.06	55.9	65.0	21.2	0	100
					2	86.2
					4	75.3
					8	62.7
					15	51.8
					30	41.6
					60	33.5
					100	29.2
					200	28.3

The terminal capillary pressure (200 psi) was obtained by porous-plate desaturation.

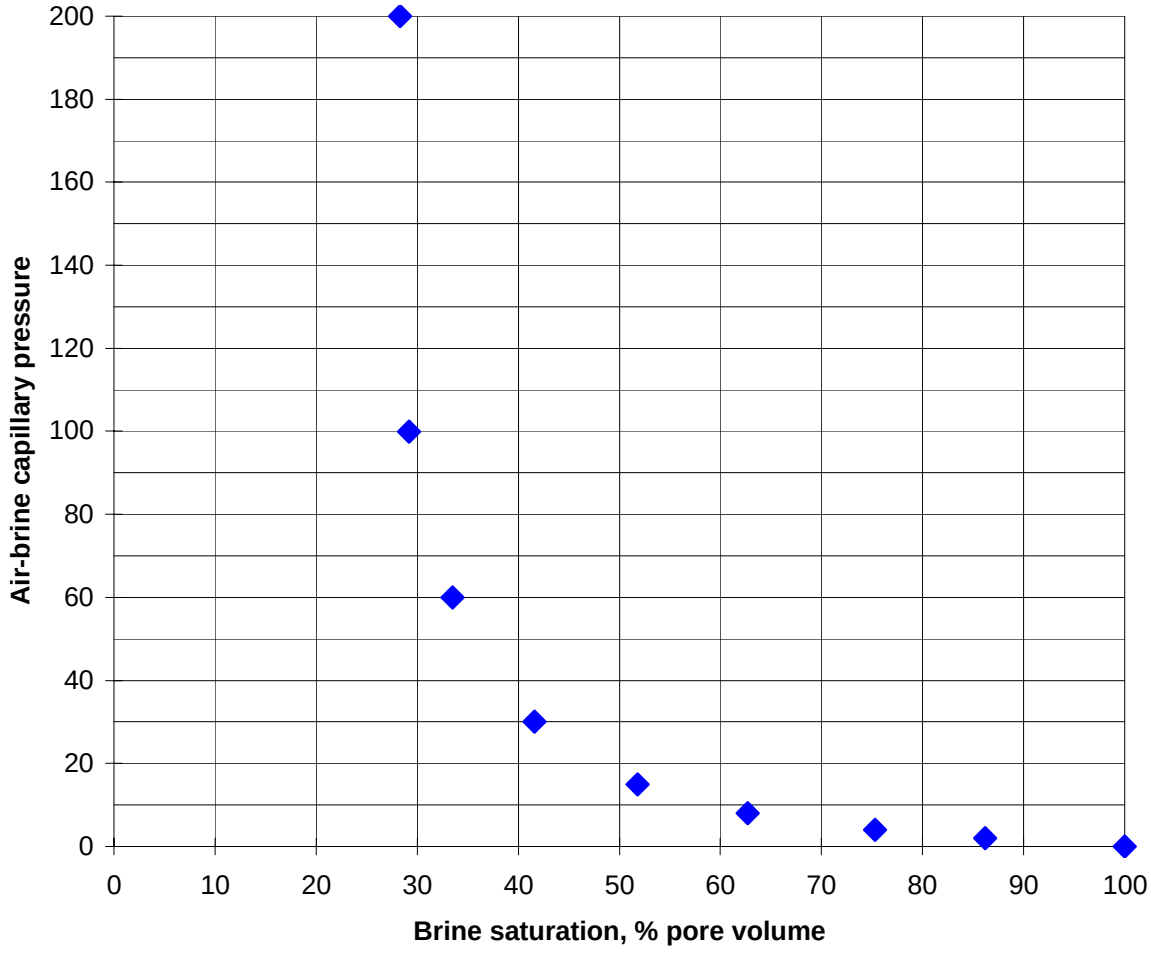

Air-brine capillary pressure by centrifuge at 1800 psi NOBP

Sample no.	Depth (m)	Determined at 1800 psi NOBP				
		Kinf (md)	Kair (md)	Porosity (%)	Capillary pressure (psi)	Brine saturation (%PV)
50	2129.56	28.9	32.9	20.3	0	100
					2	100
					4	83.1
					8	68.8
					15	58.2
					30	48.6
					60	40.7
					100	35.9
					200	32.4

The terminal capillary pressure (200 psi) was obtained by porous-plate desaturation.

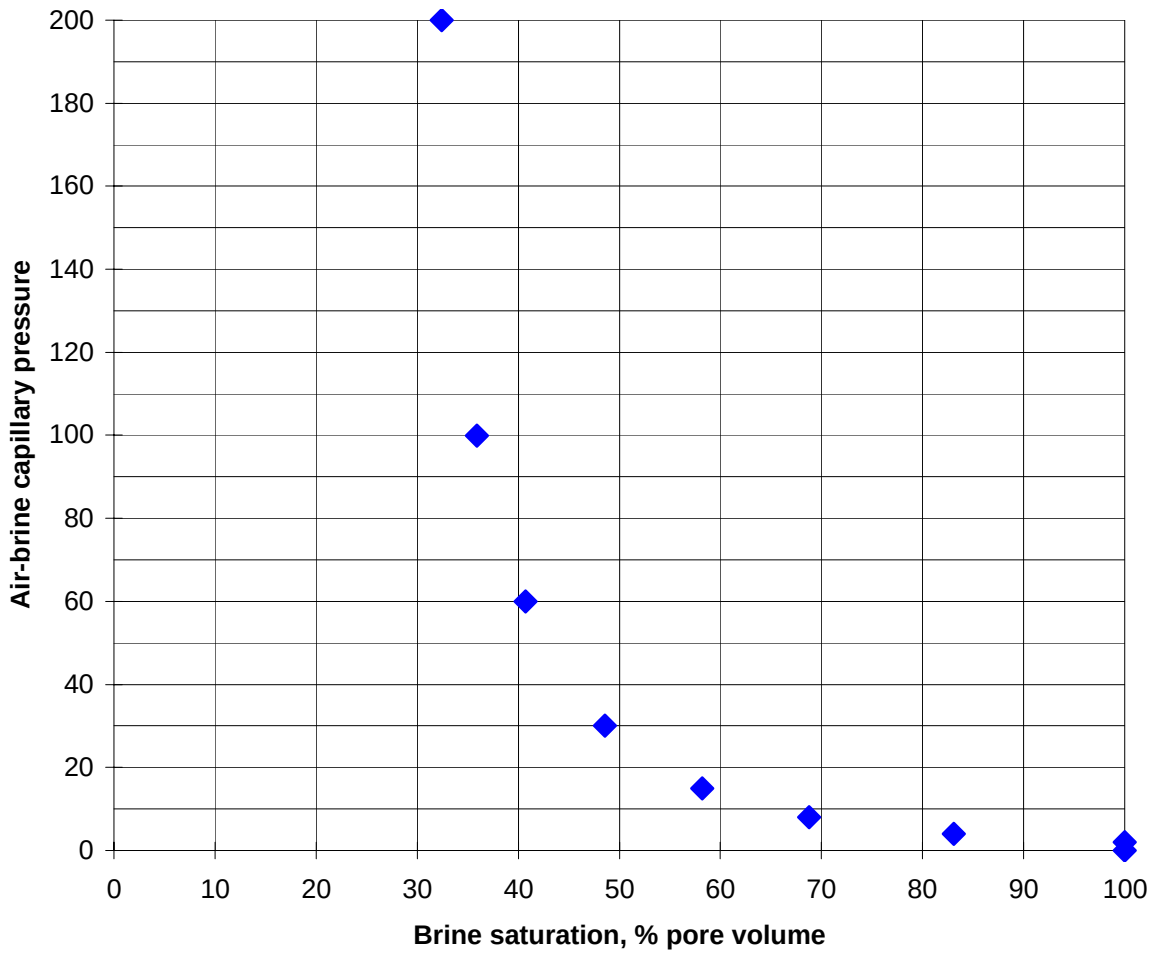

Air-brine capillary pressure by centrifuge at 1800 psi NOBP

Sample no.	Depth (m)	Determined at 1800 psi NOBP				
		Kinf (md)	Kair (md)	Porosity (%)	Capillary pressure (psi)	Brine saturation (%PV)
55	2131.13	6.81	7.79	18.3	0	100
					2	98.4
					4	89.2
					8	81.0
					15	75.1
					30	67.3
					60	61.2
					100	57.9
					200	52.0

The terminal capillary pressure (200 psi) was obtained by porous-plate desaturation.

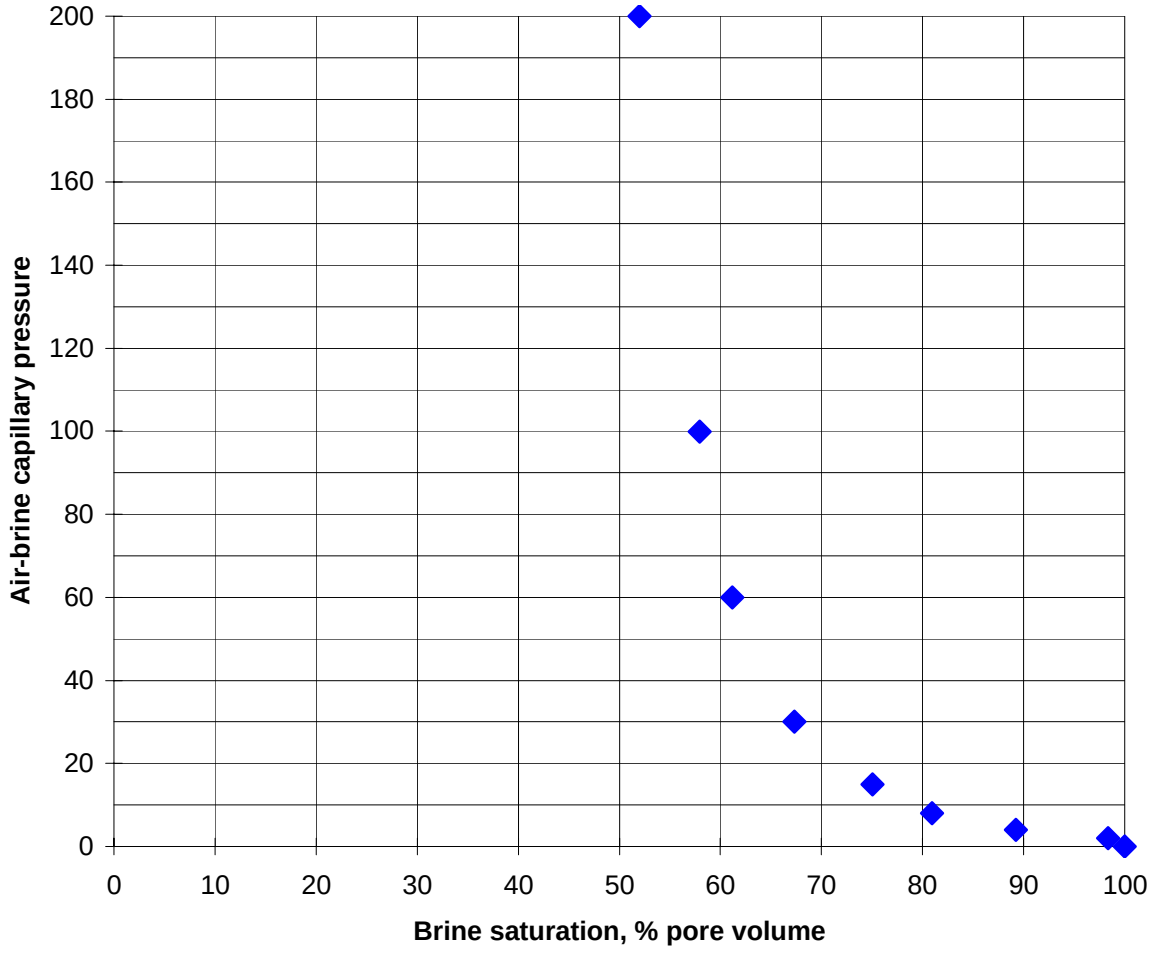

Air-brine capillary pressure by centrifuge at 1800 psi NOBP

Sample no.	Depth (m)	Determined at 1800 psi NOBP				
		Kinf (md)	Kair (md)	Porosity (%)	Capillary pressure (psi)	Brine saturation (%PV)
67	2134.75	56.4	62.3	21.9	0	100
					2	89.4
					4	78.4
					8	65.5
					15	53.5
					30	41.5
					60	32.2
					100	27.1
					200	26.2

The terminal capillary pressure (200 psi) was obtained by porous-plate desaturation.

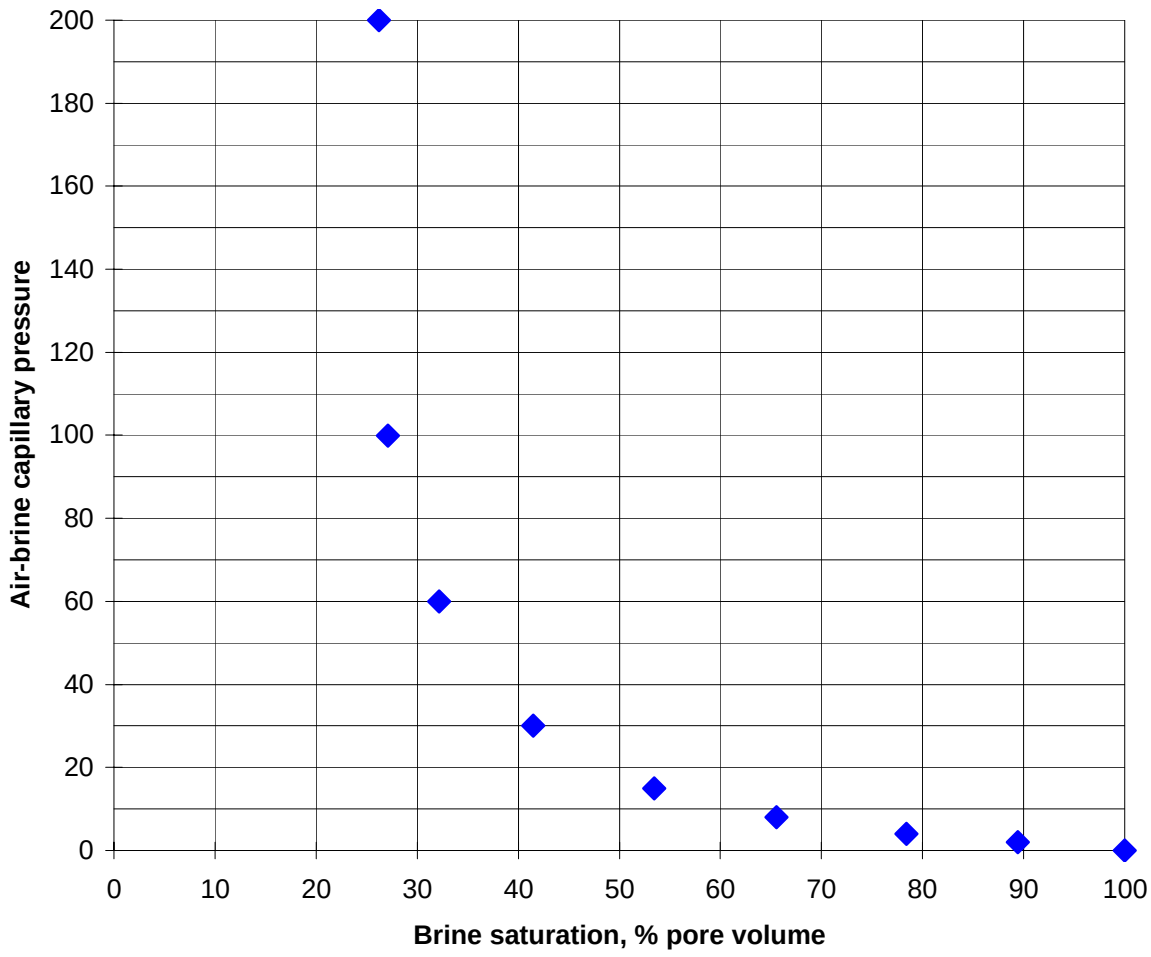

Air-brine capillary pressure by centrifuge at 1800 psi NOBP

Sample no.	Depth (m)	Determined at 1800 psi NOBP				
		Kinf (md)	Kair (md)	Porosity (%)	Capillary pressure (psi)	Brine saturation (%PV)
73	2136.44	7.93	9.06	19.0	0	100
					2	100
					4	92.9
					8	80.0
					15	73.7
					30	67.7
					60	61.6
					100	57.1
					200	51.9

The terminal capillary pressure (200 psi) was obtained by porous-plate desaturation.

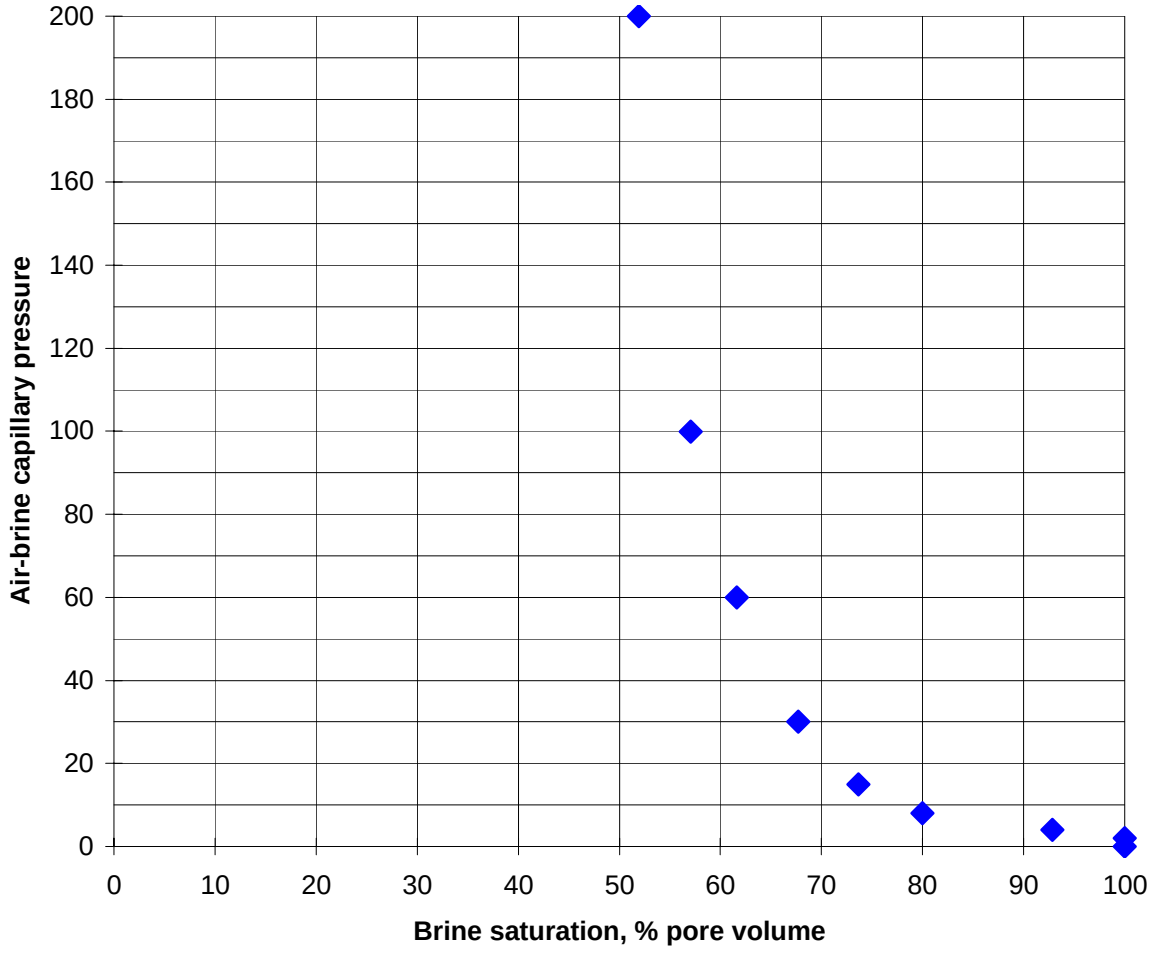

Air-brine capillary pressure by centrifuge at 1800 psi NOBP

Sample no.	Depth (m)	Determined at 1800 psi NOBP				
		Kinf (md)	Kair (md)	Porosity (%)	Capillary pressure (psi)	Brine saturation (%PV)
76	2137.38	16.0	19.3	18.8	0	100
					2	100
					4	86.2
					8	76.0
					15	68.6
					30	59.1
					60	48.2
					100	42.9
					200	40.7

The terminal capillary pressure (200 psi) was obtained by porous-plate desaturation.

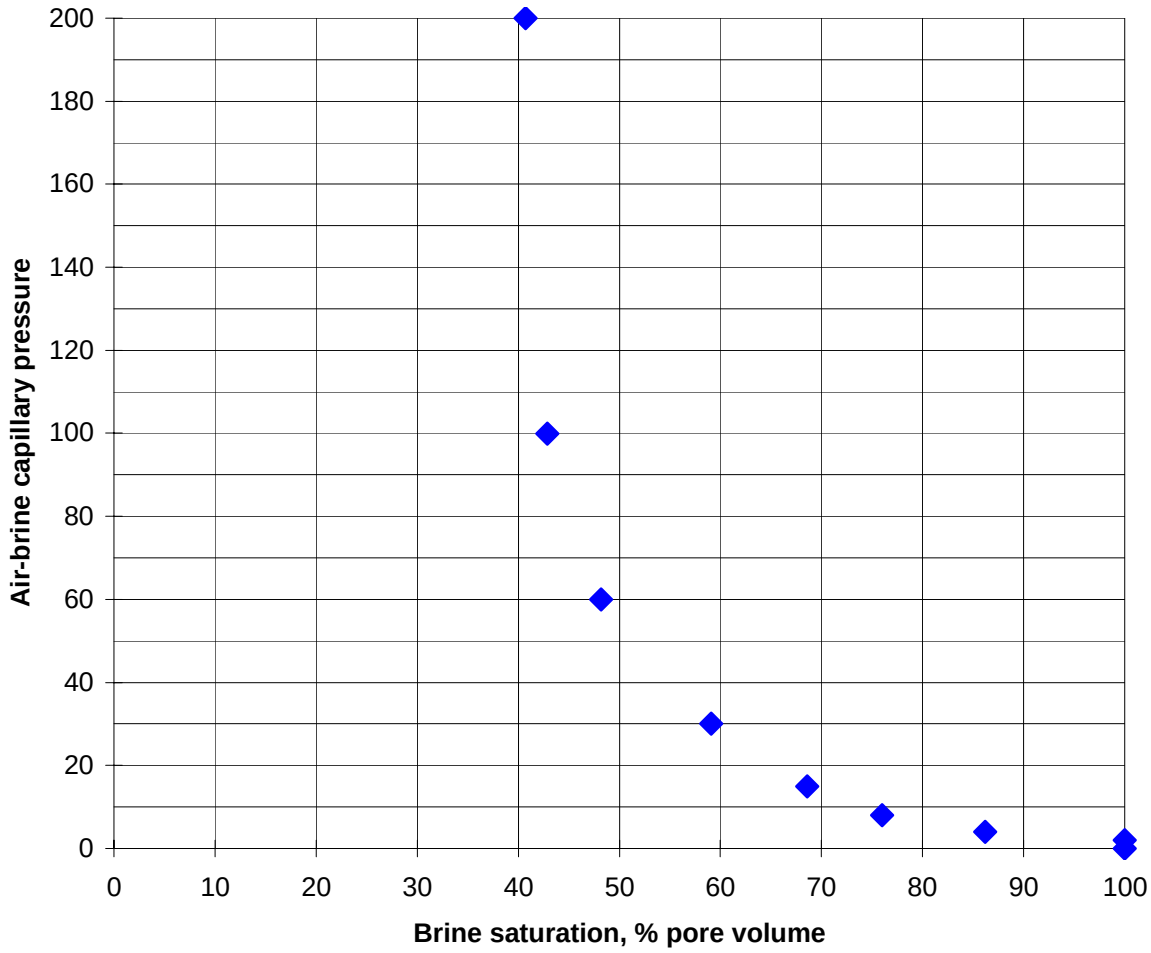

Air-brine capillary pressure by centrifuge at 1800 psi NOBP

Sample no.	Depth (m)	Determined at 1800 psi NOBP				
		Kinf (md)	Kair (md)	Porosity (%)	Capillary pressure (psi)	Brine saturation (%PV)
81	2138.88	36.2	38.7	20.6	0	100
					2	99.1
					4	81.8
					8	68.0
					15	57.8
					30	48.8
					60	41.5
					100	37.1
					200	34.0

The terminal capillary pressure (200 psi) was obtained by porous-plate desaturation.

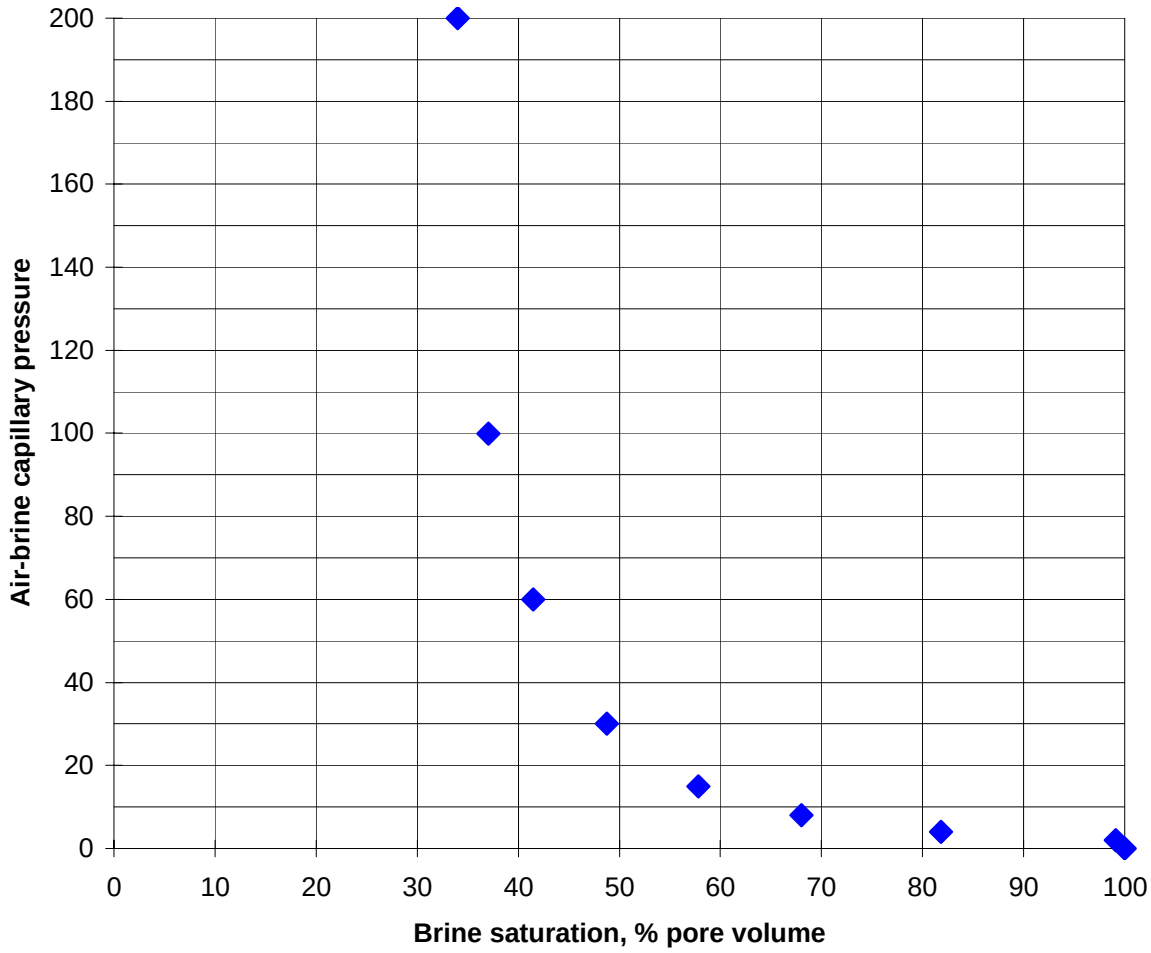

Air-brine capillary pressure by centrifuge at 1800 psi NOBP

Sample no.	Depth (m)	Determined at 1800 psi NOBP				
		Kinf (md)	Kair (md)	Porosity (%)	Capillary pressure (psi)	Brine saturation (%PV)
88	2141.05	73.5	77.7	21.5	0	100
					2	79.6
					4	56.4
					8	47.0
					15	40.9
					30	35.3
					60	31.4
					100	29.4
					200	28.1

The terminal capillary pressure (200 psi) was obtained by porous-plate desaturation.

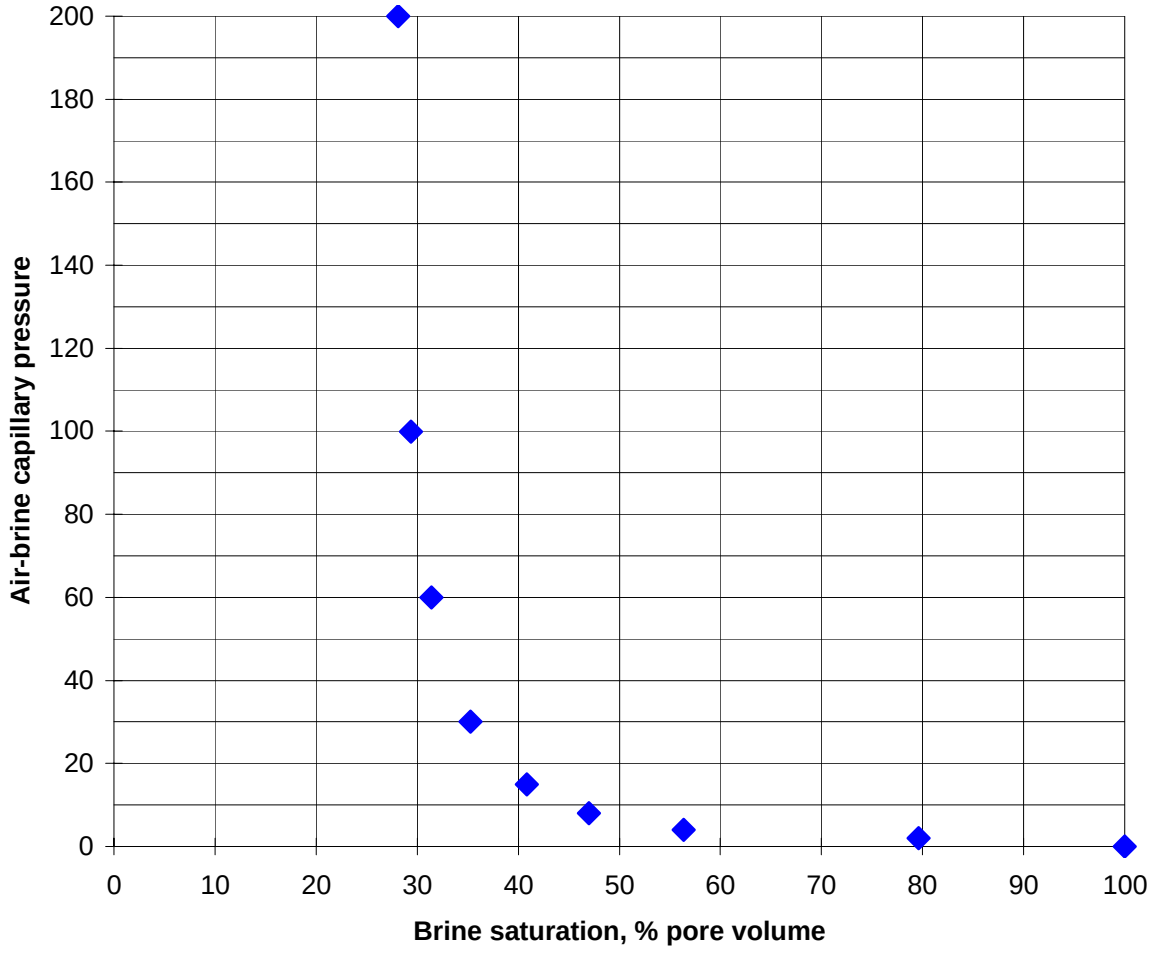

Capillary pressure by mercury injection analysis

Sample no.		25	29	45	50
Depth (m)		2120.45	2121.65	2128.06	2129.56
K air (md)		23.6	6.43	65.0	32.9
Porosity * (%)		19.1	19.7	21.7	21.2
Injection pressure (psia)	**Pore throat radii (microns)**	**Mercury Saturation, Percent pore space ****			
3	**35.5**	0	0	0	0
6	**17.7**	0	0	2.53	0
9	**11.8**	0	0	3.79	0
12	**8.9**	0	0	6.43	0
15	**7.1**	0	0	12.5	1.12
18	**5.9**	0	0	17.5	2.25
21	**5.1**	0	0	21.4	4.72
24	**4.4**	0	0.700	24.0	7.30
27	**3.9**	2.19	2.68	25.8	11.0
30	**3.6**	4.17	4.55	28.1	14.6
40	**2.7**	10.7	9.92	31.9	25.4
60	**1.8**	24.7	20.8	38.1	34.4
80	**1.3**	31.3	25.4	42.4	38.9
100	**1.1**	35.4	29.2	46.6	42.6
200	**0.53**	46.8	36.9	56.3	51.3
300	**0.36**	51.1	42.0	60.7	56.0
500	**0.21**	57.0	48.3	66.6	62.2
750	**0.14**	60.7	51.6	71.6	65.6
1000	**0.11**	63.3	53.8	74.3	67.9
1250	**0.085**	65.2	55.5	76.2	69.3
1500	**0.071**	67.0	57.4	77.4	70.2
1750	**0.061**	69.1	59.0	78.3	70.9
2000	**0.053**	71.0	60.7	79.0	71.5
% Pore Throats < 0.053 micron		29.0	39.3	21.0	28.5

* Porosity values determined on recleaned and dried samples prior to mercury injection analysis.

** Can also be considered to be the percent of pore space having pore throat entry sizes of the indicated radii or greater.

Capillary pressure by mercury injection analysis

Sample no.		55	67	73	76
Depth (m)		2131.13	2134.75	2136.44	2137.38
K air (md)		7.79	62.3	9.06	19.3
Porosity * (%)		19.8	22.4	20.0	19.5
Injection pressure (psia)	**Pore throat radii (microns)**	**Mercury Saturation, Percent pore space ****			
3	**35.5**	0	0	0	0
6	**17.7**	0	0	0	0
9	**11.8**	0	1.14	0	0
12	**8.9**	0	2.97	0	0
15	**7.1**	0	5.74	0	0
18	**5.9**	0	15.8	0	0
21	**5.1**	2.20	21.5	0.347	0
24	**4.4**	6.02	25.2	1.62	0
27	**3.9**	7.64	28.0	5.09	0
30	**3.6**	9.38	31.1	7.64	0
40	**2.7**	14.1	36.8	17.1	10.3
60	**1.8**	21.8	42.7	26.1	25.2
80	**1.3**	25.7	46.8	30.5	31.5
100	**1.1**	29.2	49.4	33.5	34.1
200	**0.53**	37.5	57.6	40.5	43.2
300	**0.36**	40.3	62.0	44.7	47.7
500	**0.21**	44.3	67.0	49.3	54.4
750	**0.14**	47.5	71.3	52.3	58.9
1000	**0.11**	49.6	73.3	54.8	62.1
1250	**0.085**	51.4	74.9	56.9	64.8
1500	**0.071**	53.3	75.9	58.8	66.4
1750	**0.061**	55.1	76.6	60.5	68.0
2000	**0.053**	56.8	76.9	62.0	69.3
% Pore Throats < 0.053 micron		43.2	23.1	38.0	30.7

* Porosity values determined on recleaned and dried samples prior to mercury injection analysis.

** Can also be considered to be the percent of pore space having pore throat entry sizes of the indicated radii or greater.

Capillary pressure by mercury injection analysis

Sample no.		81	82	88
Depth (m)		2138.88	2139.18	2141.05
K air (md)		38.7	1.13	77.7
Porosity * (%)		21.6	16.6	22.5
Injection pressure (psia)	**Pore throat radii (microns)**	**Mercury Saturation, Percent pore space ***		
3	**35.5**	0	0	0
6	**17.7**	0	0	0
9	**11.8**	0	0	2.14
12	**8.9**	0.547	0	6.09
15	**7.1**	3.06	0	19.1
18	**5.9**	11.5	0	25.5
21	**5.1**	16.4	0	30.0
24	**4.4**	20.9	0	33.8
27	**3.9**	24.4	0	35.5
30	**3.6**	26.9	0	37.3
40	**2.7**	32.8	0	42.0
60	**1.8**	39.0	2.89	47.2
80	**1.3**	42.2	10.0	50.1
100	**1.1**	44.8	17.9	52.4
200	**0.53**	51.5	29.4	58.9
300	**0.36**	55.1	33.8	62.2
500	**0.21**	59.7	39.3	66.8
750	**0.14**	63.2	43.5	70.7
1000	**0.11**	65.5	46.2	72.9
1250	**0.085**	67.5	48.7	74.3
1500	**0.071**	69.3	50.9	75.6
1750	**0.061**	70.9	52.5	76.5
2000	**0.053**	72.4	53.9	77.1
% Pore Throats < 0.053 micron		27.6	46.1	22.9

* Porosity values determined on recleaned and dried samples prior to mercury injection analysis.

** Can also be considered to be the percent of pore space having pore throat entry sizes of the indicated radii or greater.

Pore throat size distribution from mercury injection analysis

Sample no.	25
Depth (m)	2120.45
K air (md)	23.6
Porosity * (%)	19.1

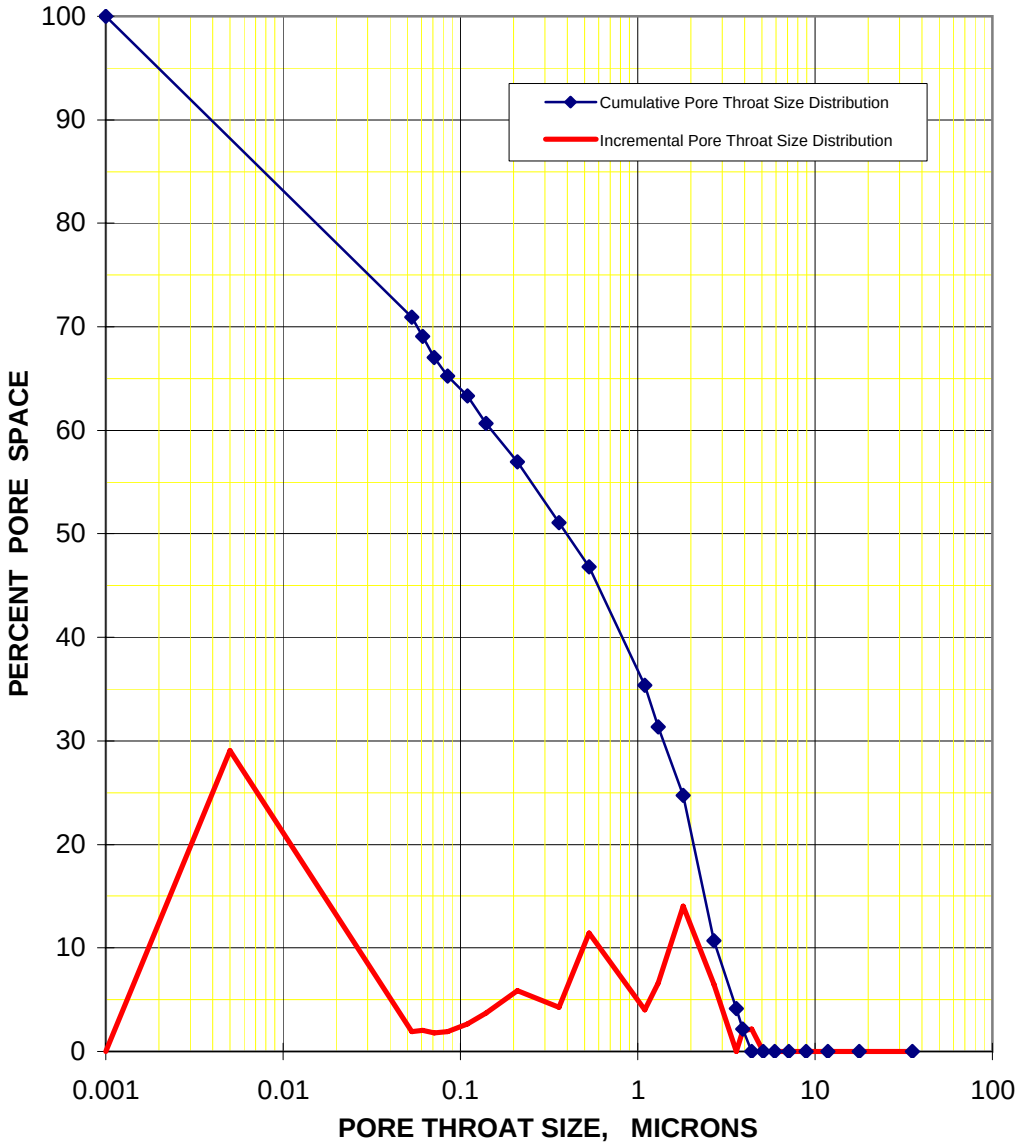

0.001 micron assumed to be the minimum pore throat size for convenience of plotting only.

* Porosity values determined on recleaned and dried samples prior to mercury injection analysis.

Pore throat size distribution from mercury injection analysis

Sample no.	29
Depth (m)	2121.65
K air (md)	6.43
Porosity * (%)	19.7

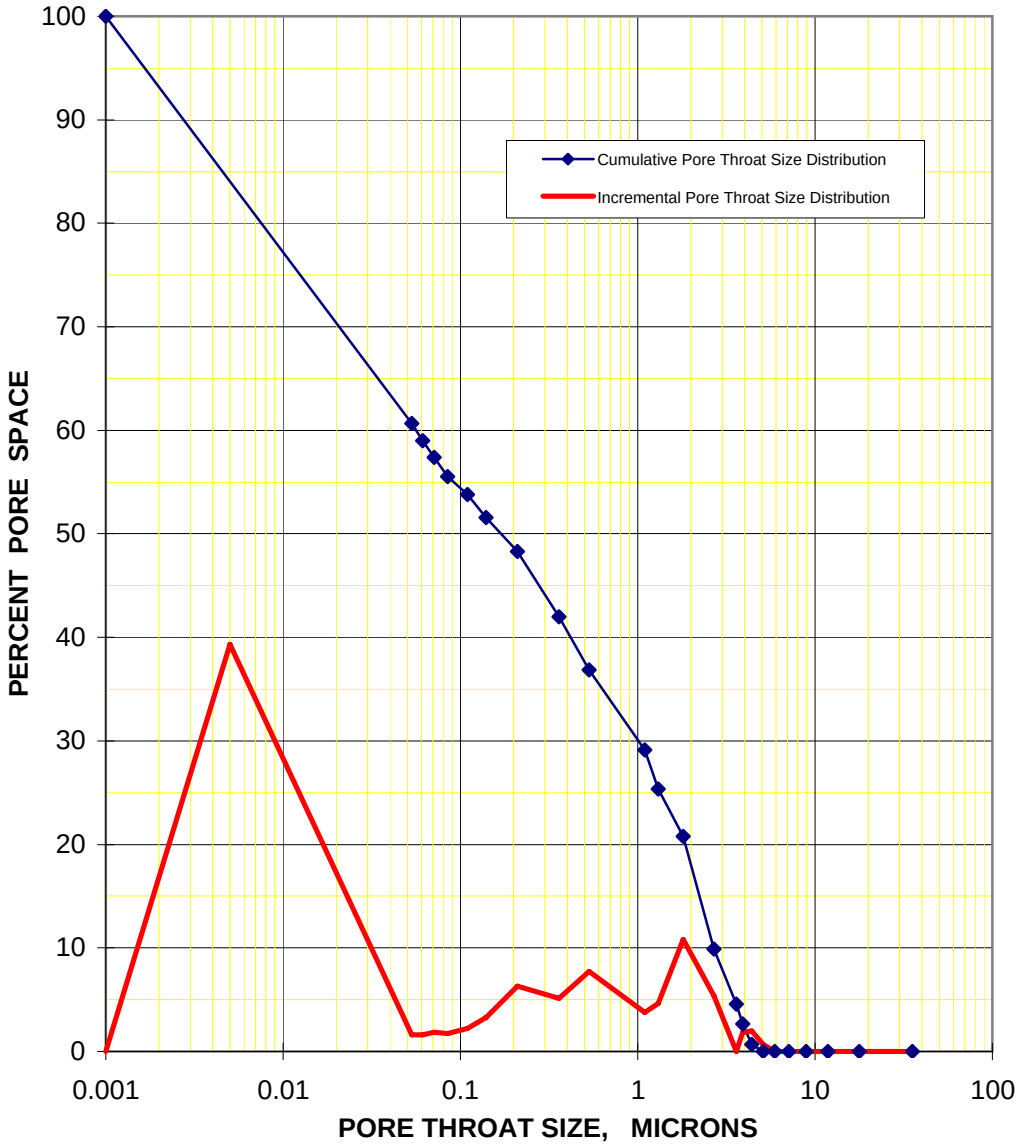

0.001 micron assumed to be the minimum pore throat size for convenience of plotting only.

* Porosity values determined on recleaned and dried samples prior to mercury injection analysis.

Pore throat size distribution from mercury injection analysis

Sample no.	45
Depth (m)	2128.06
K air (md)	65.0
Porosity * (%)	21.7

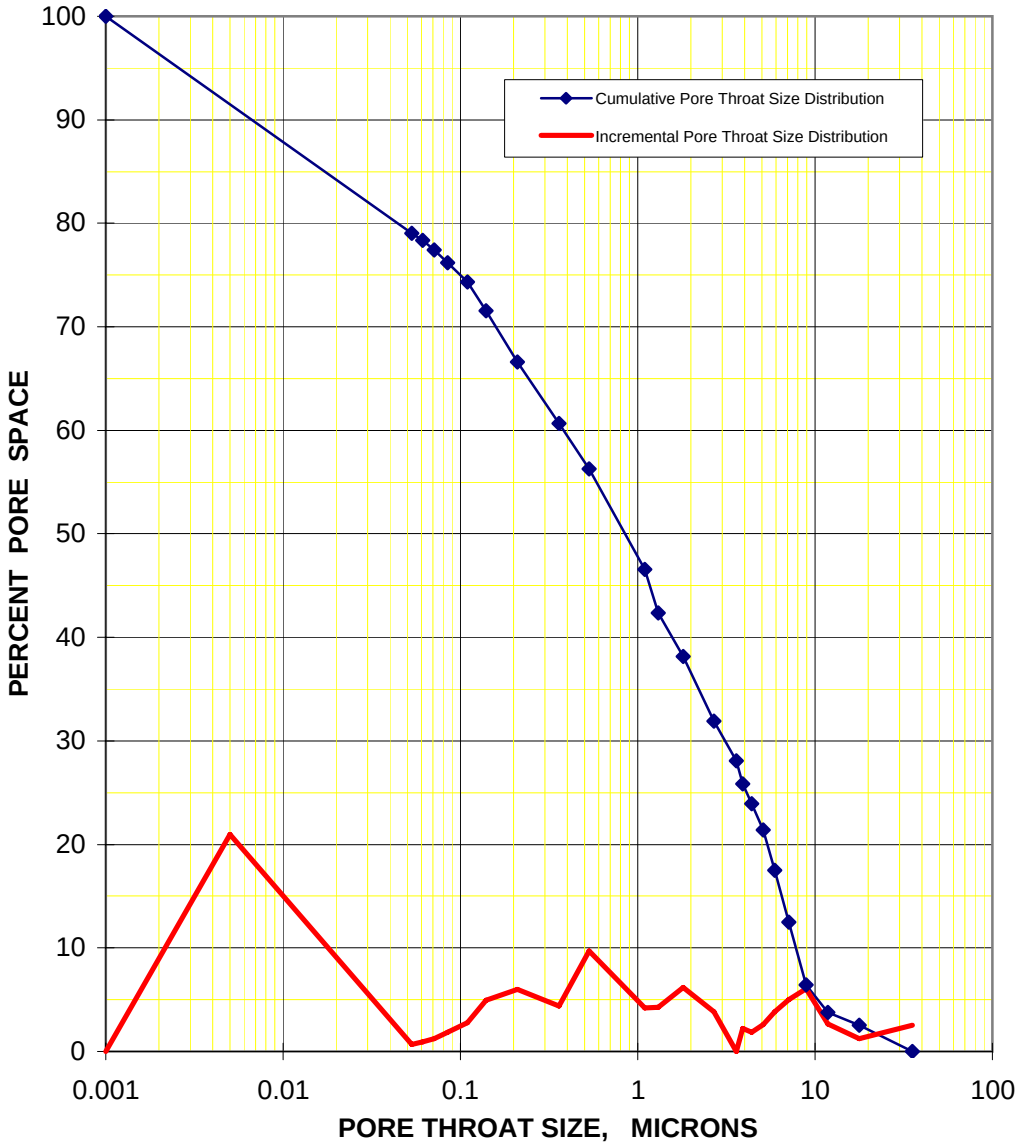

0.001 micron assumed to be the minimum pore throat size for convenience of plotting only.

* Porosity values determined on recleaned and dried samples prior to mercury injection analysis.

Pore throat size distribution from mercury injection analysis

Sample no.	50
Depth (m)	2129.56
K air (md)	32.9
Porosity * (%)	21.2

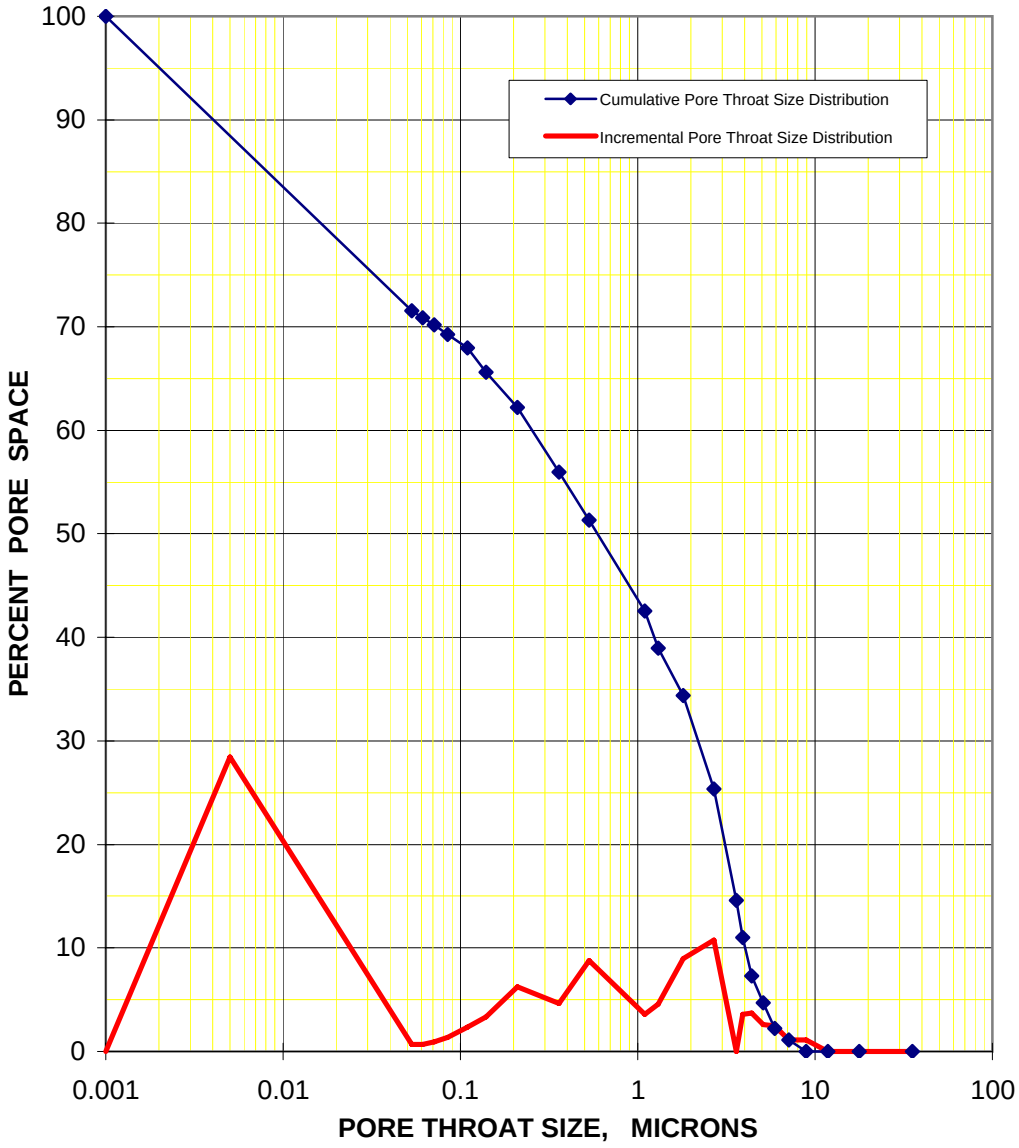

0.001 micron assumed to be the minimum pore throat size for convenience of plotting only.

* Porosity values determined on recleaned and dried samples prior to mercury injection analysis.

Pore throat size distribution from mercury injection analysis

Sample no.	55
Depth (m)	2131.13
K air (md)	7.79
Porosity * (%)	19.8

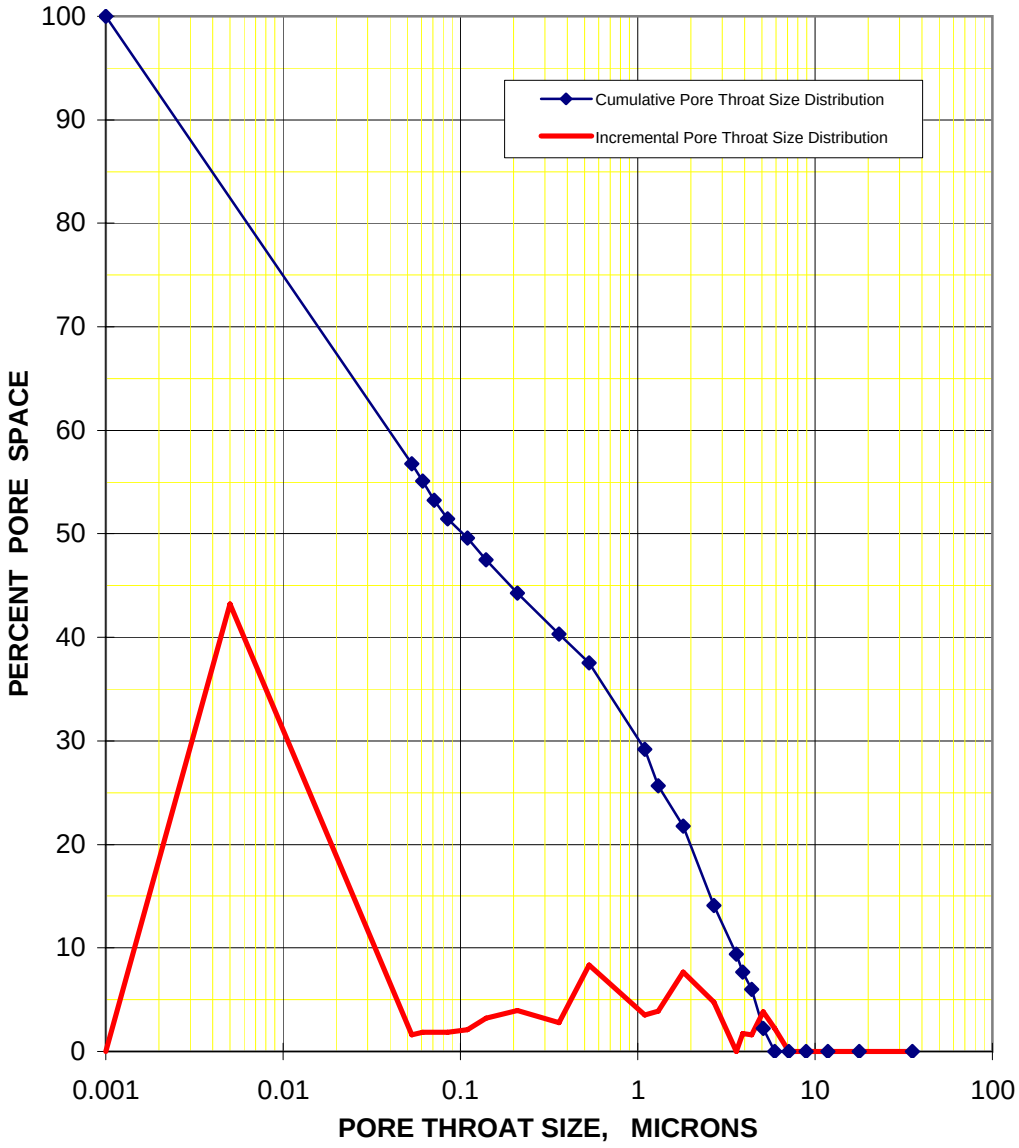

0.001 micron assumed to be the minimum pore throat size for convenience of plotting only.

* Porosity values determined on recleaned and dried samples prior to mercury injection analysis.

Pore throat size distribution from mercury injection analysis

Sample no.	67
Depth (m)	2134.75
K air (md)	62.3
Porosity * (%)	22.4

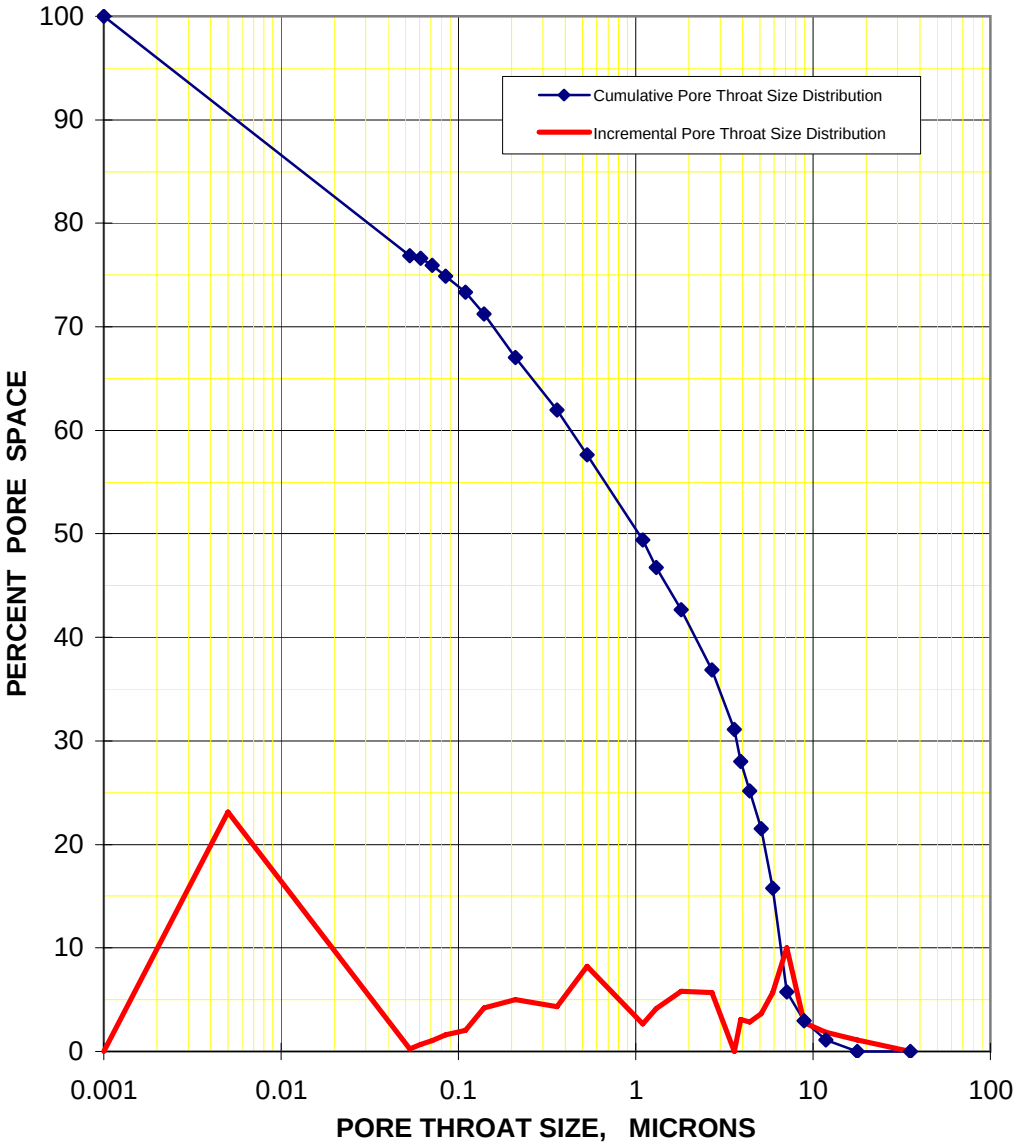

0.001 micron assumed to be the minimum pore throat size for convenience of plotting only.

* Porosity values determined on recleaned and dried samples prior to mercury injection analysis.

Pore throat size distribution from mercury injection analysis

Sample no.	73
Depth (m)	2136.44
K air (md)	9.06
Porosity * (%)	20.0

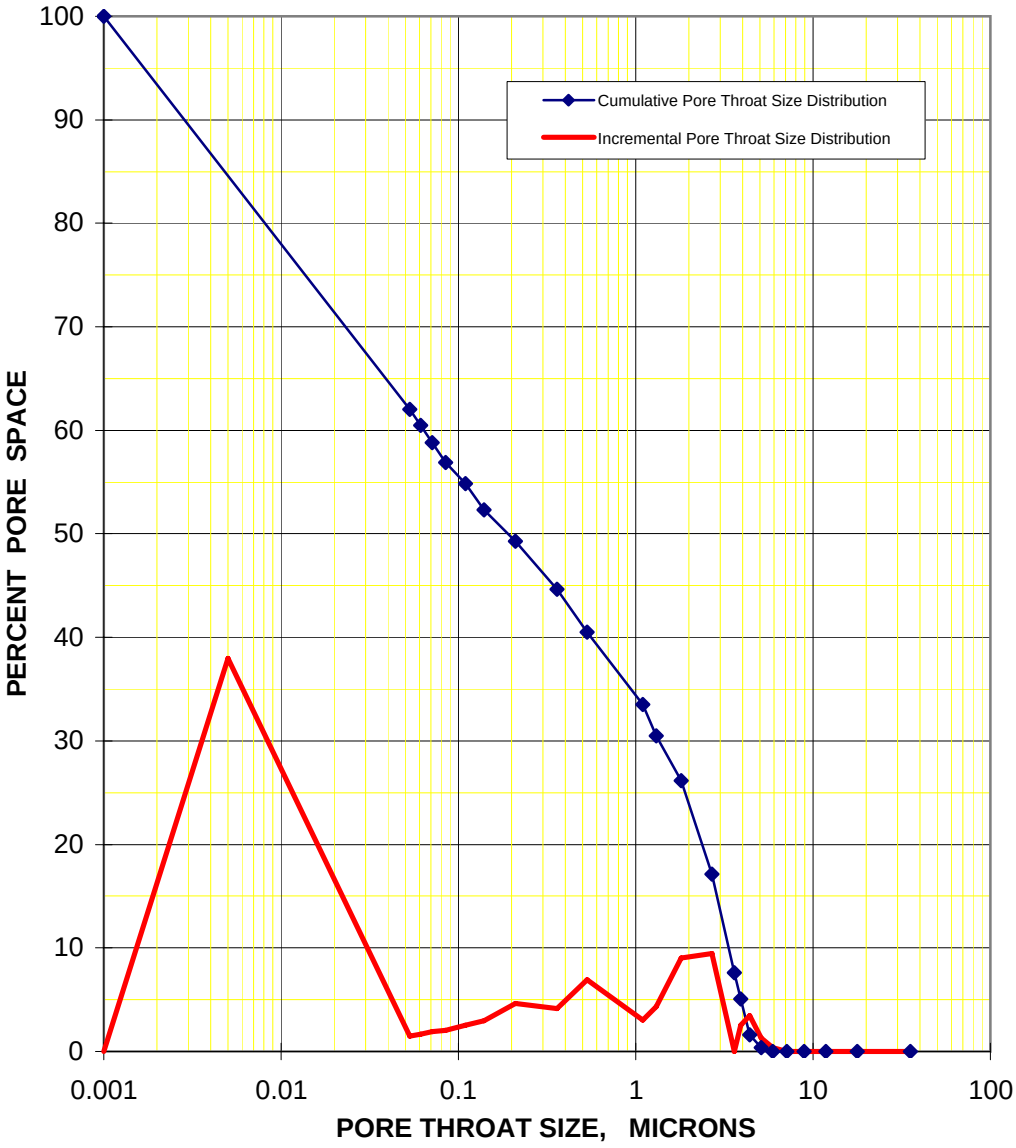

0.001 micron assumed to be the minimum pore throat size for convenience of plotting only.

* Porosity values determined on recleaned and dried samples prior to mercury injection analysis.

Pore throat size distribution from mercury injection analysis

Sample no.	76
Depth (m)	2137.38
K air (md)	19.3
Porosity * (%)	19.5

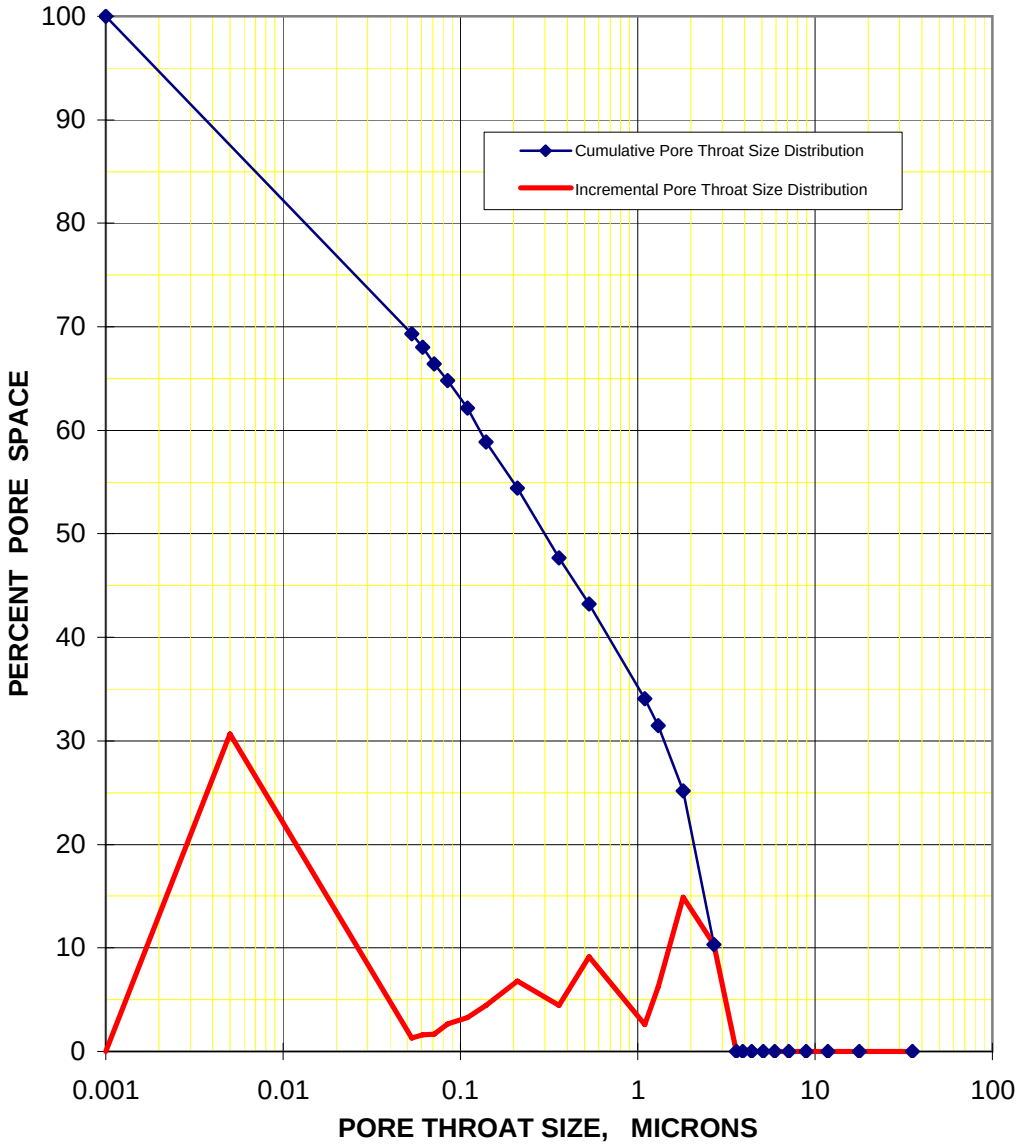

0.001 micron assumed to be the minimum pore throat size for convenience of plotting only.

* Porosity values determined on recleaned and dried samples prior to mercury injection analysis.

Pore throat size distribution from mercury injection analysis

Sample no.	81
Depth (m)	2138.88
K air (md)	38.7
Porosity * (%)	21.6

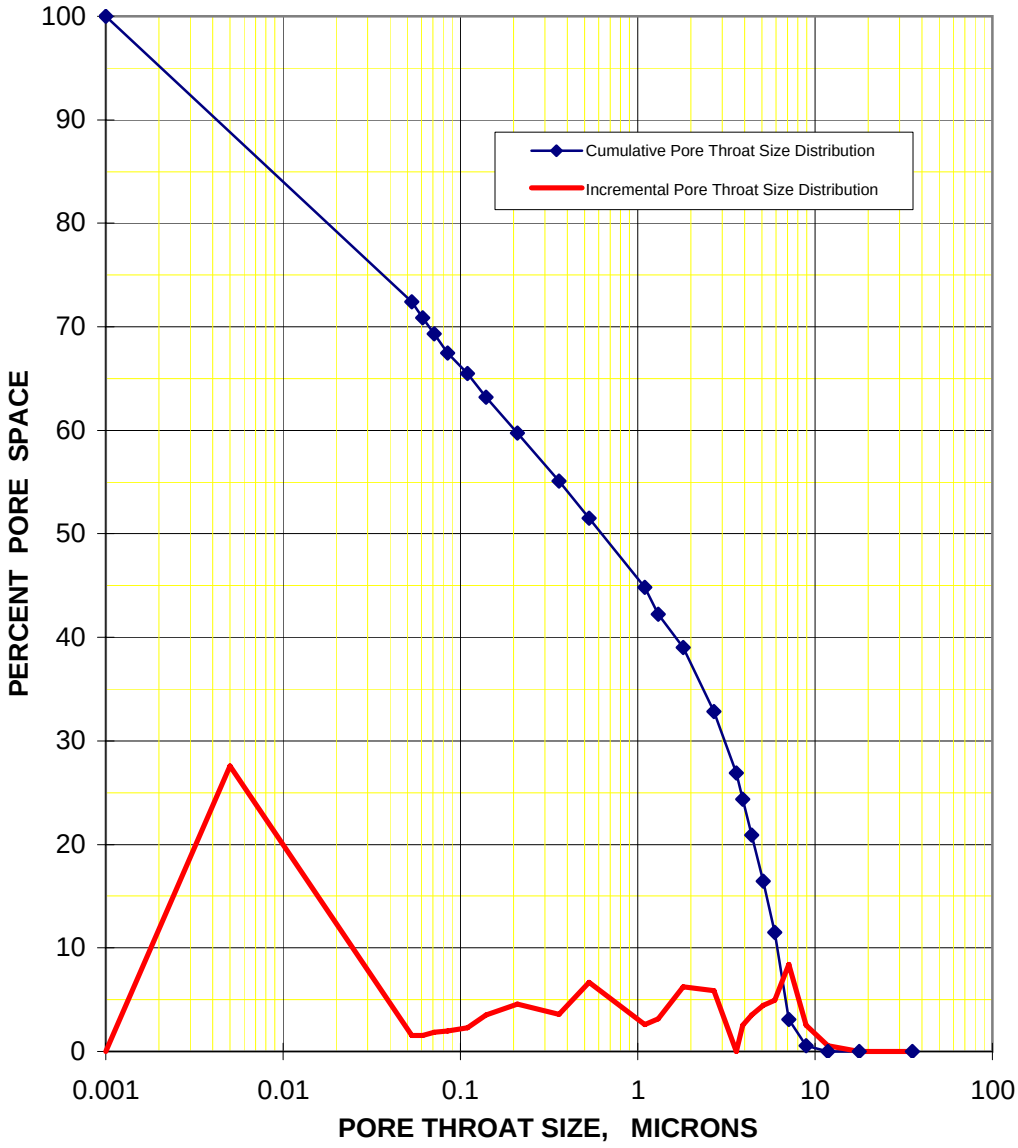

0.001 micron assumed to be the minimum pore throat size for convenience of plotting only.

* Porosity values determined on recleaned and dried samples prior to mercury injection analysis.

Pore throat size distribution from mercury injection analysis

Sample no.	82
Depth (m)	2139.18
K air (md)	1.13
Porosity * (%)	16.6

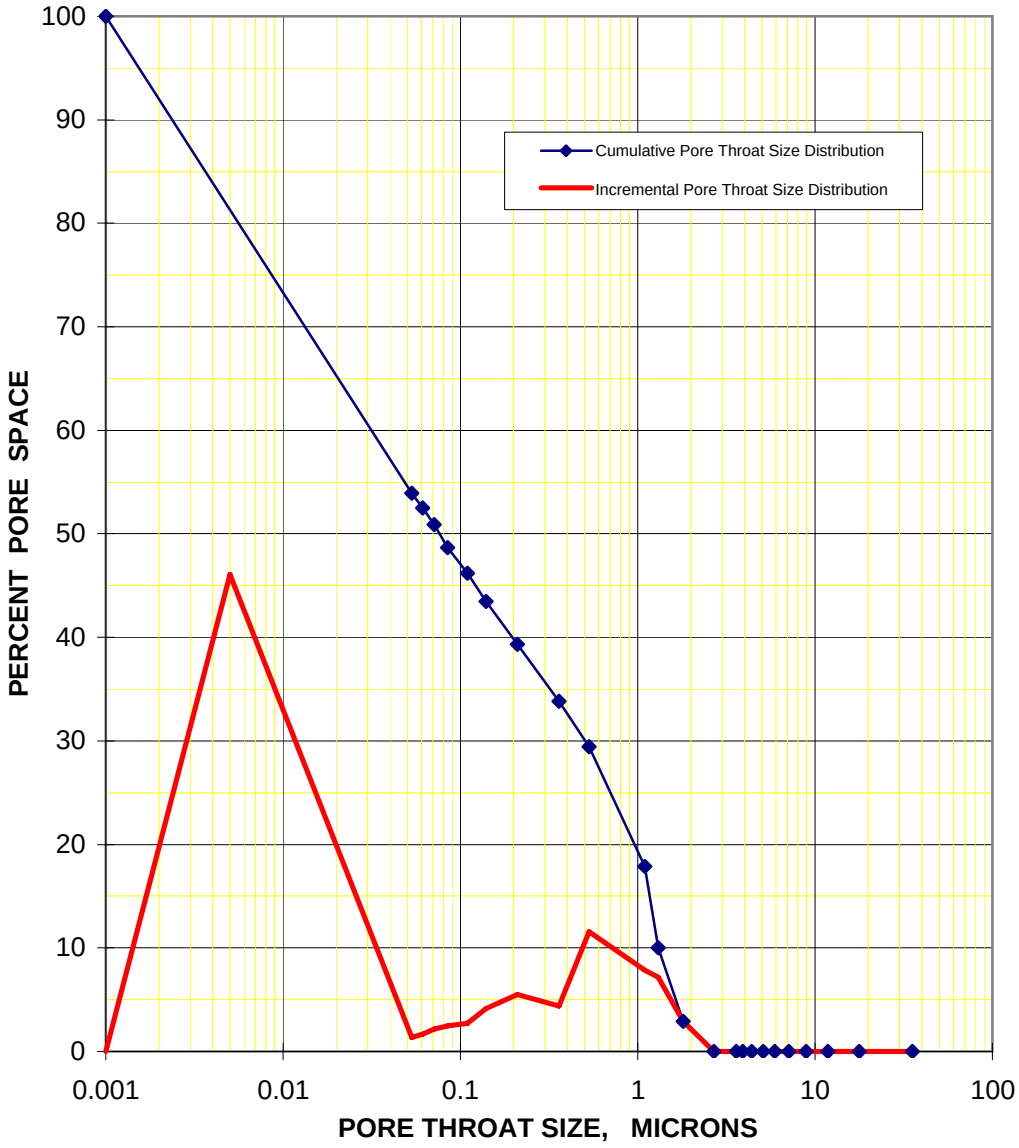

0.001 micron assumed to be the minimum pore throat size for convenience of plotting only.

* Porosity values determined on recleaned and dried samples prior to mercury injection analysis.

Pore throat size distribution from mercury injection analysis

Sample no.	88
Depth (m)	2141.05
K air (md)	77.7
Porosity * (%)	22.5

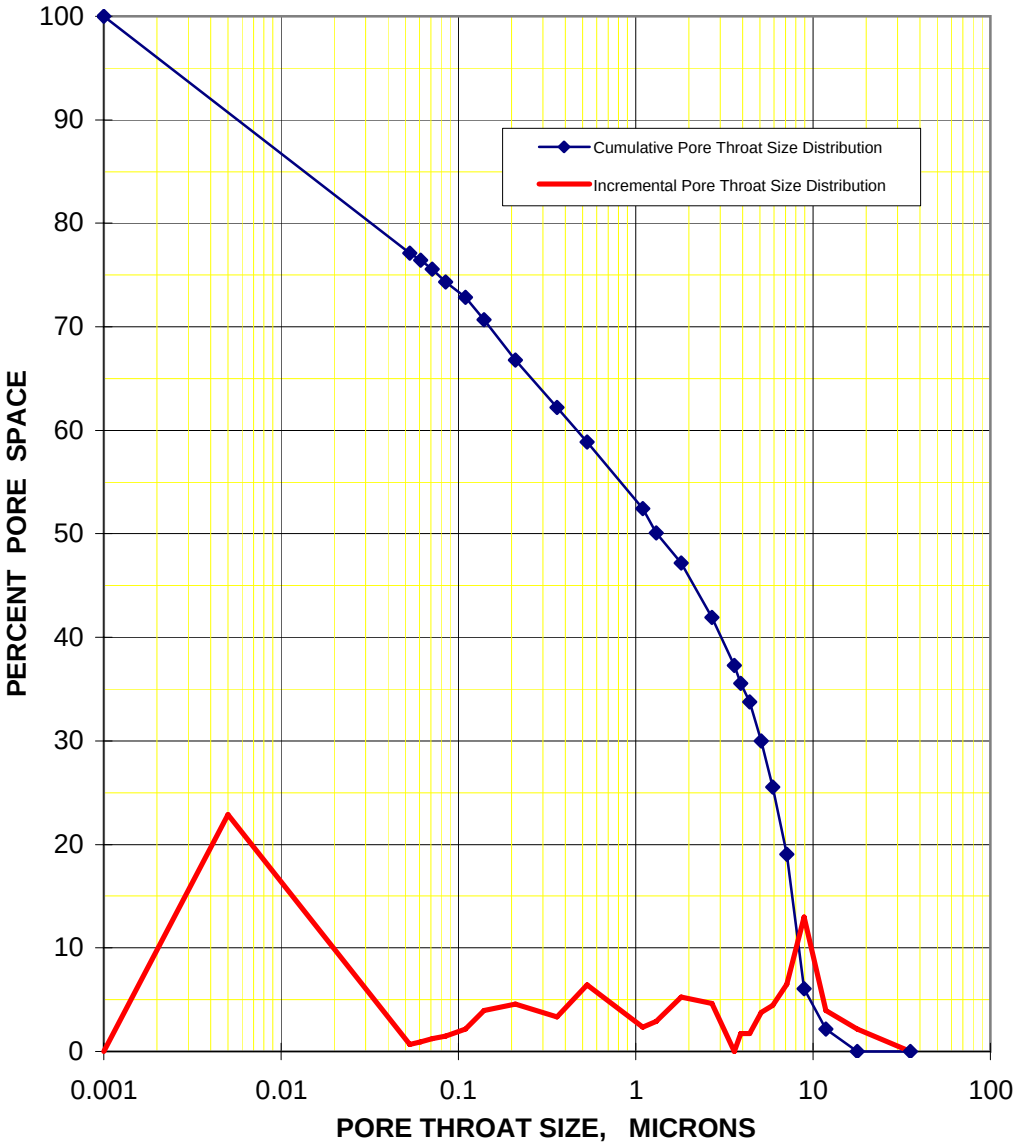

0.001 micron assumed to be the minimum pore throat size for convenience of plotting only.

* Porosity values determined on recleaned and dried samples prior to mercury injection analysis.

SECTION 4
RELATIVE PERMEABILITY

Summary of the WATER-GAS relative permeability by centrifuge (end-point) analysis results determined at 1800 psi NOBP.

Sample No.	Depth (m)	Kair NOBP (md)	Porosity (%)	INITIAL CONDITIONS			TERMINAL CONDITIONS			
				Swi (% pv)	Gas in place (% pv)	Kgas at Swi (md)	Sgr (% pv)	Gas Recovery (% pv)	Gas Recovery (% IGIP)	Kw at Sgr (md)
25	2120.45	23.6	18.9	41.2	58.8	8.63	14.2	44.6	75.9	5.30
29	2121.65	6.43	18.5	58.2	41.8	4.00	10.5	31.3	74.9	2.80
45	2128.06	65.0	21.2	29.2	70.8	36.9	20.6	50.2	70.9	15.6
50	2129.56	32.9	20.3	35.9	64.1	15.0	17.5	46.6	72.7	8.60
55	2131.13	7.79	18.3	57.9	42.1	5.04	14.3	27.8	66.0	2.55
67	2134.75	62.3	21.9	27.1	72.9	45.8	17.3	55.6	76.3	19.6
73	2136.44	9.06	19.0	57.1	42.9	5.96	10.2	32.7	76.2	3.13
76	2137.38	19.3	18.8	42.9	57.1	7.56	18.5	38.6	67.6	3.26
81	2138.88	38.7	20.6	37.1	62.9	29.5	16.8	46.1	73.3	16.8
88	2141.05	77.7	21.5	29.4	70.6	65.5	19.8	50.8	72.0	34.1

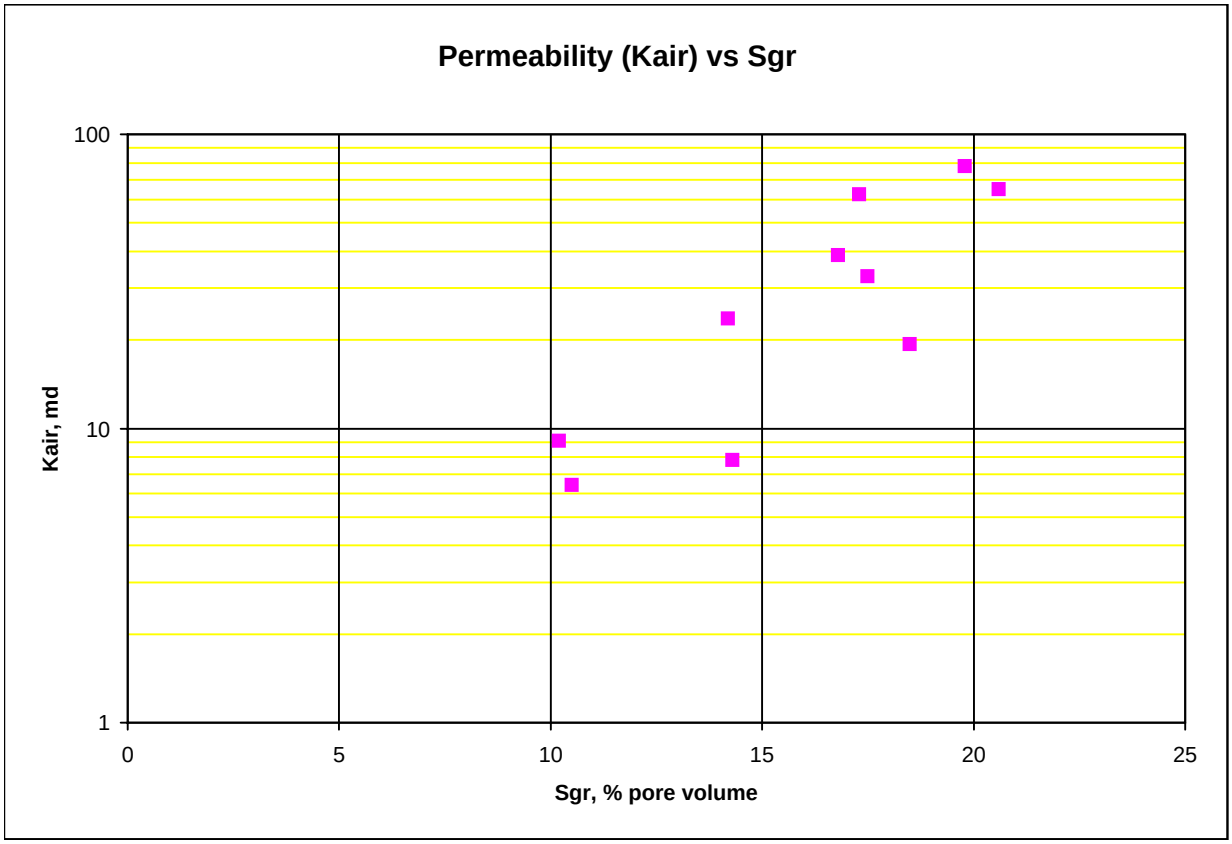
Permeability (Kair) vs Sgr
Kair, md
100
10
1
0
5
10
15
20
25
Sgr, % pore volume

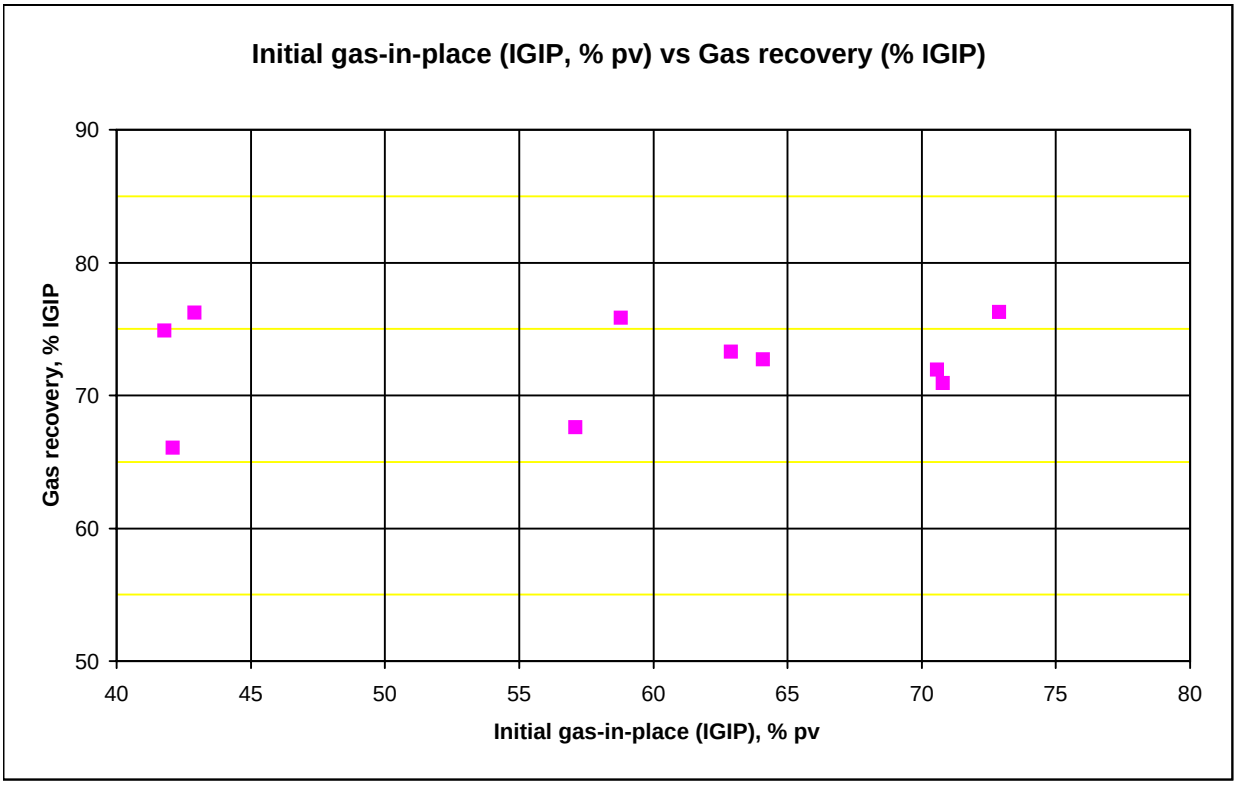
Initial gas-in-place (IGIP, % pv) vs Gas recovery (% IGIP)
Gas recovery, % IGIP
90
80
70
60
50
40
45
50
55
60
65
70
75
80
Initial gas-in-place (IGIP), % pv

APPENDIX

APPENDIX-1
SUMMARY OF LABORATORY PROCEDURES

SUMMARY OF LABORATORY PROCEDURES

Sample preparation

The selected samples were initially redried in a controlled humidity oven, maintained at 60^{o}C and 40-45% relative humidity, and the base data (permeability, porosity and grain density) at 1800 psi net overburden (NOBP) conditions confirmed.

Formation brine analysis.

For this study, a simple brine of 35,000 ppm TDS was formulated using 80% sodium chloride and 20% potassium chloride.

Air-brine capillary pressure by centrifuge

The ten selected samples were initially pressure saturated with the simulated formation brine. All samples were weighed after saturation to check measured pore volumes.

The fully saturated samples were each loaded into individual centrifuge core holders and the 1800 psi NOBP applied. The samples were then subjected to non-stop centrifugation, using the overburden centrifuge, at rotational rates that were increased incrementally to generate equivalent pressures ranging from 1 to 100 psi in an air-brine system. Effluent brine volumes were monitored as the samples achieved capillary equilibrium at each incremental pressure.

Capillary pressure and end-face saturation data were then calculated from the raw data using data reduction techniques developed by Hassler-Brunner and later modified by other workers (e.g Rajan). These results are presented within SECTION 3 of this report.

The maximum achievable air-brine capillary pressure, using the overburden centrifuge, is 100 psi. Brine saturation values at the terminal 200 psi capillary pressure were obtained by porous-plate desaturation (in conjunction with the resistivity index measurements described below).

Centrifuge water-gas relative permeability (end-point) analysis

Following the air-brine capillary pressure tests, the samples were loaded individually into hydrostatic core holders and the 1800 psi NOBP applied. Humidified gas was flowed through each sample and the permeability to gas (Kgas at Swi) determined.

Water-gas relative permeability tests were then performed in the centrifuge with water displacing gas at constant speed (equivalent to constant pressure). When gas production had stabilised, the individual core holders were removed from the centrifuge and water permeability at residual gas saturation (Krg at Swr) measured.

Results from the relative permeability analyses are presented within SECTION 4 of this report.

SUMMARY OF LABORATORY PROCEDURES … cont'd

Electrical properties

On completion of the centrifuge water-gas relative permeability measurements, the samples were re-saturated under back pressure with the simulated formation brine. All samples were weighed after saturation to check measured pore volumes.

Resistivities of both the saturated samples and the saturant brine were monitored on consecutive days until they stabilised, indicating ionic equilibrium. Each sample was then loaded into a hydrostatic core holder and the effective overburden pressure raised from ambient to the requested 1800 psi NOBP. Resistivity and pore volume reductions were monitored over a period of several days until ionic equilibrium had been achieved. Formation resistivity factors and cementation exponent "m" were then calculated. Results are presented both in tabular and graphical formats on page 2-1.

After the formation resistivity factor analyses, the samples were desaturated, using humidified air, to varying decreasing brine saturations. At each brine saturation, samples were allowed to achieve capillary equilibrium. Electrical resistivities were then determined and the resistivity indices calculated. Results are presented within pages 2-2 and 2-14 of this report.

Capillary pressure from mercury injection analysis and pore throat size distribution

On completion of the electrical properties measurements, all ten samples were recleaned, dried, pore volume and porosity values determined at ambient conditions. At a later request received from Apache Energy (email dated 31st March 2005), an additional sample (#82) was added to the set undergoing mercury injection analysis.

Each sample was placed into a sample holder, evacuated and pressure injected at incremental pressures from 3 psia to 2,000 psia. Mercury saturations were monitored at every pressure stage. From the mercury injection data, pore size distributions were calculated. These results are presented within SECTION 3 of this report.

APPENDIX-2
CT-SCAN DESCRIPTIONS

CT-Scanning

Methodology

Individual samples are CT-sliced lengthwise, effectively generating two perpendicular image slices. A third slice is a cross section through the middle of the plug. Each slice has a thickness (voxel depth) of one millimetre.

The ends of the eleven unsleeved Teflon-wrapped samples have been visually examined using a Nikon SMZ-10 polarizing binocular microscope; these visual observations have been incorporated into the descriptions. The remaining seven samples, those nickel-sleeved and screened, have not been examined.

Raw CT image data in Dicom format are electronically archived on optical disk and DVD. In addition, CT images and data acquisition parameters used at the time of interpretation are archived on negative hardcopy.

General Comments

All of the samples are moderately well indurated, upper very fine to fine grained quartz sandstones. They are generally at least moderately well sorted notwithstanding rare localised grains to medium sand size and a component of silt (the latter most evident in sample 30). Accessory particles include significant rock fragments, common very distinctive micas, traces of ‘coaly’ organic matter (most apparent in sample 55 and possibly 45), and rare greenish grains of possible glauconite (the latter not recognised in all samples).

Layering of millimetre-scale is the common fabric element. It is evident from slight to moderate attenuation variation: finer grained and therefore less porous layers are inferred to show relatively higher attenuation. Accessory cement phases, pyrite certainly and carbonate probably, also contribute to higher attenuation. For the most part, layering is planar and trends at a low angle lengthwise with the plug axis. The dip angle is most extreme in samples 30, 48 and 63. A number of samples show evidence of low angle cross bedding (ripple laminations), a feature most apparent in sample 55.

All of the samples are at least moderately homogeneous. However, a significant open defect is recognised in sample 64.

Sample Descriptions

Sample 25: 2120.45 m

A probable fine to possibly lower medium grained quartz sandstone. The attenuation fabric is essentially homogeneous although layering more or less set parallel to the plug axis may be inferred. Very rare spots of highest attenuation are probably attributable to localised pyrite cement. No defects are evident.

Sample 29: 2121.65 m

A predominantly fine grained, rarely silty, moderately well sorted quartz sandstone with millimetre-scale layering defined by slight grain size variation. Disseminated rock fragments are noted and there is a trace of 'coaly' organic matter and mica. Rare greenish grains are possibly glauconite. Planar laminations set at a low angle to the plug axis are a feature of the attenuation fabric. Domains of moderately higher attenuation are indicative of relatively less porous, finer grained (slightly silty) domains containing possible traces of cement phases carbonate and/or pyrite. The sample is moderately homogeneous and no defects are inferred.

Sample 30: 3121.93 m

A mainly fine grained quartz sandstone; it is poorly to very poorly sorted with minor localised silt, rare framework grains to at least upper medium sand size and features millimetre-scale layering defined by grain size variation. Disseminated rock fragments and rose or orange quartz grains are noted, and trace of 'coaly' organic matter occurs mainly in coarser layers. The attenuation fabric shows disturbed planar laminations set oblique to the plug axis; minor crossbedding and bioturbation is inferred. Diffuse moderately higher attenuation layers and blebs are indicative of relatively less porous finer grained domains containing possible traces of cement phases carbonate and/or pyrite. A distinctive spot of very low attenuation evident in the cross section slice is almost certainly organic matter. No defects are inferred but the sample shows moderately poor homogeneity and extreme non-parallel bedding.

Sample 45: 2128.06 m

A probable fine to lower medium grained quartz sandstone. The attenuation fabric reveals distinctive millimetre-scale planar layering paralleling the plug axis. Slight variations in attenuation predominantly are a function of grain size; higher attenuation is inferred for relatively less porous finer grained layers. Rare spots of very high attenuation are inferred as probably attributable to localised pyrite cement. Distinctive larger spots of very low attenuation are possibly open pores, however, specks of 'coaly' organic matter is more probable. The sample is moderately homogeneous and no defects are inferred.

Sample Descriptions … cont'd

Sample 47: 2128.66 m

A probable fine to possibly lower medium grained quartz sandstone. Planar layering of millimetre-scale and set more or less set parallel to the plug axis is inferred from slight variations in attenuation. Very rare spots of highest attenuation are probably attributable to localised pyrite cement. The sample is essentially homogeneous and no defects are evident.

Sample 48: 2128.94 m

A probable fine to possibly lower medium grained quartz sandstone. The attenuation fabric reveals planar millimetre-scale layering set at an oblique angle to the plug axis. Attenuation variation between layers is slight and probably attributable to minor variations in grain size. Very rare spots of highest attenuation are probably attributable to localised pyrite cement. The sample is at least moderately homogeneous and no defects are evident.

Sample 50: 2129.56 m

A probable fine to possibly lower medium grained quartz sandstone. Planar layering of millimetre-scale and set more or less parallel to the plug axis is inferred from slight variations in attenuation. Very rare spots of highest attenuation are probably attributable to localised pyrite cement. The sample is essentially homogeneous and no defects are evident.

Sample 55: 2131.13 m

A moderately well sorted, mainly fine grained, rarely silty quartz sandstone with rare scattered framework grains to medium sand size. Layering of millimetre-scale is defined by variations in grain size. Accessory particles of 'coaly' organic matter are a characteristic of some layers. Also noted are disseminated rock fragments, mica flakes (commonly distinctively golden or pinkish gold) and very rare soft greenish grains of possible glauconite. The layering dominates the attenuation fabric; it is planar, set at a low angle to the plug axis and crossbedded in part. Higher attenuation domains are inferred as relatively less porous, finer grained and possibly containing traces of cement phases carbonate and/or pyrite. Rare spots of very high attenuation are inferred as pyrite cement. Generally lower attenuation domains generally are considered more porous, however larger spots of very low attenuation within some layers are almost certainly clasts of organic matter. The sample is moderately homogeneous overall and no defects are inferred.

Sample Descriptions … cont'd

Sample 58: 2132.06 m

A moderately well sorted, mainly fine grained quartz sandstone with rare scattered framework grains to medium sand size. Layering of millimetre-scale is apparent. Accessory rock fragments, mica flakes, 'coaly' particles of organic matter and greenish grains of possible glauconite are noted. The attenuation fabric reveals the fine layering to be planar and crossbedded; it trends parallel or at a low angle to the plug axis. Slight variations in attenuation predominantly are a function of grain size; higher attenuation is inferred for relatively less porous finer grained layers. Rare spots of very high attenuation are inferred as pyrite cement. The sample is essentially homogeneous overall and no defects are inferred.

Sample 63: 2133.55 m

A moderately well sorted, fine to lower medium grained quartz sandstone. Layering of millimetre-scale is present and is defined by slight variations in grain size and orientation of common elongate framework grains. Accessory rock fragments, mica flakes, 'coaly' particles of organic matter and greenish grains of possible glauconite are noted. Planar layering set oblique to the plug axis is the main feature of the attenuation fabric. The slight variations in attenuation predominantly are a function of grain size; higher attenuation is inferred for relatively less porous finer grained layers. Rare spots of very high attenuation are inferred as pyrite cement. The sample is moderately homogeneous overall and no defects are evident.

Sample 64: 2133.89 m

A moderately well sorted, predominantly fine grained quartz sandstone containing rare localised grains to medium sand size. Traces of disseminated rock fragments, pink and orange quartz, 'coaly' and partially pyritised organic matter are noted. The attenuation fabric reveals distinctive millimetre-scale layering, visually not apparent, set oblique to the plug axis. Layers with slightly higher attenuation probably contain a greater finer grained component. Rare spots of very high attenuation are localised pyrite cement. However, most apparent is a somewhat irregular curviplanar low attenuation trace inferred as a lengthwise open defect.

Sample 67: 2134.75 m

A probable fine to possibly lower medium grained quartz sandstone. Planar layering of millimetre-scale and set more or less parallel to the plug axis is inferred from slight variations in attenuation. Rare spots and blebs of highest attenuation are almost certainly attributable to localised pyrite cement. The sample is essentially homogeneous and no defects are evident.

Sample Descriptions … cont'd

Sample 73: 2136.44 m

A moderately well sorted, mainly fine grained quartz sandstone with rare scattered framework grains to medium sand size. Layering of millimetre-scale is inferred from slight grain size variation and orientation of elongate framework grains. Rose and orange quartz grains are common, along with accessory rock fragments, mica flakes, 'coaly' particles of organic matter and greenish grains of possible glauconite. The attenuation fabric reveals the fine layering to be planar and at a low angle to the plug axis. Slight variations in attenuation predominantly are a function of grain size; higher attenuation is inferred for relatively less porous finer grained layers. Rare spots of very high attenuation are inferred as pyrite cement. The sample is moderately homogeneous and no defects are inferred.

Sample 76: 2137.38 m

A probable fine to possibly lower medium grained quartz sandstone. Slight variations in the attenuation fabric are suggestive of layering set slightly oblique to the plug axis. Rare spots and blebs of highest attenuation are almost certainly attributable to localised pyrite cement. Traces of disseminated carbonate cement also may be present. The sample is essentially homogeneous and no defects are evident.

Sample 80: 2138.59 m

A mainly fine, rarely medium grained quartz sandstone; it is layered and poorly sorted overall but individual layers are quite well sorted. Rose and orange quartz is common and there is accessory rock fragments, mica flakes, 'coaly' particles of organic matter and greenish grains of possible glauconite. The attenuation fabric shows planar layering developed steeply oblique to the plug axis. However, for the most part, the fabric is quite homogeneous. Lesser higher attenuation layers are millimetre-scale and inferred as relatively less porous and finer grained. Traces of pyrite cement may be contributing to the diffuse higher attenuation in places and rare spots of very high attenuation are almost certainly attributable to localised pyrite. No defects are evident but the sample shows extreme non-parallel bedding and is moderately poorly homogeneous overall.

Sample Descriptions … cont'd

Sample 81: 2138.88 m

A moderately well sorted, mainly fine, rarely medium grained quartz sandstone. Traces of disseminated rock fragments, pink and orange quartz, 'coaly' organic matter and greenish grains of possible glauconite are noted. The attenuation fabric reveals distinctive millimetre-scale layering, visually not apparent, set more or less parallel to the plug axis. Layers with slightly higher attenuation probably contain a greater finer grained component. Rare spots of very high attenuation are localised pyrite cement. The sample is moderately homogeneous and no defects are inferred.

Sample 87: 2140.71 m

A moderately well sorted, fine to lower medium grained quartz sandstone. Accessory rock fragments, pink and orange quartz, 'coaly' organic matter and greenish grains of possible glauconite are noted. The attenuation fabric reveals distinctive millimetre-scale planar layering, visually not so apparent, set at a low angle to the plug axis. Layers showing slightly higher attenuation probably contain a greater finer grained component and possible associated pyrite 'dust'. However, very distinctive but rare spots of very high attenuation are almost certainly localised pyrite cement. The sample is moderately homogeneous and no defects are evident.

Sample 88: 2141.05 m

A moderately well sorted, mainly fine, rarely medium grained quartz sandstone. Traces of disseminated rock fragments, iron-stained grains, 'coaly' organic matter and very rare soft greenish grains of possible glauconite are noted. The attenuation fabric reveals distinctive millimetre-scale layering, visually not so apparent, set at a low angle to the plug axis. Layers with slightly higher attenuation probably contain a greater finer grained component along with traces of cement phases, pyrite 'dust' and possible carbonate. Distinctive but rare spots of very high attenuation are localised pyrite cement. The sample is moderately homogeneous and no defects are inferred.

APPENDIX 4

Petrophysical Analysis

PETROPHYSICAL REPORT

LONGTOM-2

VIC/P-54

VICTORIA

Paul Bingaman

January 2006

1. INTRODUCTION

Longtom-2 was drilled as a deviated appraisal well to test the 251 metre gas column encountered in the Longtom-1/ST-1 discovery well drilled by BHPP in 1995. The primary objectives in the well were sandstones of the Admiral Formation (Emperor Sub-group) within a three-way dip buttress closure. The gas accumulation was confirmed.

Log analysis was performed using PETROLOG software (Crocker Data Processing) Rev 9.3 7 September 2004. The interpretation workflow comprised temperature gradient determination, environmental corrections using service company-specific algorithms, Vcl and porosity calculations using a complex lithology crossplot method, and water saturation calculation using an Indonesian algorithm. Formation water resistivity (salinity) of 35,000 ppm NaCl equivalent was assumed based on nearby analogues.

2. MUD PROPERTIES AND TEMPERATURE DATA (Section of Interest)

Type	Wt. (sg)	Cl (ppm)	KCl (%)	Rm @ °C	Rmf @ °C	Rmc @ °C
KCl/IDCAP	1.30	48,000	5.5	0.10 @ 28.0	0.08 @ 28.0	0.15 @ 28.0

Depth (m)	Temperature (°C)	Gradient (°C/100m)
0.0	15.0	
2214.2	102.8 *	3.97

(* - DST 1)

3. ANALYSIS PARAMETERS (Zone of Interest)

Input Parameter	Value	Input Parameter	Value
Bit Size (inch)	8.5	RHOB clay (g/cc)	2.48
Rw @ 75° F	0.185	PHIN clay (dec)	0.50
Rw Salinity (ppm)	35,000	DT clay (msec/ft)	97
RHOH (g/cc)	0.60	a	1.0
RHOF (g/cc)	1.048	m	2.0
RHOMA (g/cc)	2.65	n	2.0
GR clean (API)	50	Clay Cutoff	0.50
GR clay (API)	145	Phi Cutoff	0.10
R clay (ohm-m)	3.0	Sw Cutoff	0.70

4. DISCUSSION

Log quality at Longtom-2 is excellent with the borehole in-gauge through the primary objectives.

The Admiral Formation at this location comprises a series of interbedded sandstones and claystones. The sandstones are poorly to moderately sorted with common lithic grains and argillaceous matrix. A 259.3 metre gross gas column is interpreted with 94.9 metres of net pay (36.6% net-to-gross). The sandstones exhibit average porosities of 18.9% and average calculated water saturations of 39.9%. The base of the sandstone units represents a ‘gas-down-to’ with no gas/water contact evident.

The results of the analysis for the Admiral Formation Sandstones are summarised in the tables and log analysis plots on the following pages:

Log Analysis Summary for Longtom-2 - Admiral Formation

Depth - TVD SS		Gross	Net	Avg Sand	Net	Avg HC	Avg
From	To	Interval	Sand	Porosity	HC Pay	Porosity	Sw
metres	metres	metres	metres	percent	metres	percent	percent
1,992.3	1,998.0	5.7	1.2	16.3 %	1.2	16.3 %	50.1 %
1,998.0	2,004.0	6.0	1.2	19.7 %	1.2	19.7 %	42.7 %
2,004.0	2,010.0	6.0	2.7	24.9 %	2.7	24.9 %	36.0 %
2,010.0	2,016.0	6.0	1.6	24.4 %	1.6	24.4 %	31.4 %
2,016.0	2,022.0	6.0	0.8	19.6 %	0.8	19.6 %	31.0 %
2,022.0	2,028.0	6.0	-	6.1 %	-	0.0 %	0.0 %
2,028.0	2,034.0	6.0	1.0	17.5 %	0.9	18.1 %	62.1 %
2,034.0	2,040.0	6.0	-	5.5 %	-	0.0 %	0.0 %
2,040.0	2,046.0	6.0	-	6.0 %	-	0.0 %	0.0 %
2,046.0	2,052.0	6.0	-	2.2 %	-	0.0 %	0.0 %
2,052.0	2,058.0	6.0	-	7.0 %	-	0.0 %	0.0 %
2,058.0	2,064.0	6.0	-	7.8 %	-	0.0 %	0.0 %
2,064.0	2,070.0	6.0	-	7.9 %	-	0.0 %	0.0 %
2,070.0	2,076.0	6.0	-	5.6 %	-	0.0 %	0.0 %
2,076.0	2,082.0	6.0	0.8	15.5 %	0.8	15.5 %	57.1 %
2,082.0	2,088.0	6.0	4.3	19.3 %	4.3	19.3 %	36.7 %
2,088.0	2,094.0	6.0	3.7	23.1 %	3.7	23.1 %	29.7 %
2,094.0	2,100.0	6.0	5.3	21.3 %	5.3	21.3 %	36.0 %
2,100.0	2,106.0	6.0	6.0	22.2 %	6.0	22.2 %	31.6 %
2,106.0	2,112.0	6.0	6.0	18.6 %	6.0	18.6 %	36.8 %
2,112.0	2,118.0	6.0	0.8	18.8 %	0.8	18.8 %	51.4 %
2,118.0	2,124.0	6.0	1.4	14.8 %	1.4	14.8 %	60.0 %
2,124.0	2,130.0	6.0	3.4	19.2 %	3.4	19.2 %	48.9 %
2,130.0	2,136.0	6.0	2.7	18.8 %	2.7	18.8 %	48.6 %
2,136.0	2,142.0	6.0	-	5.1 %	-	0.0 %	0.0 %
2,142.0	2,148.0	6.0	-	5.4 %	-	0.0 %	0.0 %
2,148.0	2,154.0	6.0	1.0	16.5 %	1.0	16.5 %	56.5 %
2,154.0	2,160.0	6.0	6.0	20.8 %	6.0	20.8 %	40.5 %
2,160.0	2,166.0	6.0	1.1	20.1 %	1.1	20.1 %	38.6 %
2,166.0	2,172.0	6.0	-	7.3 %	-	0.0 %	0.0 %
2,172.0	2,178.0	6.0	-	4.8 %	-	0.0 %	0.0 %
2,178.0	2,184.0	6.0	1.6	15.8 %	1.6	15.8 %	51.1 %
2,184.0	2,190.0	6.0	4.8	15.6 %	4.8	15.6 %	49.0 %
2,190.0	2,196.0	6.0	5.8	16.7 %	5.8	16.7 %	40.8 %
2,196.0	2,202.0	6.0	6.0	21.9 %	6.0	21.9 %	30.8 %
2,202.0	2,208.0	6.0	6.0	19.6 %	6.0	19.6 %	31.8 %
2,208.0	2,214.0	6.0	2.2	17.0 %	2.2	17.0 %	40.4 %
2,214.0	2,220.0	6.0	0.7	15.9 %	0.7	15.9 %	54.6 %
2,220.0	2,226.0	6.0	0.7	17.6 %	0.7	17.6 %	56.4 %
2,226.0	2,232.0	6.0	0.9	14.3 %	0.9	14.3 %	53.4 %
2,232.0	2,238.0	6.0	5.5	15.3 %	5.5	15.3 %	49.5 %
2,238.0	2,244.0	6.0	6.0	16.2 %	6.0	16.2 %	40.5 %
2,244.0	2,250.0	6.0	3.3	15.1 %	3.3	15.1 %	49.9 %
2,250.0	2,251.6	1.6	0.7	14.7 %	0.7	14.7 %	54.8 %
Total / Averages		259.3	95.0	18.9 %	94.9	18.9 %	39.9 %
Net/Gross Ratio			36.6 %		36.6 %		

Cutoffs Applied	Vclay = 50.0 %	Porosity = 10.0 %	Sw = 70.0 %

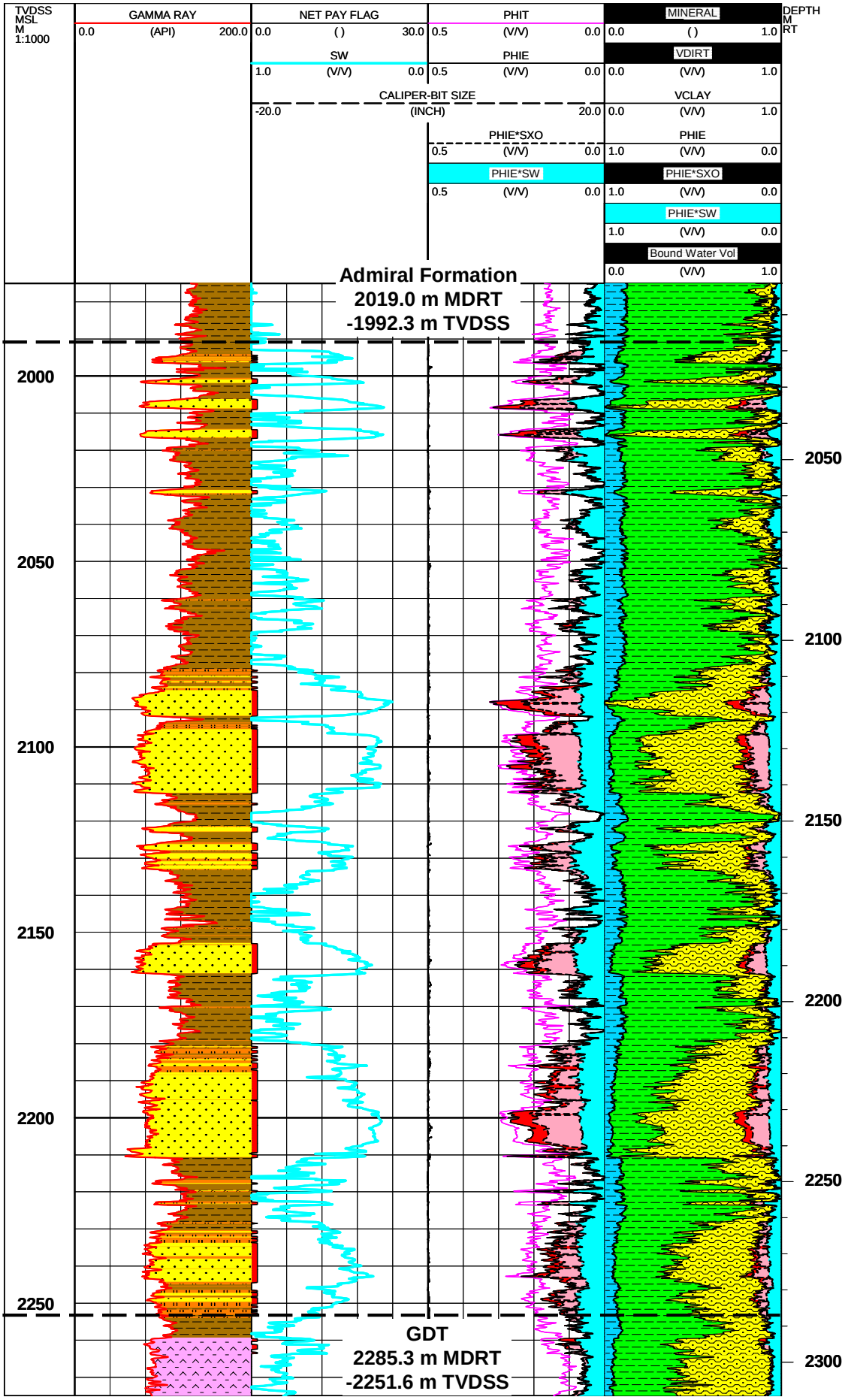
TVDSS
MSL
M
1:1000
GAMMA RAY
0.0 (API) 200.0
NET PAY FLAG
0.0 ( ) 30.0
SW
1.0 (V/V) 0.0
CALIPER-BIT SIZE
-20.0 (INCH) 20.0
PHIT
0.5 (V/V) 0.0
PHIE
0.5 (V/V) 0.0
PHIE*SXO
0.5 (V/V) 0.0
PHIE*SW
0.5 (V/V) 0.0
MINERAL
0.0 ( ) 1.0
VDIRT
0.0 (V/V) 1.0
VCLAY
0.0 (V/V) 1.0
PHIE
1.0 (V/V) 0.0
PHIE*SXO
1.0 (V/V) 0.0
PHIE*SW
1.0 (V/V) 0.0
Bound Water Vol
0.0 (V/V) 1.0
DEPTH
M
RT
Admiral Formation
2019.0 m MDRT
-1992.3 m TVDSS
GDT
2285.3 m MDRT
-2251.6 m TVDSS
2000
2050
2100
2150
2200
2250
2050
2100
2150
2200
2250
2300

APPENDIX 5

Geochemistry

VITRINITE REFLECTANCE MEASUREMENT

LONGTOM-2 / ST1

Sample Details		Mean	Range	Std Dev	N° of Readings	Sample Description Including Liptinite Fluorescence, Maceral Abundances, Mineral Fluorescence
2124.0m Core	2_vmax	0.73	0.67-0.84	0.053	6	Abundant lamalginite and sparse liptodetrinite yellow to orange, rare cutinite orange. (Claystone. Dom abundant, L>I>V. Liptinite abundant, inertinite common, vitrinite rare. Mineral fluorescence weak orange. Pyrite rare.)
	2_lmax	1.62	0.90-2.56	0.442	25	
2148.0m Core	2_vmax	0.68	0.55-0.82	0.061	27	Sparse lamalginite and rare liptodetrinite yellow to orange, rare sporinite orange, rare cutinite orange to dull orange. (Argillaceous siltstone and claystone with traces of "coal". "Coal" rare, V>L, vitrite>clarite and may represent drifted wood and leaves. Dom abundant, I>V>L. Inertinite and vitrinite common, liptinite sparse. Rare coalified leaf tissue fragments. Mineral fluorescence moderate to weak orange. Iron oxides rare. Pyrite rare.)
	2_lmax	1.63	1.00-2.12	0.347	10	
2170.0m Ctgs	2_vmax	0.69	0.58-0.81	0.053	25	Rare lamalginite and liptodetrinite orange to dull orange, rare sporinite dull orange. (Argillaceous siltstone>sandstone>claystone. Dom common, I>>V>L. Inertinite common, vitrinite rare to sparse, liptinite rare. Mineral fluorescence moderate orange Iron oxides rare. Pyrite rare.)
	2_lmax	1.64	1.10-2.58	0.317	15	
2200.0m Ctgs	2_vmax	0.71	0.59-0.91	0.069	25	Rare lamalginite and liptodetrinite orange to dull orange, rare sporinite orange, rare cutinite dull orange. (Argillaceous siltstone>claystone>sandstone. Dom common, I>>V>L. Inertinite common, vitrinite rare to sparse, liptinite rare. Mineral fluorescence moderate orange. Iron oxides rare. Pyrite rare.)
	2_lmax	1.64	1.20-2.22	0.287	10	
2250.0m Ctgs	2_vmax	0.72	0.62-0.91	0.067	25	Rare sporinite and liptodetrinite greenish yellow and orange to dull orange, rare cutinite dull orange. (Argillaceous siltstone> claystone>sandstone>coal>carbonate. Coal abundant, V>>I>L, vitrite>>duroclarite. Dom common, I>V>L. Inertinite common, vitrinite rare to sparse, liptinite rare. The mean reflectance of the coal population is 0.45%. The coals show desiccation cracks probably represent cavings and/or contaminants. Greenish yellow fluorescing liptinite is associated with coals. Mineral fluorescence moderate to strong orange. Glauconite rare. Iron oxides rare. Pyrite rare.)
	2_lmax	1.67	1.12-2.32	0.377	10	
2290.0m Ctgs	2_vmax	0.70	0.64-0.81	0.048	11	Rare sporinite and liptodetrinite orange to dull orange. (Argillaceous siltstone>sandstone>ferruginous claystone. Dom sparse to common, I>V>L. Inertinite sparse, vitrinite and liptinite rare. Mineral fluorescence weak orange to none. Iron oxides abundant. Pyrite rare.)
	2_lmax	1.68	1.14-2.24	0.310	20	

VITRINITE REFLECTANCE MEASUREMENT

LONGTOM-2 / ST1

Sample Details		Mean	Range	Std Dev	N° of Readings	Sample Description Including Liptinite Fluorescence, Maceral Abundances, Mineral Fluorescence
2310.0m	2_vmax	0.73	0.61-0.83	0.063	8	Rare lamalginite and liptodetrinite orange to dull orange, rare
Ctgs	2_lmax	1.71	1.10-2.88	0.396	25	sporinite dull orange. (Argillaceous siltstone>claystone>sandstone> ferruginous claystone. Dom sparse, I>V>L. Inertinite sparse, vitrinite and liptinite rare. Inorganic mud additives abundant. Mineral fluorescence weak dull orange. Iron oxides sparse. Pyrite sparse, locally abundant.)
2422.0m	2_vmax	?0.81	0.76-0.87	0.047	4	Fluorescing liptinite absent. (Sandstone>argillaceous
Ctgs	2_lmax	3.58	1.72-4.90	1.353	3	siltstone>claystone>carbonate. Dom rare, V>I. Vitrinite and inertinite rare, liptinite absent. Measured vitrinite population may be cavings and inertinite population may also include cavings. Low rank coal cavings present. Mineral fluorescence mostly none, weak dull orange in fine grained sediments. Iron oxides sparse. Pyrite sparse, locally abundant.)

The upper part of the section has vitrinite reflectance values that indicate it lies in the middle of the main oil generation zone. Some of the deeper samples contain low rank coals, but these appear to be a contaminant, either cavings, or an additive. The deepest sample includes some fluorescing liptinite but many of the grains show very weak fluorescence. The fluorescing liptinite may be cavings, and the sample could be from a much more mature part of the section. In the absence of stratigraphic data, it is difficult to be more definitive about assigning the populations of vitrinite that were found.

ANALYSIS OF ORGANIC MATTER BY ROCK-EVAL PYROLYSIS

LONGTOM-2 / ST1

Depth (m)		*Tmax*	*S1*	*S2*	*S3*	*S1+S2*	*S2/S3*	*PI*	*TOC*	*HI*	OI
2124.0	Core	434	0.06	0.62	0.11	0.68	5.64	0.09	0.70	89	16
2148.0	Core	439	0.05	0.62	0.15	0.67	4.13	0.07	0.91	68	16
2170.0	Ctgs	439	0.26	1.12	1.47	1.38	0.76	0.19	1.11	101	132
2200.0	Ctgs	436	0.25	1.12	1.17	1.37	0.96	0.18	1.13	99	104
2250.0	Ctgs	439	0.25	1.33	2.51	1.58	0.53	0.16	1.50	89	167
2290.0	Ctgs	442	0.19	0.93	0.81	1.12	1.15	0.17	0.72	129	113
2310.0	Ctgs	441	0.08	0.61	6.16	0.69	0.10	0.12	0.52	117	1185
2420.0	Ctgs	nd	nd	nd	nd	nd	nd	nd	0.22	nd	nd

A TMAX value is not reported if the S2 is <0.2mg/g

TMAX = Max. temperature S2 (^{o}C)

S1 = Volatile hydrocarbons (HC) (mg/g rock)

S2 = HC generating potential (mg/g rock)

S1+S2 = Potential yield (mg/g rock)

S3 = Organic carbon dioxide (mg/g rock)

PI = Production index

OI = Oxygen Index

TOC = Total organic carbon (wt % of rock)

HI = Hydrogen index

nd = no data

GEOTECHNICAL SERVICES PTY LTD

Sample : **LONGTOM-2/ST1, 2340m, Mud**
File ID : **347010XB**

Chromatogram obtained from analysis of the whole extract by GC-MS

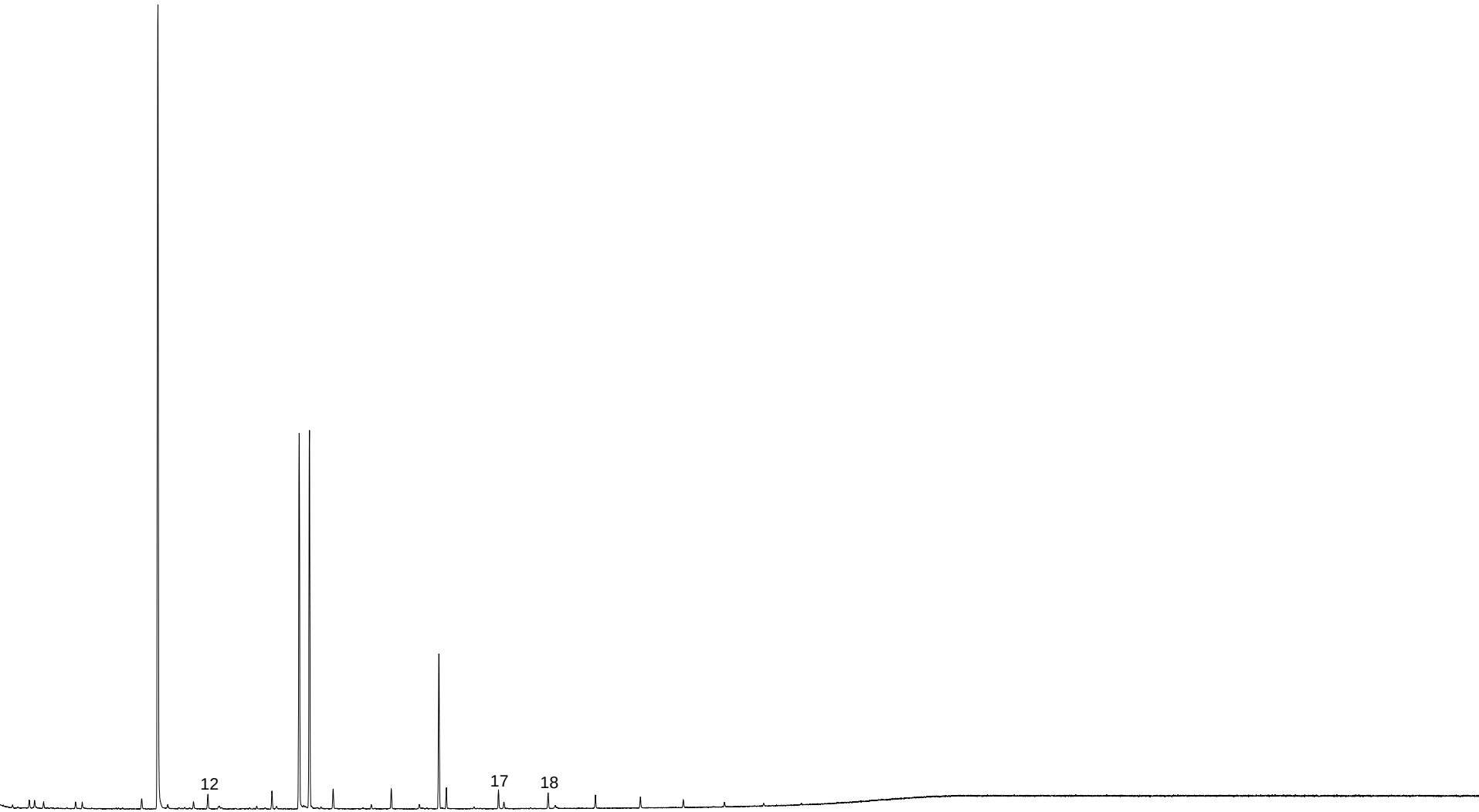

SOLVENT EXTRACTION DATA

LONGTOM-2/ST1

DEPTH	Sample Type	Weight of Material Extd. (g)	Total Extract (mg)	Total Extract (ppm)
2340m	Mud	99.9	11.5	115

nd = no data

ENCLOSURE 1

Longtom-2

Composite Log 1: 500 TVD

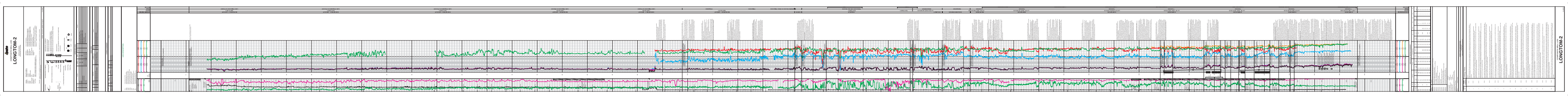
LONGTOM-2
LONGTOM-2